

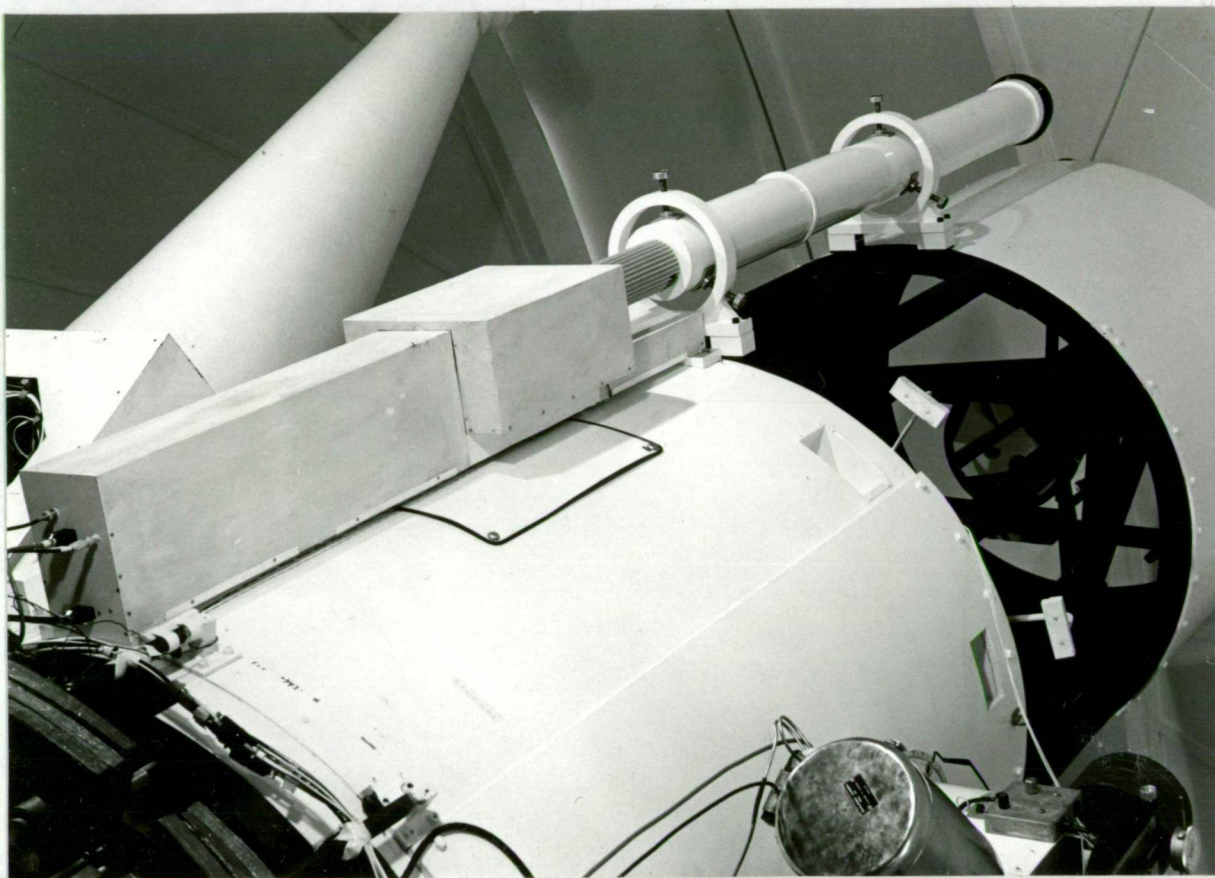
AN EFFICIENT ASTRONOMICAL
IMAGE INTENSIFIED TELEVISION
ACQUISITION AND GUIDING SYSTEM

AN ERDINAND
J F JOURKE
BOERSMA B.Sc. (Hons.)

Submitted in fulfilment of the
requirements for the degree of
Master of Science.

UNIVERSITY OF TASMANIA

1980.



Frontispiece : (a) The intensified television system mounted on the 1.04 metre telescope.

(b) The complete system with covers removed.

ABSTRACT

A four field television star acquisition and guiding system incorporating image intensification has been designed, constructed and evaluated. The system which includes a 152mm objective, a three stage cascaded electrostatic image intensifier, a newvicon target low light level television camera is mounted on the 1.04 metre reflecting telescope of the Canopus Hill Observatory near Hobart.

An extensive testing programme on fields of $3\frac{1}{2}$, 9, 25 and 60 arc min has yielded the excellent results of a limiting sensitivity of 13.7^m and a resolution in the $3\frac{1}{2}$ arc min. field of 1.4 arc sec. Some proposals are discussed to push these limits even further.

C O N T E N T S

ABSTRACT	Page iii
PROLEGOMENON	1.
CHAPTER 1. INTRODUCTION	2.
2. GENERAL SYSTEM DESIGN FACTORS	
Overall Magnification	6.
Effects of Seeing	7.
3. THE IMAGE INTENSIFIER	
Characteristics	12.
Magnification and Distortion	15.
Projected Investigations	17.
4. TELEVISION SYSTEM	
Camera Characteristics	18.
Target Characteristics	19.
Camera Field Tests	21.
5. IMAGE TRANSFER SYSTEM	27.
Photon Flux Collection Efficiency	27.
Operating Point Selection	33.
Field Tests	34.
Vignetting and Focal Lengths	36.
6. COMBINED ELECTRONIC SYSTEM EVALUATION	39.
Resolution	39.
TV Optical Transfer Characteristics	41.
Variation of Intensifier Gain	46.
7. FIELD SELECTOR SYSTEM	51.
Distribution	52.
Simple Field Selector/Transfer System	52.
Two Lens Field Selector/Lens Transfer	54.

7.	FIELD SELECTOR SYSTEM (contd.)	
	Possible Optical Configurations of Selector	58.
	Single lens	58.
	Single lens plus field lens	61.
	Twin lens (fixed focus)	64.
	Twin lens selector including a zoom	67.
	Cadadioptric folded system	71.
8.	PROJECTED PERFORMANCE	73.
9.	BACKGROUND & NOISE	
	Sky Background	76.
	Stellar magnitude equivalent	80.
	Background as function of magnification	81.
	Intensifier Noise	
	Thermal emission	84.
	Shot noise	86.
	Phosphor boil	87.
10.	TECHNICAL ASPECTS OF CONSTRUCTION	
	Field Selector Table Rotations	89.
	Increasing the effective field	92.
	Table Mechanics	94.
	Acquisition Support Frame	98.
	Location of System Optical Centre	102.
11.	SYSTEM EVALUATION	103.
12.	FUTURE DEVELOPMENTS	115.

APPENDICES

I	Vignetting in Rokkor Transfer Lens Pair	118.
II	Scene Illumination v. Target Illumination	121.
III	Resolution Tests on MD Rokkor lenses	123.
IV	Photon flux collection from phosphor star image	124.
V	Real Time Observations:	126.
	Minor Planet Appulses	126.
	Lunar Eclipse Occultation	130.

REFERENCES	132.
------------	------

PROLEGOMENON

The prime experimental problems confronting an observational astronomer are to collect as much light as possible from the object of interest and to concentrate this with minimal loss and at an appropriate scale on to a detector of high efficiency for a sufficient time to record the desired information. At the present time such desires need not necessarily be flights of fantasy. Moderate size telescopes have had their effective apertures increased when first efficient reflective and antireflective coatings became available, and then gain elements in the form of photoelectronic imaging devices employing high quantum efficiency photocathodes were introduced. Components such as fibre optics, low noise amplifiers, etc., have made considerable contributions and advanced technologies have made otherwise difficult processes possible. In many cases theoretical limits are within sight of realisation. Practical limitations such as sky background are now readily reached quite aside from our city floodlit society.

Cost reductions of similar nature to the adjacent areas of micro-electronics have meant that such devices are no longer the prerogative of large budget institutions; with some ingenuity sophisticated ancillary telescope equipment may now be constructed for a modest outlay. Not only light flux but telescope time, always at a premium, is thus more effectively used. It is in this context that the present project is concerned.

Chapter 1.

INTRODUCTION

It is desired to design and construct an efficient television system to detect faint stars and to provide a display at the console and other key points of a one metre telescope primarily for the purpose of star field acquisition and guidance. To reach stars of fainter magnitudes image enhancement by photo-electronic intensification is a first necessity. A second requirement is that several appropriate fields of view be readily accessible at the behest of the astronomer.

Such a TV system will of course also have ready application to other low light level detection areas of spectroscopy and microscopy, etc. Two examples of real time observation of planetary occultations are illustrated in Appendix V.

At the outset there must be an optoelectronic chain of components that will collect the light flux from a star field, magnify the prime image produced, intensify the optical signal by a suitable gain factor, and reimage this on a photocathode for display on a television monitor. The sequence will be as illustrated in Fig. (1.1) although the exact form has yet to be justified.

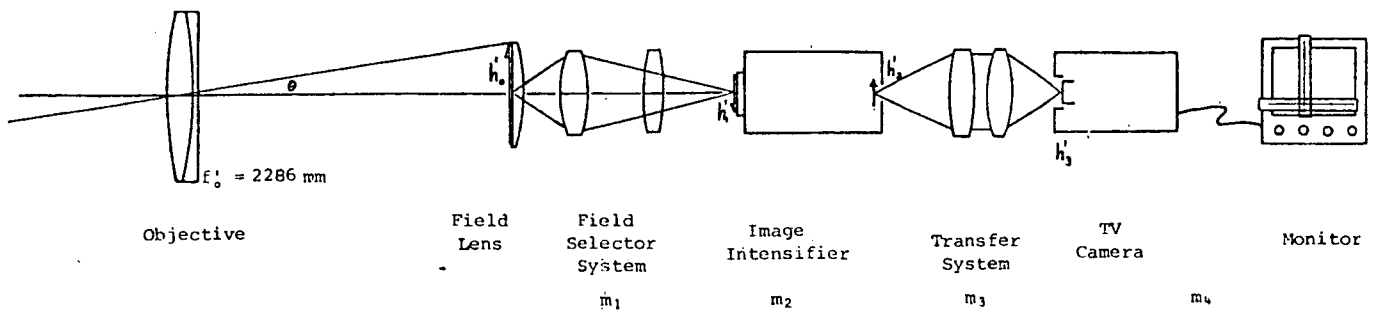


Fig. (1.1) The sequential layout of the overall system.

A doublet objective receives a quantity of illumination determined by its 152mm aperture which, after being focussed in the prime image plane, is redirected by a field lens into one of several lens configurations (called the field selector) to re-image with magnification on the fibre optic faceplate of an image intensifier. Electron multiplication occurs in three cascaded stages with a considerable increase in image brightness. The intensifier phosphor screen image is transferred as efficiently as possible to the TV target so that the star field is viewed via the monitor screen at the normal television framing rate. As shown in the figure the magnification is distributed between several components in the chain with m_1 and m_3 in front of and behind the image intensifier respectively being so chosen as to give appropriate fields of view while maintaining optimum resolution. Degeneration in resolution carries with it an automatic loss in sensitivity so that switching a field of view requires careful check on image disc scales from section to section. For example no purpose is served imaging down before the intensifier and then magnifying up the blob onto the TV target. It is this question that requires paramount attention.

In this thesis the chapters are in the order in which the important choices and analyses are to be made although some anticipation is necessary and some retrospective modification may also be required.

Fields of View

How should the fields of view be specified? The wide field is taken at 60 arc mins chiefly for initial star field recognition although some clusters do in fact have outer diameters a substantial fraction of this. The criterion for the narrowest field is more precisely determined by the need to keep a star accurately guided on the TV fiducial markers to within at least one star diameter and preferably better.

Taking an initial narrow field example of $2\frac{1}{2}$ arc min yields approximately three TV line pairs per arc sec so that if atmospheric seeing is three arc sec then the stellar image is nine line pairs in diameter. The original specifications stated that fields be 60, 20 and 2.5 arc min. However these were relaxed when it became evident that other benefits could be obtained with only slight modifications.

It is maintained that the design criteria for all components in the optoelectronic chain following the objective should allow for the possibility of transmitting one arc sec resolution. This was in the end justified since the final system has resolved stellar discs 1.4 arc sec in diameter (see Fig. 11.4).

Since the photometer at Cassègrain focus is sometimes at rather inconvenient locations it is also desirable to set and guide the telescope with confidence on a star situated in the centre of the smallest diaphragm. With an aperture range of 7 to 40 arc sec this should be achieved without difficulty.

GENERAL SYSTEM DESIGN FACTORS

In general terms the performance of an image intensifier television system will be dependent upon a number of factors including at least:-

- (a) Seeing conditions.
- (b) Sky background.
- (c) Telescope aperture and F number.
- (d) Magnification of field selection and image transfer elements.
- (e) Resolution of all components in chain.
- (f) Photocathode characteristics of intensifier and TV target.
- (g) Image tube gain.
- (h) TV target integration time

Other factors will be related to these such as photocathode area, diameters and transmission coefficients of optical elements, equivalent background input, etc.

Some are predetermined by the atmosphere or by the state of the art; others can be controlled and optimised by suitably trading off one variable against another. An over-riding limitation difficult to put into equations describing laws of nature is cost which must inevitably be low. Choice of components will be rather influenced by the latter. However even with such restriction the completed system achieved a sensitivity to 14th magnitude and 1.4 arc sec resolution while employing a 150mm aperture objective.

Overall Magnification, Effects of Seeing

The overall magnification of the image on the TV target must be such that the specified field of view will fill the TV monitor screen.

If Q is the width of the TV quality rectangle,

$$h_3 = \frac{h_3'}{m_3} = \frac{Q}{m_3}$$

$$h_2 = \frac{h_2'}{m_2} = \frac{Q}{m_2 m_3}$$

$$h_1 = \frac{h_1'}{m_1} = \frac{Q}{m_1 m_2 m_3}$$

h_1 is determined for each of at least three fields by

$$h_1 = h_0' = 2 f_0' \tan \theta$$

where θ is the half field angle.

Hence

$$m_1 m_2 m_3 = \frac{Q}{2 f_0' \tan \theta} \quad \text{..... (2.1)}$$

A similar equation is obtained in terms of smallest resolution elements. If ΔQ is a picture element on the TV target and $\Delta\theta$ is the half angle as set by atmospheric seeing or objective resolving power,

then

$$m_1 m_2 m_3 = \frac{\Delta Q}{2 f_0' \tan \Delta\theta} \quad \text{..... (2.2)}$$

This is the minimum magnification required to exactly match the atmospheric seeing to the smallest resolvable element on the TV photocathode. Increasing $m_1 m_2 m_3$ above this value causes the stellar image to spill over onto adjacent resolution elements with consequent reduction in photon flux density and hence sensitivity to fainter stars. If seeing conditions momentarily improved below "typical" value the image point spread function merely contracts to below ΔQ , sensitivity is unaffected and resolution is limited by the target. See Fig. (2.1)

The above presumes that no image degradation occurs in the intervening optical components and intensifier.

Equations (2.1) and (2.2) therefore suggest an optimum field for which matching occurs. It is

$$2\theta_0 = 2 \arctan \left(\frac{Q}{\Delta Q} \tan \Delta\theta \right) \quad \dots\dots (2.3)$$

Magnifying a field to below $2\theta_0$ produces a decrease in sensitivity proportional to $\left(\frac{1}{m_1 m_2 m_3} \right)^2$. For a field selected such that $\theta_1 < \theta_0$ the brightness loss in stellar magnitudes becomes

$$\begin{aligned} m_v &= 2.5 \log \left(\frac{2\theta_1}{2\theta_0} \right)^2 \\ &= 5.0 \log \frac{2\theta_1}{2\theta_0} \end{aligned}$$

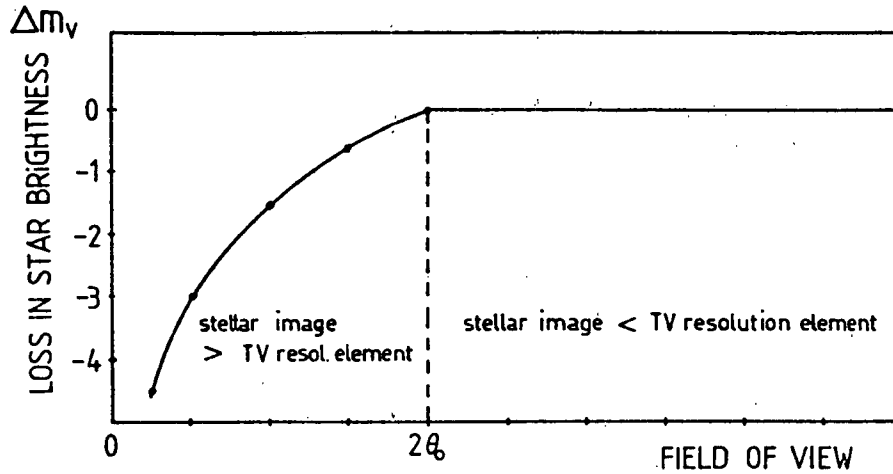


Fig. (2.1) Change in star image brightness as function of magnification.

To find numerical values as listed in Table 2.1, the performance figures of the component equipment justified and tested in later chapters are merely quoted at this stage. A 2/3 inch Newvicon TV camera has a quality rectangle of 6.6 x 8.8mm and a photocathode resolution tested at 38 line pairs/mm or 334 line pairs total.

An F15 objective doublet of 152.4mm aperture was available for use in the final system although for virtually all prototype testing a 100mm F15 lens was employed as indicated on various photographs in Chapters 7. and 11.

For the 152mm aperture lens the focal length is thus $f_0' = 2286\text{mm}$.

Table 2.1 Magnification at narrowest most sensitive field as function of seeing conditions. Measured photocathode resolution 38 lp/mm.

Seeing	$m_1 m_2 m_3$	m_1 for $\frac{m_2}{m_3} = \frac{0.82}{1}$	$2\theta_0$ (optimum field)
1 arc sec	2.38	2.90	5.6 arc min
2 arc sec	1.19	1.45	11.1 arc min
3 arc sec	0.79	0.97	16.7 arc min
4 arc sec	0.60	0.73	22.3 arc min

In the final analysis ΔQ may not be set solely by the transfer/TV components. Putting $m_3 = 1$ already limits resolution to that slightly lower value of the intensifier (31 lp/mm). Final tests by photography of real star fields show that some significant image degradation also occurs for some fields at the field selector stage.

To estimate the drop off in sensitivity with magnification it is important to attach a typical value to atmospheric seeing as observed with a 150 mm objective. For example, if seeing limits stellar discs to 3 arc sec and then a $2\frac{1}{2}$ arc min field of view was called, the star image area will be enlarged $\left(\frac{16.7}{2.5}\right)^2$ times i.e. there will be a limiting sensitivity change of $44.6 = 4^{m.12}$ stellar magnitudes, a considerable drop indeed. The graph is illustrated in Fig. (2.1)

It appears that general seeing conditions over Hobart as viewed with the one metre telescope are in fact about 3 arc sec. However in smaller telescope apertures the optical wave front distortion due to atmospheric temperature cells is less than for larger instruments so that seeing is correspondingly better (Young 1). Of course greater image motion may occur. Empirical evidence suggests that an optimum aperture seems to be about 400mm (16 inch) where good seeing will allow about one arc sec resolution. Since TV viewing corresponds to the taking of very short exposures with integration times of 20m sec higher resolution will be achieved than by normal astro-photographic exposures. It is therefore proposed to take the angular resolution for the 152 mm objective at between one and two arc sec as a basis for system design work. Note that the theoretical Rayleigh diffraction limit gives 0.8 arc sec.

The switching from an intermediate to a narrow $2\frac{1}{2}$ min field should then not cause such a dramatic fall off in sensitivity. It will be born in mind that accurate guiding normally demands narrow fields. That this thinking is correct is demonstrated by analysis of photographs taken with the completed system where the sensitivity reduction to the narrowest field is $1^{m.7}$ as discussed in Chapter (11).

Chapter 3.

THE IMAGE INTENSIFIER

High quantum efficiency photoelectric surfaces positioned at the front end of the electron imaging devices have made available high gain elements in opto-electronic chains that are strictly linear with respect to incident light flux and do not suffer from reciprocity failure at low light levels. Several such intensifiers may be cascaded thus multiplying gains and being limited only by photon noise of the leading surface, and the restriction on minimum acceptable resolution and image distortion.

The theory of operation and development of intensifiers have been well described for example by McGee (2), Wampler (3), Lowrance and Succino (4), Sauermann (5), and Bibermann and Nudelman (6). While these devices were originally invented several decades ago they have achieved a high degree of sophistication and reliability only in the last decade. Developments in diversified technologies such as high vacuum, solid state physics, fibre optics, integrated and miniaturized high voltage components, have permitted the introduction of variant generations of intensifiers. The chief groups are multi-stage electrostatic tubes with diameters 18-40mm and gains of the order of 50 per stage, and microchannel plates (MCP) available up to 25mm diameter with gain of 30,000 in a single stage. It should be noted that a contract has just been awarded (July 1980) to RCA for a special project for the production of a 90mm diameter MCP.

One of the advantages of MCPs is that the threshold of damage through overloading (such as by bright stars) is very much higher than for the generation I type (ref. 7) since the microchannel amplifiers simply saturate locally.

For this project a 3-stage image electrostatic intensifier assembly with an extended red response S-20 photocathode (11% QE) and 40mm nominal diameter of Varo manufacture was selected as the gain element in the chain. The near infra red response demands that careful choice needs to be made of refracting components before the faceplate. Whereas the minimum gain is normally offered at 35000 (33 per stage) for this particular assembly it was 145000 (52 per stage) while maintaining a centre resolution of 31 lp/mm at limiting visibility. This was directly tested by projection of a Cobb resolution graticule onto the faceplate.

Figure (6.1b) shows photographically the contrast still visible when a 500 1/inch grating (24 lp/mm) at the output screen) pressed to the faceplate is transmitted by the intensifier, transfer lens pair, and TV camera in tandem. Note that this is not yet the limiting resolution. Strictly speaking it would be a modulation transfer function that is desired for each component and the whole system. Only a sketch of the intensifier MTF is shown in Figure (3.1).

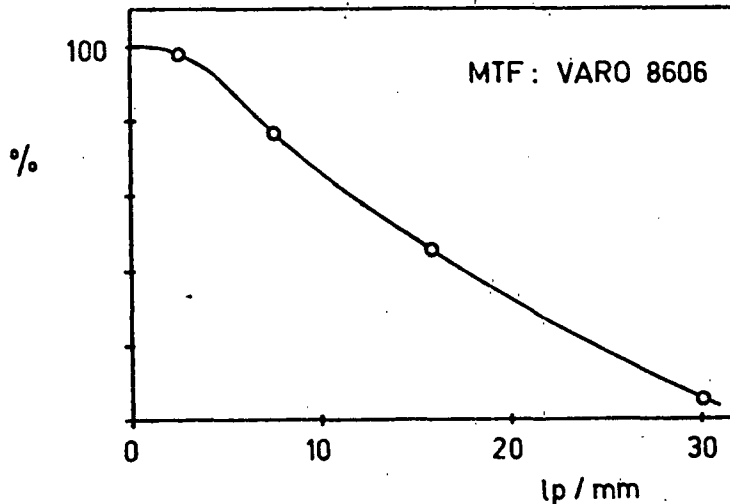


Fig. (3.1) Modulation Transfer Function of Image Tube.

The electrostatically focussed assembly is compact, light and easily mounted in an optical train. Both input and output plates are field flattening fibre optics whose small fibre diameter is 5 microns and mean separation is 6 microns. The hexagonal array of fibre ends is clearly visible on the screen by direct viewing with a microscope. Theoretically, only if image detail greater than 100 line pairs/mm is necessary could this become a limitation. Even though transparent phosphor screens can be produced by evaporation techniques some scattering still occurs and becomes a practical limitation (Eberhardt and Mertel 8).

The nominal input requirements are 2800 volts peak to peak at 1500 Hz and maximum illumination of approximately 10 mlx after which an automatic brightness control becomes effective to limit the gain. At this point screen luminance has a respectable value of over 200 cd/m . When a photocathode illuminance of 10 lux is reached there is no output and damage is likely. The latter effect was not tested (!). The automatic brightness control (ABC) is of little significance to this project as it operates on the averaged illumination over the entire

photocathode and astronomy tends to be concerned with imaging in discrete points. However it does raise the question of photocathode burn-in due to high intensities within images of bright stars. Calculation suggests a star magnitude limit of four be imposed and this is experimentally supported by brief exposures causing an image persistence of several minutes. Protection is afforded by the addition of an objective diaphragm whose extinction is equivalent to $\Delta m_V = 6$, so that the stellar brightness threshold for damage becomes $m_V = -2^m$.

Intensifier Magnification and Distortion

Although nominally unity the magnification is a function of the linear field radius i.e. significant distortion exists. This is immediately evident when a millimetre graticule is pressed to the faceplate as in Figure (3.2a). For comparative scaling the output screen has an eight division reference scale permanently inscribed at 1.25mm per division. The axial magnification is simply calculated at $m_2 = 0.82$. Figure (3.2b) shows a similar result when a 10 lines/mm grating is positioned on the faceplate and the output screen is photographed directly rather than imaging with the television system.

The variation in magnification from field centre to 10mm radius is $m_2 = 0.82$ to 1.01 and hence the percentage distortion (pincushion) is

$$\left(\frac{m_{21}}{m_{22}} - 1 \right) 100 = 23\%$$

for the three stage assembly. While this does appear large it will become apparent later that with optimum choice of variables for the entire

system the area of intensifier tube to be utilized is equal to the quality rectangle on the T.V. target whose radius is about half of the above.

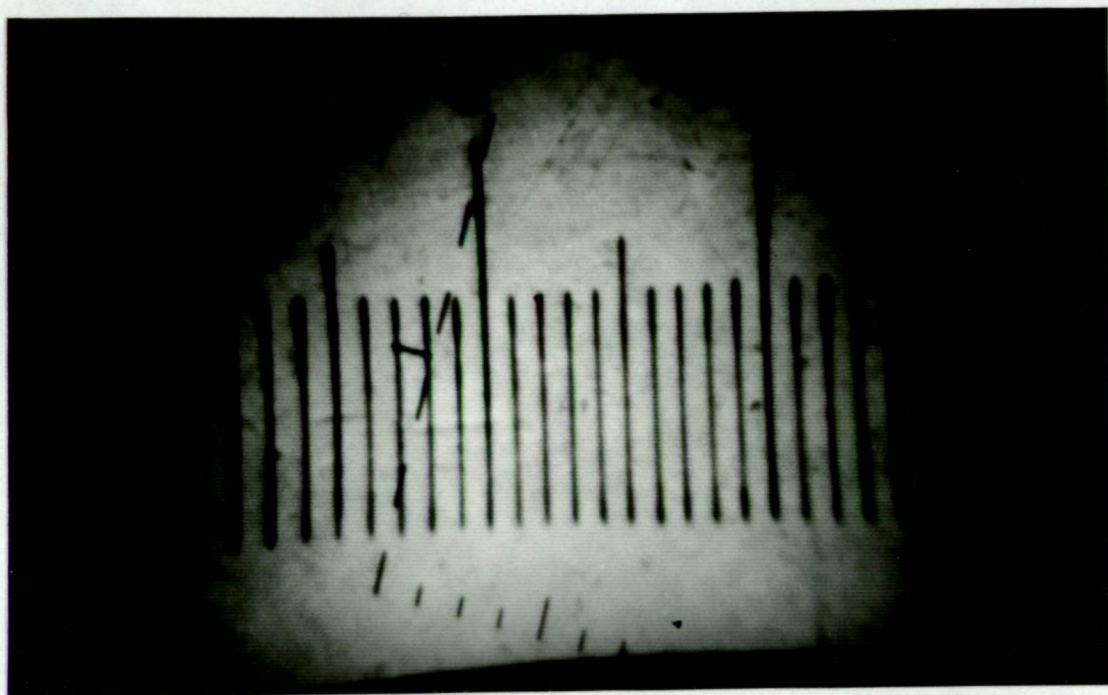


Figure (3.2a) Image intensifier magnification and distortion tests. The image of the millimetre scale may be compared with the 8 division reference scale (1.25 mm/div.) on the phosphor screen.
Axial $m_2 = 0.82$

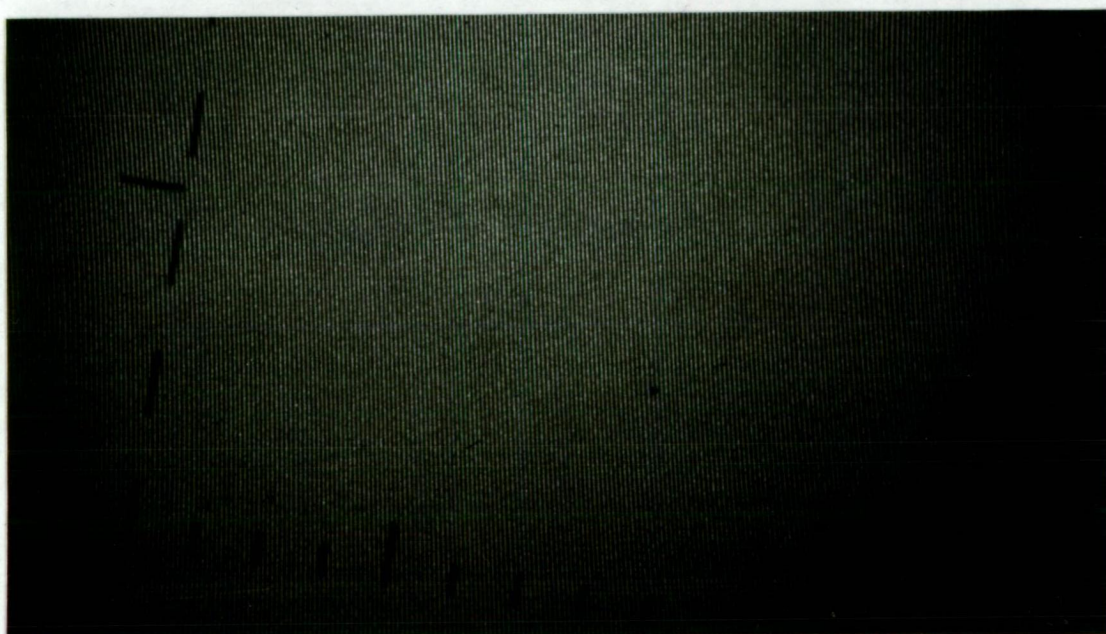


Figure (3.2b) The object is a 10 lp/mm grating and the image obtained by direct photography.

Projected Investigations

A number of leading experimental questions relate to intensifier operation:

- (a) How does the phosphor output screen brightness vary as a function of the applied voltage for a constant input? Can the gain be usefully increased?
- (b) What is the equivalent background input (EBI) as a function of voltage?
- (c) How does this compare with sky background noise?
- (d) How significant is the ever present random ion shot noise?
- (e) It is realistic to entertain the idea of a fourth stage of intensification?
If so what signal to noise ratio?
- (f) What is the resolution of the combined II + transfer + T.V. system?
- (g) The output image appears on a phosphor screen whose luminous emittance is Lambertian. How should this affect the image transfer to the T.V. Target?

As these are to be investigated in conjunction with the T.V. camera the parameters of this segment will be discussed first.

TELEVISION SYSTEM

Camera Characteristics

The television tube target is the second photocathode in the chain and since it will be shown that noise is not a prime limitation in either image tube or camera, maximizing sensitivity is a first priority.

A second requirement will be that picture elements must match those of the intensifier phosphor. Some juggling in terms of scale is possible with the image transfer system but generally the resolution of television tubes in terms of line pairs/mm is equal if not slightly better than that of three stage intensifiers.

The third question of tube window diameter rises rapidly with budget in importance. Traditional tube diameters have ranged from small (25mm) to large ($\geq 75\text{mm}$). The broadcasting industry has standardised on the former so that 25mm tube costs have been pushed "down to only" \$4,000 - \$8,000 per camera. Another group of cameras has been largely ignored for precision work. It is the 17mm diameter miniature vidicon that originated for low grade surveillance work but is now able to compete with big brother.

Advantages of 17mm tubes (6.6 x 8.8mm window)

- (a) The trend in TV camera development seems to be towards miniaturisation so that resolution of 17mm tubes are now much the same as 25mm tubes of a few years ago.

- (b) Any lenses required can have correspondingly smaller apertures and hence are also at much reduced cost.
- (c) Almost all photocathode surface on 25mm tubes can now be obtained in the 17mm range so that low light level sensitivity is available.
- (d) The whole star acquisition system in which it is to be used can be scaled physically smaller and lighter.
- (e) They are cheaper in cost by a factor of 5 to 10.

Target Characteristics

The array of tubes that now present themselves for consideration

include:

- Lead oxide vidicon - Plumbicon, Leddicon, Vistacon
- Silicon vidicon
- Standard vidicon
- Newvicon
- Chalnicon
- Saticon

It is not the intention to give an exhaustive analysis of each tube but to examine those characteristics relevant to making an appropriate choice of one for this project. Since the lead oxide and saticon tubes have very low lag and low dark current they are suitable for broadcast quality colour work and attract a premium price while still not being particularly sensitive. The standard antimony trisulphide vidicon has been a work horse for 25 years, is very cheap and easy to run but now seems to be the historic standard by which all new tubes are compared. The silicon diode array vidicon is exceptional in its sensitivity. Because its spectral response extends far into the infra

red it has application for surveillance purposes. However this characteristic makes its high sensitivity misleading for this project as the camera will only be looking at a green P20 phosphor of the image tube. Tube spectral response and transfer characteristics shown in Fig. (4.1) are mostly from Philips internal papers marked "not for publication" (1976). See also refs. 9, 10, 11.

The chalnicon and newvicon were innovations introduced in 1972 and 1974 with increases in both quantum efficiency and spectral response. The newvicon is rather distinct from the others in that it exhibits a quantum efficiency greater than unity, i.e. an incident photon produces more than one pair of charge carriers. Consequently it has the highest sensitivity of any of the commercially available photoconductive tubes, this being twenty times that of a standard vidicon and double that of a silicon vidicon. Another exceptional feature appropriate to astronomy is the newvicon's ability to withstand high overloads. It shows virtually no blooming as star photographs in this thesis indicate. In other factors such as beam discharge lag the newvicon is not as good as in the colour tubes but then, there is no intention of detecting rapidly moving stellar objects. Hence it appears that a newvicon tube is the clear leader for a star acquisition and guidance system.

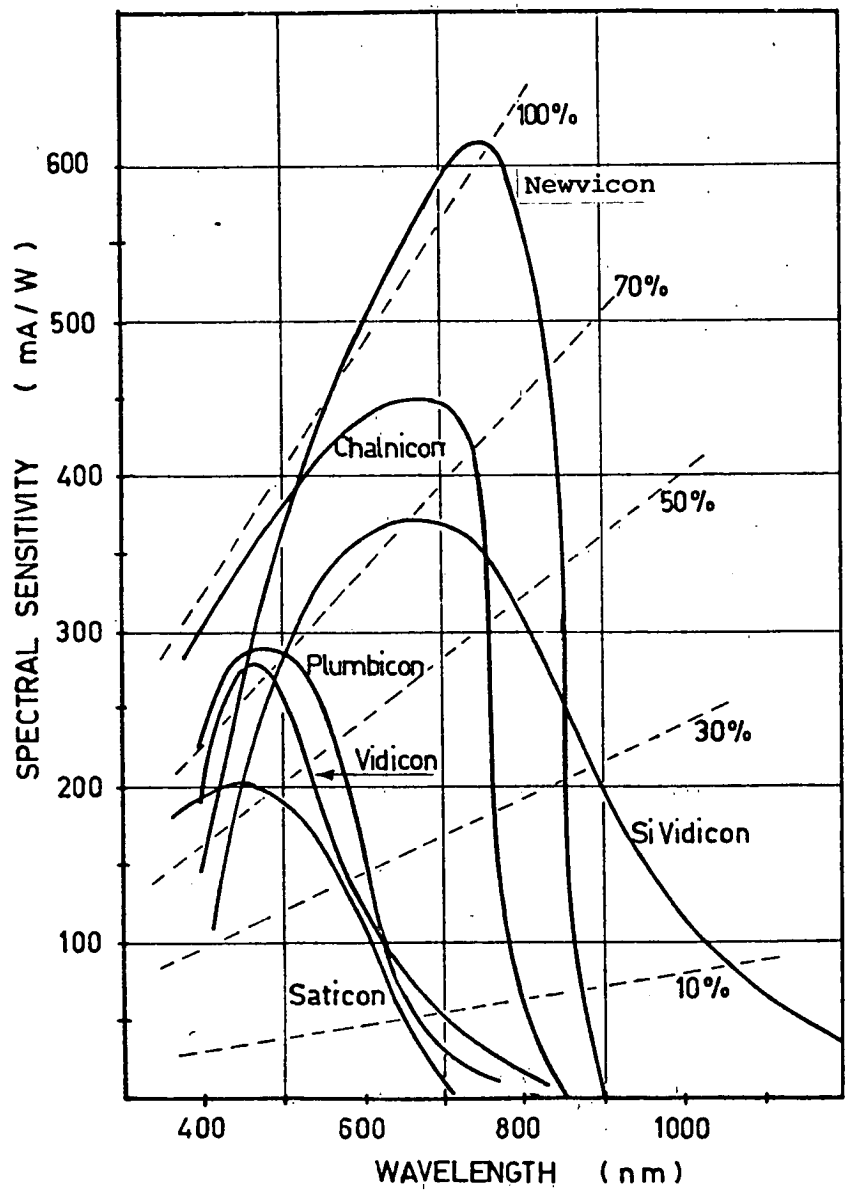


Fig. (4.1a) Spectral response of photoconductive camera tubes.

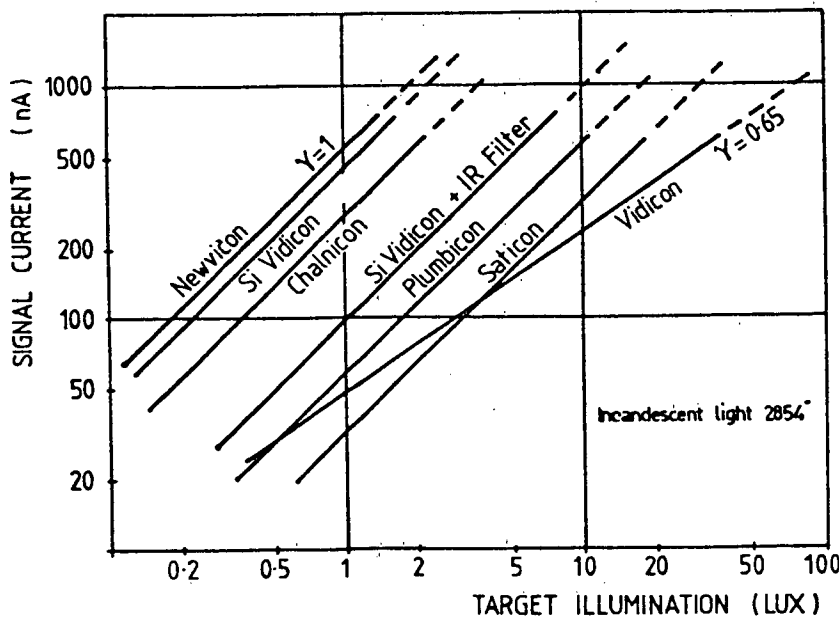


Fig. (4.1b) Transfer characteristic of photoconductive tubes.

Camera Field Tests

It was possible to borrow for testing with the option to purchase a Si diode array Vidicon and a Newvicon camera. Some of their nominal specifications are set out in Table 4.1.

Table 4.1

	VCS-3000 Silicon diode array	WV - 1350 Newvicon
Horizontal resolution	400 lines at centre 350 lines at corners	400 lines at 0.3 lux 500 lines at 0.6 lux
S/N ratio	43 dB	43 dB
Sensitivity	1 lux	0.3 lux

Both cameras were tested for point source imaging in the laboratory with artificial sources as well as on actual star fields. Since the lens aperture determines the flux and the target sensitivity is specified, the temptation is to expect to decrease the image point area, thereby increasing the illuminance (lux) and hence improve the detection of fainter stars. As this is not in fact fruitful what then determines the limiting point sensitivity?

Certainly a very fine point charge may develop on the target. However as Cope, Gray and Hutter (Ref. 12) point out the electron beam reads electrical potential rather than electric charge. Therefore a larger optical point spread function that leaves the target potential distribution unchanged will read the same as a small spread function, and if the bandwidth is sufficient will appear the same size on the TV monitor screen.

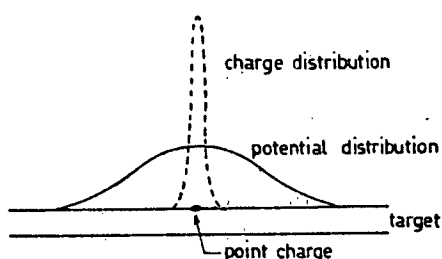


Fig. (4.2) Scan beam senses potential distribution.

This is ^{the} inherent limitation of the tube and lens resolution need not be finer than this. Other limitations of course are the preamplifier and monitor bandwidth and phosphor resolution.

Laboratory tests included the imaging down of fine pinhole objects (10-60 microns) with a range of magnification onto the target. At no stage for either camera could the T.V. image be reduced to less than $2\frac{1}{2}$ TV lines yielding a resolution of 251 line pairs per picture height or 502 TV points/pic. ht.

The insertion of neutral density filters facilitated the simulation of a star magnitude range and the effects for a constant diameter (small hole) source were very clear. Fig. (4.3) shows the image intensity profile as the object increases brightness (a to f).

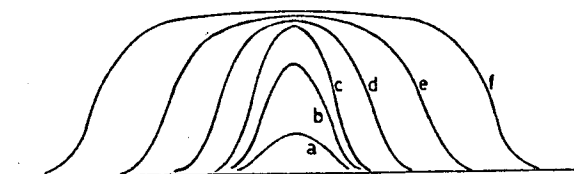


Fig. (4.3) Intensity profiles of images as function of increasing source brightness.

It was here that silicon diode camera showed wide divergence from the newvicon. Very rapidly "point" images spread to 30 times their low height level diameters for the Si tube. The newvicon on the other hand showed remarkable resistance to this "blooming" effect and even on real star field tests bright images did not increase by a factor of more than two.

That resolution is a function of illumination is demonstrated by imaging a standard Retma resolution chart at 15 and 3 lux respectively in Fig. (4.4a & b). Using the formula derived in appendix II the corresponding target illumination for the 50mm Ultron F1.8 lens is 0.6 and 0.12 lux respectively. It is apparent that the resolution falls from 450 to 360 TV points.

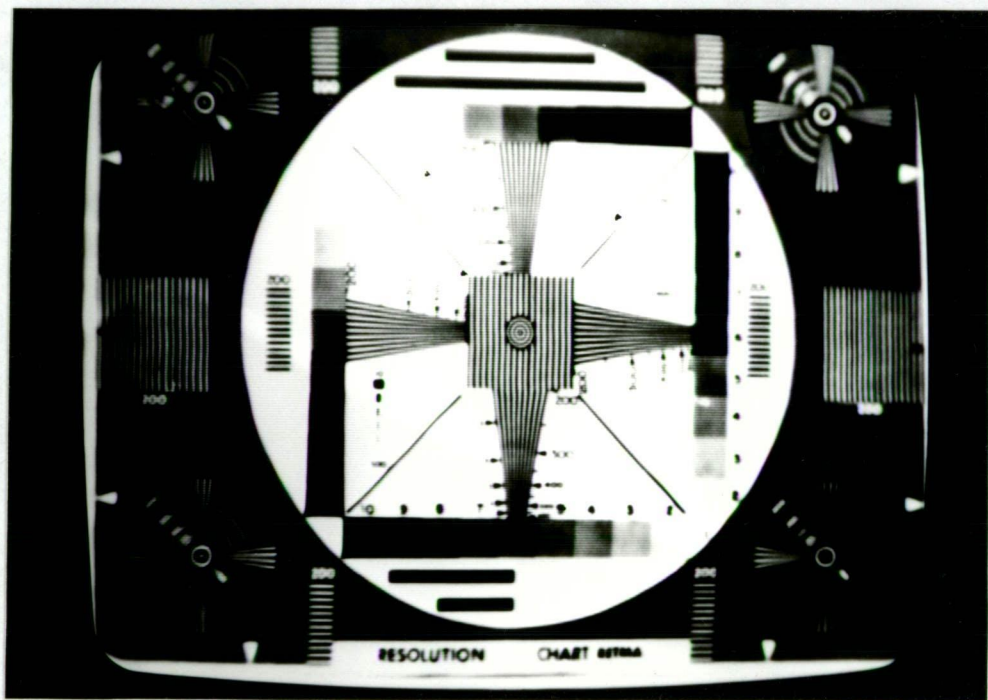


Fig. (4.4a) Retma chart resolution test.
Chart illumination 15 lux.

For sensitivity comparisons a range of at least 20 southern stars were imaged with the cameras. Lenses used were 25mm F1.4, 50mm F1.8, and 135mm F2.8. The different F number lenses could be compared by calculating relative aperture areas.

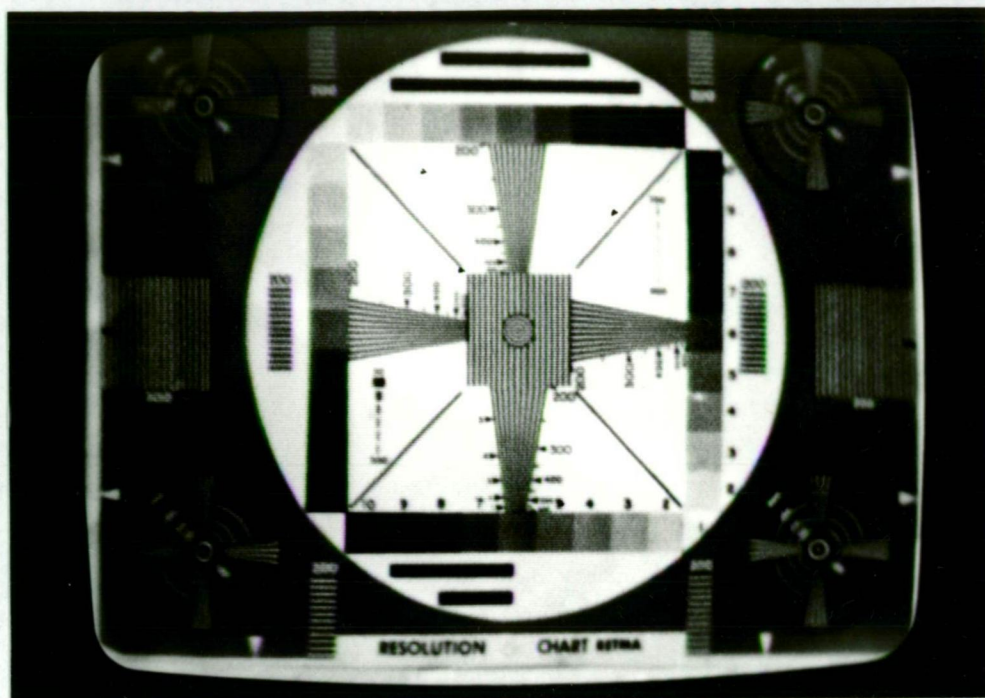


Fig. (4.4b) Retma chart resolution tests.
Chart illumination 3 lux.

The limiting sensitivities for each camera related to the 50mm F1.8 lens are:

VCS-3000 Si diode 3.7 ± 0.2

WV-1350 newvicon 4.3 ± 0.2

Although the newvicon performance appears to have only a marginal improvement here over the silicon it should be noted that the silicon also responded to infra-red which will certainly not be present when imaging P20 phosphors. The dynamic range that could be handled was simply ascertained by addition of neutral density filters to peak white star images. It was at least 10 : 1 for each camera.

Of all the TV tubes considered above the newvicon therefore emerges as a very clear choice and that with a cost factor less than all the others. It is of general interest to note that the National Newvicon WV-1350 camera obtained was in fact the first model to arrive in Australia.

IMAGE TRANSFER SYSTEM

After three stages of intensification the star field image appears on the final phosphor screen for coupling to the TV photocathode. The use of a fast lens or mirror system to transfer the output to a tube is obvious; however, the requirements on the optical system are severe. Not only is it necessary that the optical system have a high numerical aperture so that a large fraction of the photons emitted by the phosphor can be collected, but the resolution requirements are high for large field angles. The use of a fibre optic cylinder allows a very efficient transfer of photon flux at excellent resolution. In this instance however the existing image intensifier fibre optic output screen is covered by a plane glass window as a high voltage shield and is not removable according to the manufacturer. In any case fibre optic target face plates in the 17mm diameter television tube range were not yet very plentiful. These restrictions therefore demand a return to the lens system.

PHOTON FLUX COLLECTION EFFICIENCY

To maximise light transfer and thereby increase limiting sensitivity it is necessary to make a comparison of efficiencies and characteristics of the transfer system with respect to conjugate ratio, F number, resolution, and the lens availability. Once the optimum parameters have been established the specifications of the field selector system can be determined. The chief inherent problem of phosphor imaging is the very wide radiation distribution. Minor questions concern the spectral emittance of the P20 phosphor and ^{the} Gaussian spread function of a point image.

To a good approximation the intensity pattern is Lambertian, i.e.

$I = I_0 \cos\theta$ where I_0 is the luminous intensity directed normally (e.g. see Levi 13). In appendix IV it is shown that the fraction of the light flux emitted by a star image on a phosphor into the cone of half angle θ subtended by a lens is,

$$E = \sin^2\theta$$

so that E becomes an efficiency factor of light flux collection by the transfer lens.

LENS PAIRING

At the outset it is therefore clear that low F number lenses will be required and that budget and time restrictions dictate that these shall be available commercially. The photographic industry provides a ready supply of some well designed lenses (and some others!) albeit largely intended for infinite conjugates. This can be turned to advantage by placing a pair of lenses in juxtaposition front to front.

The benefits are:-

- (a) Aberrations have been minimised since each lens is used at optimum position.
- (b) The system is compact.
- (c) The scale of the output image is readily altered by exchanging the second lens.
- (d) The system is largely insensitive to the spacing between the lenses, i.e. the position of the TV camera.
- (e) For testing purposes, the intensifier screen can be conveniently photographed by aiming a still camera directly through the front (collection) lens.

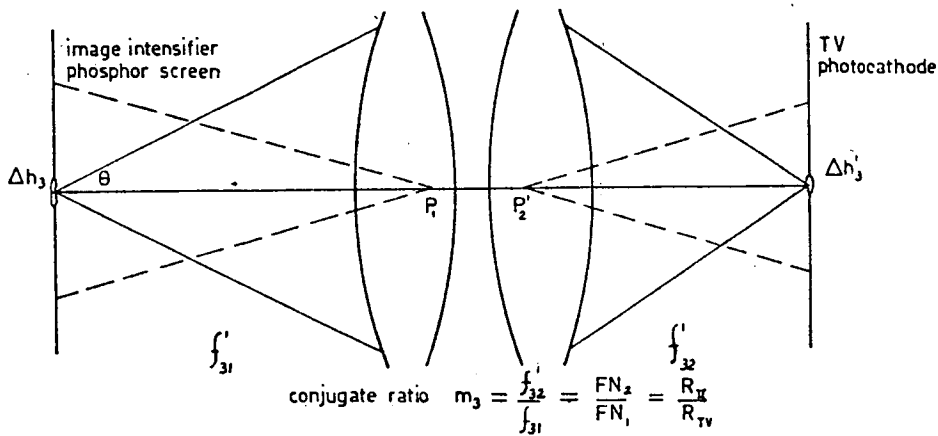


Fig. (5.1) Image transfer from intensifier screen to TV photocathode.

With the notation in the Fig. (5.1) the F number of the leading or collection lens is

$$\begin{aligned} FN_1 &= f'_{31}/2a \\ &= \frac{1}{2 \tan \theta} \end{aligned}$$

so that for axial object points the light fraction collected becomes

$$\begin{aligned} E &= \sin^2 \theta \\ &= \sin^2 \left(\arctan \frac{1}{2FN_1} \right) \end{aligned}$$

Provided that no significant degrading of resolution occurs by the lens pair, this fraction is transferred and concentrated into a small area dA' on the TV photocathode depending on the magnification.

$$\text{Now } m_3 = \frac{f'_{32}}{f'_{31}} = \frac{FN_2}{FN_1}$$

Therefore the ratio of the star disc flux densities, TV image to II object is,

$$\begin{aligned}
 F &= T_t \frac{E}{m_3^2} \\
 &= T_t \left(\frac{f'_{31}}{f'_{32}} \right)^2 \sin^2 \left(\arctan \frac{1}{2FN_1} \right) \\
 &= \frac{T_t}{m_3^2} \sin^2 \left(\arctan \frac{1}{2FN_1} \right) \quad \dots\dots (5.1)
 \end{aligned}$$

where T_t is the transmittance of the lens pair.

Legitimately it may well be said that T_t is a function of θ and therefore of FN . However the Fresnel reflection coefficient remains almost constant for both polarisations up to the Brewster angle, so that T_t is virtually constant for $FN > 0.4$. It is thus possible to choose values for the parameters FN_1 and m_3 independently within certain limits.

Fig. (5.2) demonstrates the relative brightness of the image attainable for a range of leading lens F numbers and magnifications.

It is seen that for brightest images the lowest values for FN_1 and m_3 reasonable should be chosen. Examples of efficiencies for F1 and F1.4 lenses are 20% and 11% respectively.

The lower limit on m_3 is determined by the restrictions,

- (a) that the resulting image disc diameter $\Delta h'_3$ must not be less than a television target pixel ΔQ . Imaging down further does not increase either sensitivity or resolution.
- (b) the lower limit on FN_2 . Since $m_3 = \frac{FN_2}{FN_1}$ a small FN_1 with a low m_3 requires an even lower FN_2 , probably much less than one.

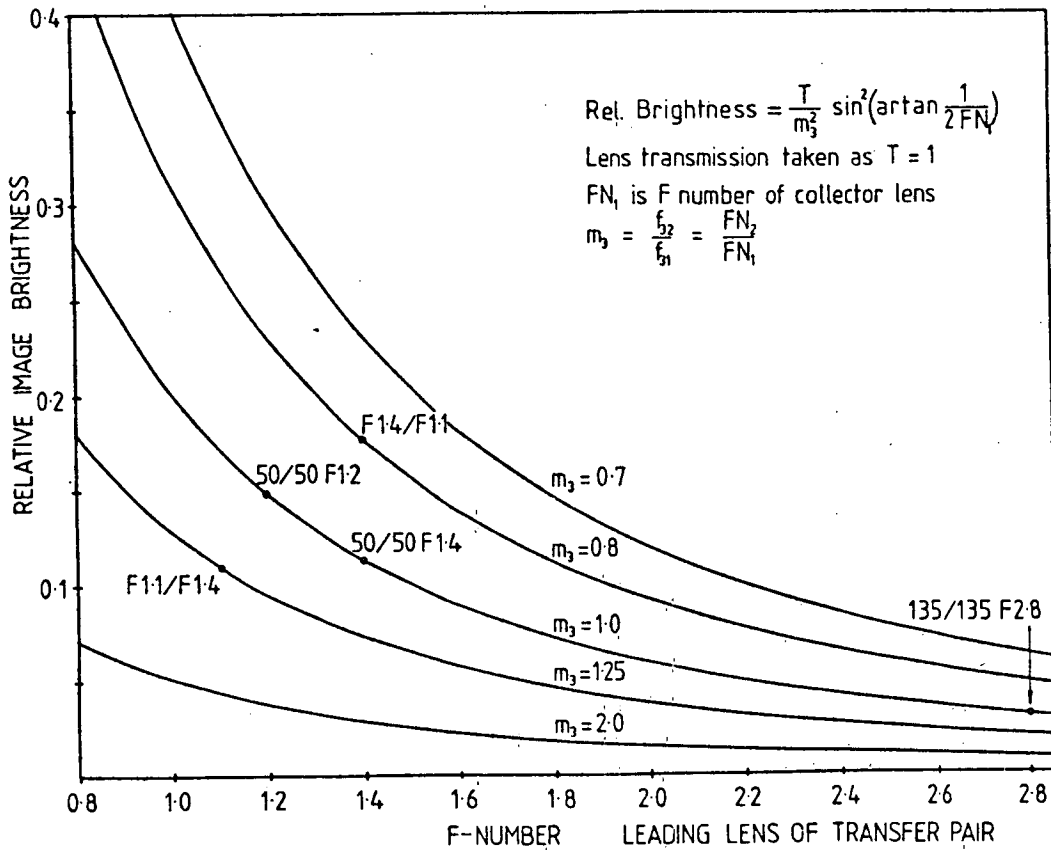


Fig. (5.2) Relative brightness image to object discs as function of FN and m_3 .

If R_{TV} and R_{II} are the resolutions of the TV target and intensifier screen, in line pairs per millimetre, then

$$\Delta h_3' = \frac{m_3}{R_{II}} \quad \text{and} \quad \Delta Q = \frac{1}{R_{TV}}$$

so that the condition of (a) above becomes

$$m_3 \leq \frac{R_{II}}{R_{TV}} \quad \dots\dots\dots (5.2)$$

and a typical value from experimental analysis may be $m_3 \leq 29/36 = 0.81$.

Strictly speaking R_{II} is the resolution of information on the II screen as a result of all preceding segments in the system including atmospheric seeing.

Combining equations (5.1) and (5.2) with (8.1) a relationship is obtained giving the expected limiting magnitude of stars detectable as a function of m_3 , FN_1 , R_{II} and R_{TV} .

$$\begin{aligned} m_V &= 5 \log D - 2.5 \log S - 2.5 \log \frac{\pi \left(\frac{m_3}{R_{II}} \right)^2}{4} + \\ &\quad 2.5 \log \sin^2 \left(\arctan \frac{1}{2FN} \right) - 2.62 \\ &= 9.63 - 5 \log \frac{m_3}{R_{II}} + 5 \log \sin \arctan \frac{1}{2FN} \end{aligned}$$

Families of curves are graphed in Fig. (5.3) with typically possible values for m_3 and FN_1 , and values for R_{II} as experimentally determined and listed in Table 5.1

Table 5.1 Limitation by atmospheric seeing on R_{II} .

Field	3½'	9'
19.3 lp/mm	1".2	3".2
11.9	2".0	
8.0	3".0	

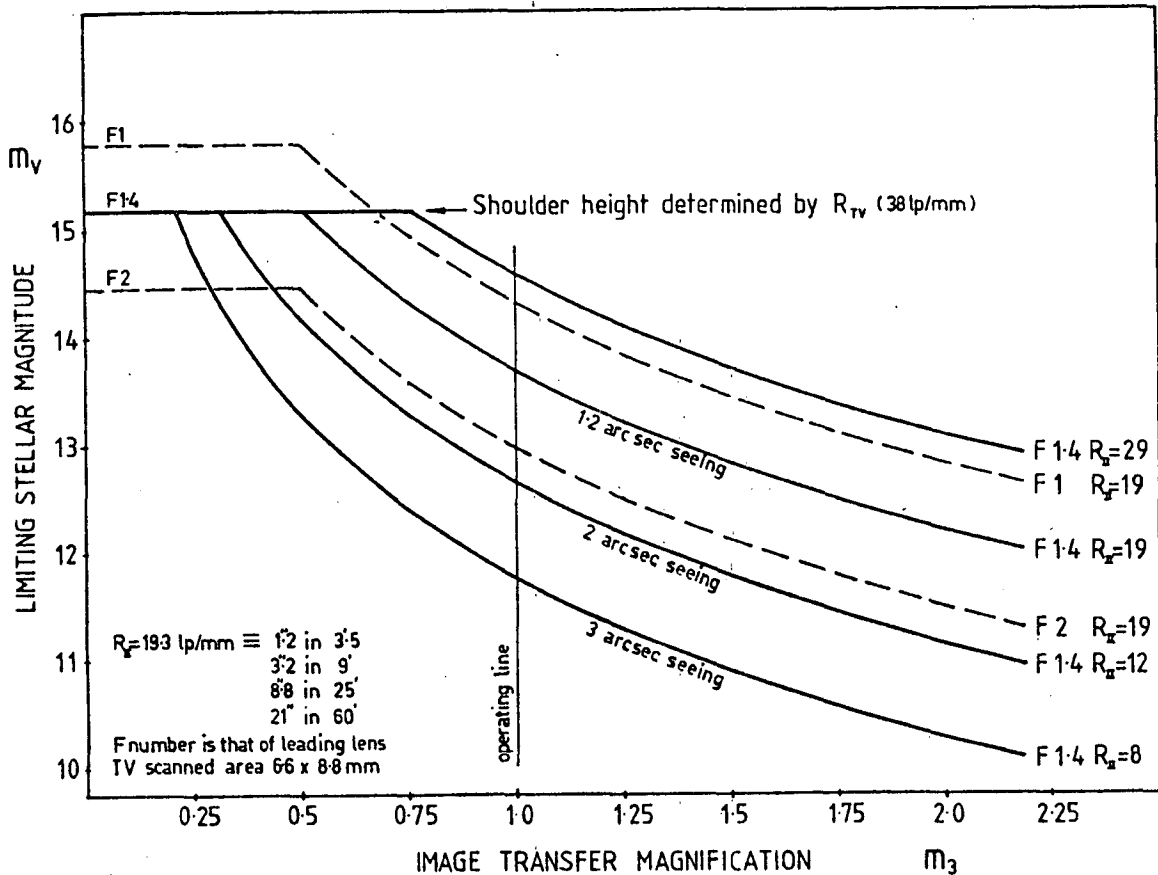


Fig. (5.3) Limiting m_v detectable as function of m_3 , FN and R_{II} .

SELECTION OF OPERATING POINT

For each F number a family of curves sweeps up to a shoulder representing the highest stellar magnitude detectable. Decreasing the magnification to the left of the shoulder reduces the best resolution attainable. Taking a particular magnification, as the seeing deteriorates the operating point falls vertically to lower magnitudes due to image spread. Hence for good resolution and maintenance of high sensitivity it is evident that parameters need to be sought in the neighbourhood of and to the right of the shoulder.

A suitable compromise appears to be $m_3 = 1$ since then $FN_1 = FN_2$ and only budget considerations dictate the trade off between limiting magnitude and F number. $14^m.3$ can be reached with F1 lenses while $13^m.7$ is obtained with F1.4.

It should be pointed out that most camera tubes tend to have similar resolutions and this is therefore not treated as a variable beyond that discussed in the section on TV cameras. On the graph a better TV resolution lifts the shoulder up marginally.

FIELD TEST

The prototype acquisition system was employed to test the effect of altering m_3 and leaving all other variables unchanged. For Fig. (5.4) and Fig. (5.5) the transfer system was changed from a 135/135mm F2.8 to 125/50mm F4 so that magnification decreased from $m_3 = 1$ to $m_3 = 0.37$. Even though the star images appear finer in Fig. (5.5) the resolution has in fact decreased in angular terms while the sensitivity, as it appears on the photographs is similar. As the curves indicate one additional stop should make an increase in sensitivity of $0^m.75$. However this is not practicable as the second lens would have to operate at F1.



Fig. (5.4) Image transfer system evaluation $m_3 = 1$.
100mm F15 objective.
NGC 6752 Scale: 1 arc min/10mm



Fig. (5.5) Image transfer system evaluation.
 $m_3 = 0.37$ 100mm F15 objective.
NGC 6752 Scale: 2.6 arc min/10mm

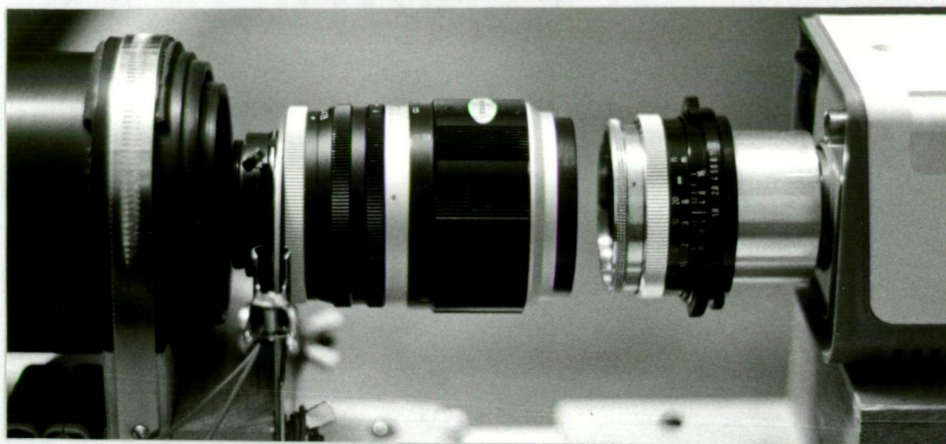


Fig. (5.6) Prototype image transfer system $m_3 = 0.37$
Lenses are 135mm and 50mm focal lengths.
Gap between lenses is not critical.

VIGNETTING AND FOCAL LENGTHS

Thus far the general behaviour of the transfer lens system has been established and specifications that $m_3 = 1$ and that F number be F1 to F1.4. The focal length is yet a free parameter. Putting $m_3 = 1$ fixes the linear scale of the object on the II screen to that of the quality rectangle of the TV tube, and as illustrated in Fig. (5.7), for off axis points the chief ray has least inclination for longest focal lengths. It is this inclination that can cause significant vignetting when a fraction of skew rays miss the entrance pupil of the second lens. This is calculated in detail for the particular lenses used in appendix III. 50 to 100mm focal lengths are to be preferred over 25mm. However at low F numbers the linear apertures of 100mm lenses are prohibitively costly, thus leaving 50mm as the final choice for focal length. With off axis points at 4.4mm the steepest rays enter the system at 5.0. Since photographic lenses normally cater for far wider fields the aberrations will be negligible.

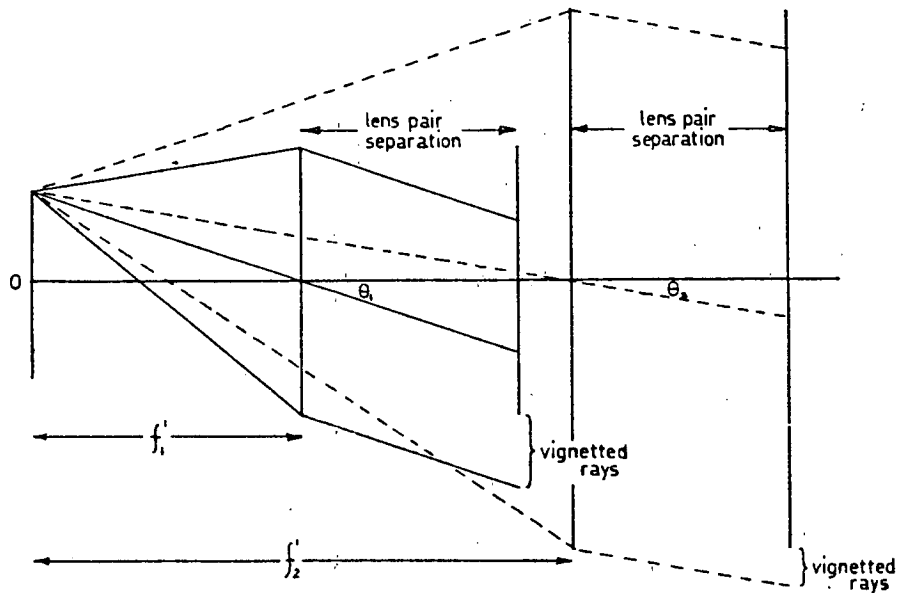


Fig. (5.7) Comparative vignetting for F1 lenses of different focal length.

The P20 phosphor's spectral emittance centred around the green 520 nm region guarantees achromaticity in the imaging.

Specification of Transfer System - Summary

A pair of lenses to be used mounted front to front.

$$m_3 = 1$$

F-number: between F0.8 and F1.4

Focal Length: preferably 50mm or longer

Centre resolution: greater than 50 lpp mm line pairs per millimetre (must not degrade image in transfer)

Achromatic over P20 phosphor range.

Correspondence with several dozen manufacturers and suppliers of commercial lenses indicate a large range available, e.g. 50mm F0.75 Heligon by Rodenstock intended for X-ray intensifier purposes and Angenieux 25mm F0.95 for cinematography, to 50mm F2 standard 35mm camera lenses. (The corresponding price bracket is \$1000 to \$100 each).

The resolution restriction on the combined lens system rules out the bottom of the range while cost rules out the very low F numbers. A sharp increase in cost occurs for F numbers below F1.4 partly because the mass production benefit no longer applies and partly because aperture and component numbers increase. A pair of 50mm F1.4 MD Rokkor lenses were selected and tested on resolution charts to considerable satisfaction. The results are shown in appendix III. It was thus deemed to be an optimised image transfer system.

Chapter 6.

COMBINED ELECTRONIC SYSTEM PERFORMANCE

Thus far have been considered separately the intensifier, the image transfer system, and the television system although each segment was evaluated with the subsequent in mind. At this stage the combined system needs to be assessed with respect to:

- (a) Resolution
- (b) TV Light transfer characteristics
- (c) Optimisation of gain

RESOLUTION

A large range of gratings or resolution graticules not being available a fixed 20 line pair/mm was pressed to the intensifier face-plate and a variable magnification provided at the image transfer stage. The permanent Rokkor lens pair were replaced temporarily by 135mm fixed focus and 17-70mm zoom system so that minification over a considerable range was possible. With a 31 lp/mm limiting resolution for the intensifier already demonstrated the lens pair was not expected to impose a significant limiting factor. Photographs were taken of the monitor screen as the zoom focal length was progressively varied. Fig. (6.1) was taken to be the situation near a limiting resolution of 36 line pairs per mm on the TV photocathode. The scale can be determined by comparing the horizontal television scan lines that are clearly visible.

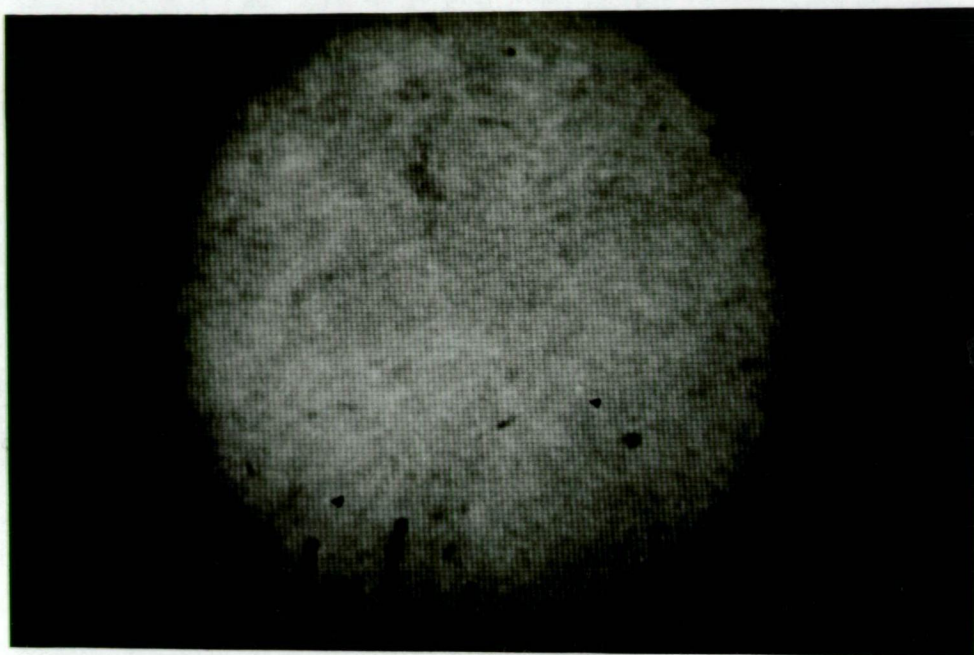


Fig. (6.1) Limiting resolution test (II + transfer + T.V.)
Horizontal lines = TV scan lines
Vertical Lines = Image of test grating
 (Mark space ratio 1:1).

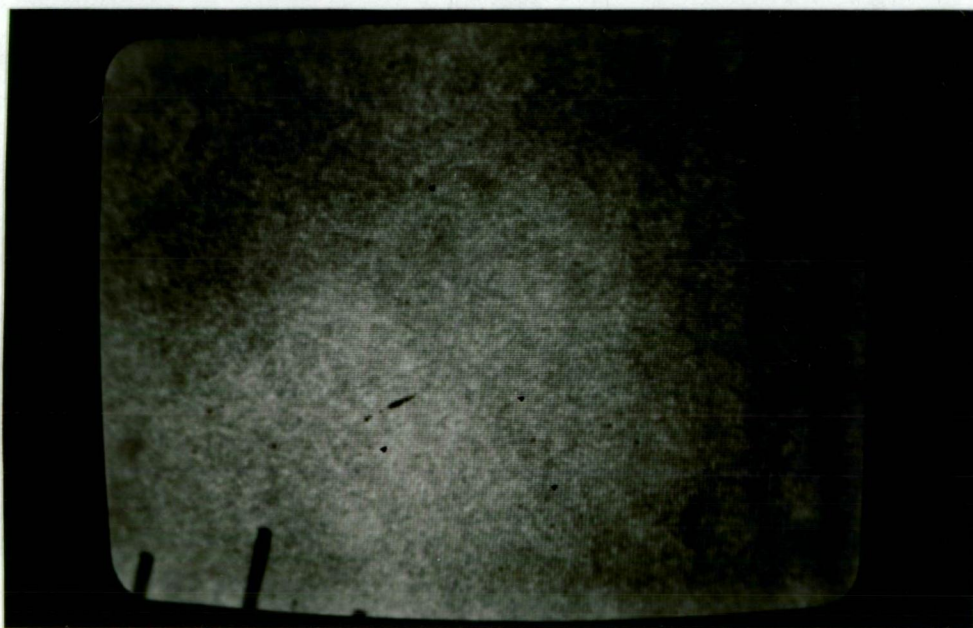


Fig.(6.1b)

TV OPTICAL TRANSFER CHARACTERISTIC

As final component in the optoelectronic chain the television camera must be capable of displaying a large range of image disc intensities preferably at good contrast on the monitor screen in front of the astronomer.

The response of the newvicon tube in terms of resolution and highlight overloads (blooming) has already been discussed and its quoted low light level sensitivity of 0.3 lux was a key factor in its favour. It is now necessary to seek the empirical characteristic between incident luminous flux on the camera target and luminous excitation of the picture tube. This can then be related to F number of the image transfer lens pair, and further, to the gain of the intensifier by control of voltage input. In the process an important question that must be answered is : how worthwhile is it to design a transfer lens system of very low F number?

GAMMA OF CAMERA PICTURE TUBE COMBINATION

As for sensitometric curves of photographic emulsions, photo electronic systems also have gamma characteristics and when two systems such as a camera and picture tube are cascaded the experimental value will be a combined effect.

For a picture tube the output brightness, B is given by the equation (see e.g. Carnt and Townsend 14 and Grob 15)

$$B = k_1 V^{\gamma_1}$$

where V is the signal voltage
and $\gamma_1 = 2.0 - 3.5$

Gamma is therefore seen to be the slope on a log graph. Similarly the output signal characteristic for a TV camera is -

$$V = \kappa_2 L \gamma_2$$

where L is the illumination on the target
and normally $\gamma_2 \leq 1$

A combined system therefore yields the luminance

$$\begin{aligned} B &= \kappa_1 (\kappa_2 L \gamma_2) \gamma_1 \\ &= \kappa_3 L \gamma_1 \gamma_2 \end{aligned}$$

In broadcast applications where realistic rendering is required $\gamma_1 \gamma_2$ is arranged equal to unity by appropriate gamma correction circuits. This project requires high contrast and high $\gamma_1 \gamma_2$ is desired.

Since a complete prototype system was first constructed a very simple technique was possible to control TV target illumination. A pair of off-the-shelf good quality 135mm telephoto lenses constituted the transfer system so that the half click stops of the aperture control of one lens produced 50% incremental steps of light flux transfer. The aperture area and hence the illumination L is then simply proportional $(1/FN)^2$.

The light source is provided by the output of the phosphor screen of the intensifier with a 6.8 millilux input source on the faceplate.

For all tests requiring a constant illumination an extended area disc containing phosphorescent tritium was used reduced in intensity by the insertion of suitable neutral density filters, generally ND3 or ND4.

The screen brightness, B was measured with a Gossen UVA luxmeter whose 90mm diameter selenium photosensitive element was pressed directly to the TV surface as shown in Fig. (6.2)

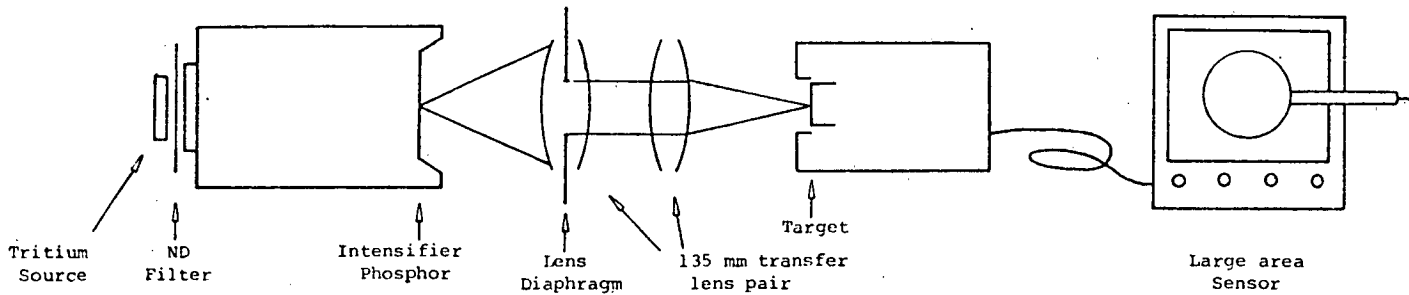


Fig. (6.2) Arrangement to determine TV Optical Transfer characteristic
The lens diaphragm controls flux input to TV target.

Graphing log screen brightness against log aperture area gives a mostly linear TV optical transfer characteristic and the value for gamma. See Fig. (6.3).

The equation is,

$$\log B = 2.57 \log L + 4.35$$

$$\text{or} \quad B = 2.24 \times 10^4 L^{2.57} \quad \dots\dots (6.1)$$

$$\begin{aligned} \text{and overall} \quad \gamma &= \gamma_1 \gamma_2 \\ &= 2.57 \end{aligned}$$

All the camera tubes discussed previously except the standard vidicon have $\gamma_1 = 1$ (e.g. ref. 16 and 17) so that for the picture tube $\gamma_2 = 2.57$ which fits well into the range suggested by Carnt and Townsend and Grob.

Inspection of the graph shows departure from linear above $\log B = 1.5$ (30 cd/m^2). This is consistent with repeated measurements, not included here, using different and larger aperture transfer lenses and represents the movement towards the shoulder of the maximum white or saturation of the picture tube phosphor. This will also be evident later when intensifier gain is investigated.

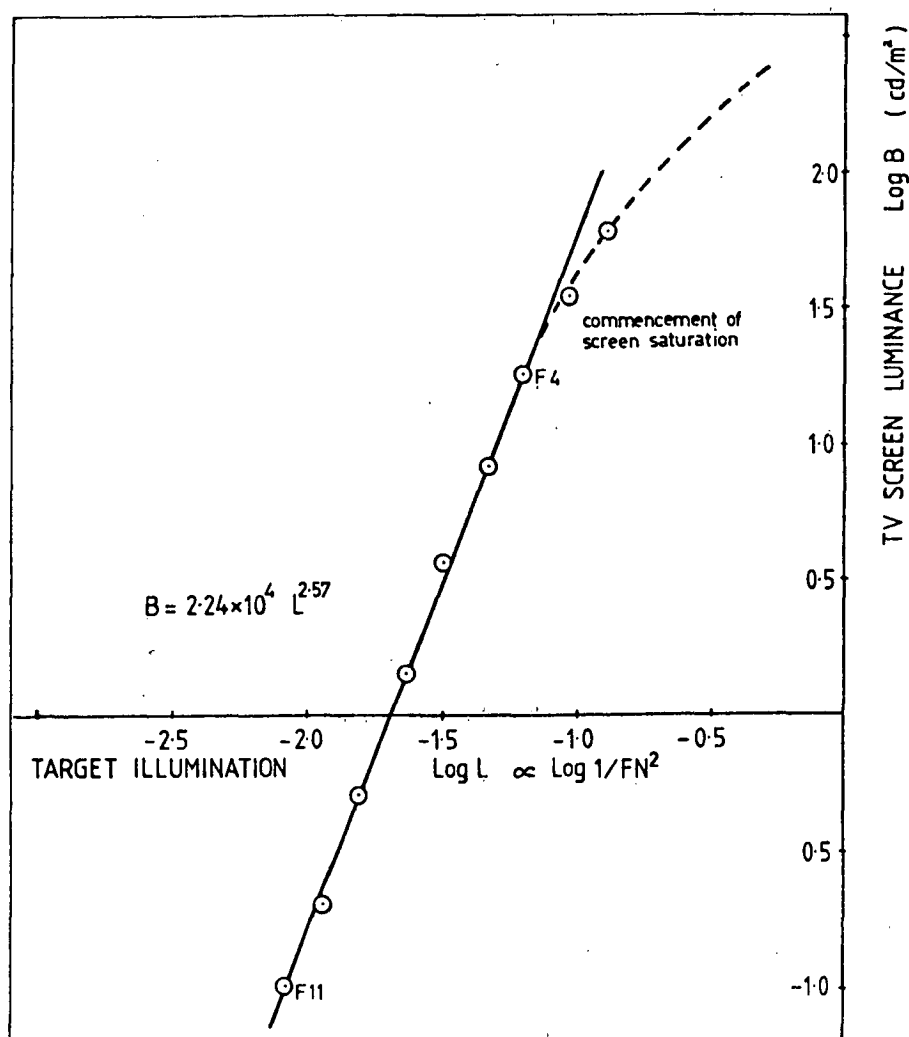


Fig. (6.3) TV Optical Transfer Characteristic.
Screen luminance v. target illumination
Extrapolation is from separate measurements.

Each consecutive point on the graph indicates an increment of a photographic half stop. It is instructive to find the TV screen sensitivity in terms of stellar magnitude per F.N. stop of transfer lens pair.

For $\Delta FN = 1$ stop (factor of 2 in area)

$$\Delta B = 2^{2.57}$$

$$= 5.94$$

$$= 1^m.93$$

This means a lower F number of one stop has a potential for increasing star brightness by $1^m.9$ a highly desirable feature. Just how low an F number should be chosen depends upon,

- (a) when the background becomes visible on the TV screen and this will be a function of magnification or field of view.
- (b) the expense allowed for a tremendous lens.

For wide fields sky background is concentrated on the II photocathode and this can become visible. An investigation was therefore made into background and this is discussed in Chapter 9.

Commercial lenses are available in a vast range of qualities and corresponding costs. The light collection efficiencies and cost benefit analysis of lenses are considered under Image Transfer System.

VARIATION OF INTENSIFIER GAIN

In the desire to squeeze the system for every photon possible, coupled with the need to establish the limitations of the chain components, the question that arises is how does the luminance gain vary as a function of voltage. Can the voltage be increased to advantage and if so to what maximum ratings?

The intensifier can be safely investigated at least up to the nominal 1000 V rms 1500 Hz. It is pointed out that a practical problem existed in that the maximum voltage attainable with a temporary power supply was 890 V and all tests in this project including sensitivity photographs were limited by this factor. Whatever limiting sensitivities have been demonstrated can therefore certainly be expected to increase for the two reasons above and it is these that are to be determined.

For a constant faceplate illumination it is necessary to measure the intensifier screen luminance as a function of applied voltage. Since the transfer lens pair and TV camera were already in situ and of known behaviour (see previous section) this system could readily be used as a photometer with the Gossen luxmeter again as the sensor. The tritium disc source with neutral density ND4 filter provided a constant 0.34 millilux input. It will be shown from equation (9.1) that this is equivalent to the illumination in the image disc of a $11^m.2$ star and is therefore a realistic input.

The resulting rather linear log graph function shown in figure (6.4) has equation,

$$\begin{aligned} \log B &= 7.80 \log V - 21.56 \\ \text{or} \quad B &= 2.74 \times 10^{-22} V^{7.80} \\ &= k_4 V^{7.80} \end{aligned} \quad \dots\dots (6.2)$$

Even a superficial glance makes such a high power law appear very promising.

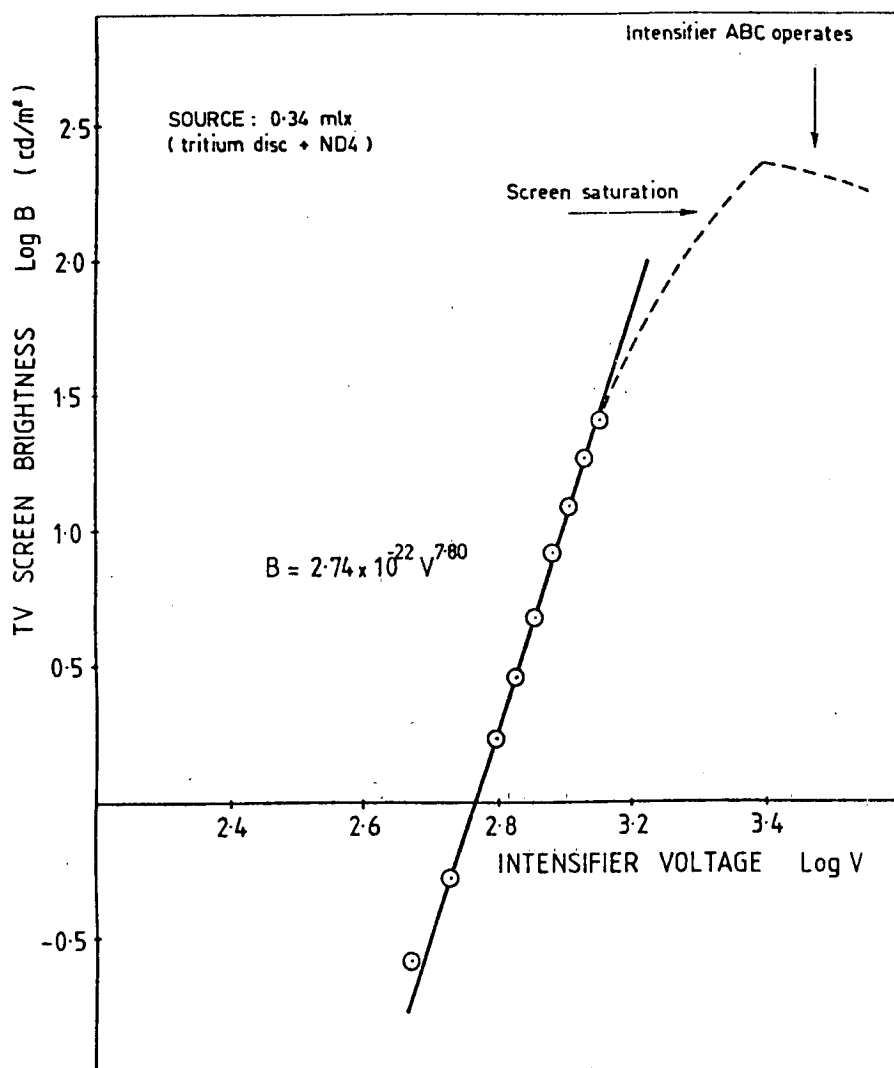


Fig. (6.4) Monitor Luminance as function of intensifier voltage. Extrapolation is from additional experiments.

It is tempting to suppose that an extrapolation of the graph would continue to be linear. However, this is not the case. Repeated experiments with higher faceplate illumination e.g. 3 millilux show a deviation from linear commencing at 35 cd/m^2 ($1.5 \log$ luminance) and this must be attributed to the saturation of the TV phosphor. This is indicated by the dashed line and corresponds to the shoulder of the TV transfer characteristic illustrated in Figure (6.4). Before full saturation is reached however the automatic brightness control (ABC) of the intensifier takes effect sharply at 225 cd/m^2 ($\log B = 2.35$) TV luminance which is equivalent to approximately 560 cd/m^2 on the intensifier screen. The ABC is not of course effective for point sources and highlight whiteness is then limited only by TV saturation or intensifier phosphor damage which has been calculated can occur for 4th magnitude stars.

Intensifier Screen Brightness

The empirical relationship between intensifies output screen brightness and applied voltage is now immediately deduced. From the fact that

$$B = k_4 V^{7.80}$$

and that the TV transfer characteristic is

$$B = k_3 L^{2.57}$$

it is evident that

$L = k V^{3.04}$ (6.3)
------------------	-------------

It is now possible to construct a table of increments in stellar magnitude, Δm that should be visible as a variation of applied voltage as in Table 6.1.

Table 6.1 Incremented limiting magnitudes visible as function of intensifier voltage. 890V was maximum obtainable with existing supply.

	V	$\frac{L}{L_0} = \left(\frac{V}{V_0} \right)^{3.04}$	Δm (stellar mag.)
1200V	135%	2.48	0.99
1100V	124%	1.90	0.70
1000V	113%	1.42	0.38
890V	100%	1.00	0
	90%	0.73	-0.35
	80%	0.51	-0.74
	70%	0.34	-1.18
	60%	0.21	-1.68

It is clear that increasing the supply voltage from the present 890V to the recommended 1000V increases the stellar limiting sensitivity by 0^m.4. Direct correspondence with the manufacturers Varo gave a tolerance of 10% on the voltage. Thus over-running the intensifier at 1100V allows a further gain of 0^m.3 and hence a total advantage over the present situation of 0^m.7.

It should be noted that internal noise is not the prime limitation at present and is further discussed in the section under sky background and noise (Chapter 9.).

Table 6.2 Limiting magnitudes attainable as function of voltage.
 The 60 arc min field is just sky background limited.

Field of View	m_V limit		
	890V (present)	1000V (normal)	1100V (possible)
$3\frac{1}{2}'$	11.3	11.7	12.0
9'	12.3	12.7	13.0
25'	13.0	13.4	13.7
60'	12.6	12.6	12.6

FIELD SELECTOR SYSTEM

At least three fields of view are required for convenient and precise operation of the telescope : One wide for initial field recognition, one intermediate for locating the particular object of interest and a narrow field for accurate guiding on fiducial markers. Consequently at least three selections of magnification must be made available as distributed before and behind the intensifier. The selector takes the image in the focal plane of the objective to reimage this with magnification onto the faceplate of the intensifier. The practicalities of effecting mechanical displacements or rotations by remote control influence the design in no small way. If lenses are to be switched in and out of position very high accuracy in seating or location is necessary. For example, the maximum depth of field acceptable for a F1.4 lens in this project is approximately 15 microns and any longitudinal movement in the transfer system would have to relocate to this accuracy repeatably. Optics in front of the intensifier will have higher F numbers but the stringency in location is more in lateral displacements due to mounting table rotation.

Reversibility of Lenses

Since some interchanges in lenses will have to occur the question arises as to whether this can be done to some extra profit. Moving one lens in and another out is wasteful of optics and therefore costly. A simple solution is to use each lens reversibly, that is, to rotate the lens

through 180° to its conjugate position so that for any magnification its reciprocal $\frac{1}{m}$ is also available. Such magnifications are not necessarily all useful from the view point of sensitivity and resolution. It is possible to imagine a demagnification below the resolution limit of the intensifier faceplate which if magnified up in a later stage has lost information.

DISTRIBUTION OF MAGNIFICATION

Notwithstanding the analysis in the chapter on the transfer system, for the sake of generality, the magnification m_3 is still to be regarded for the moment as a variable. Some possible distributions of magnification for several field selector/transfer systems to achieve the initial specified fields of view are then considered.

(i) SIMPLE FIELD SELECTOR/TRANSFER SYSTEM

By choosing one lens each before and after the intensifier of suitable conjugate ratio and using these reversibly, four fields of view are possible. The total magnifications available will be:

$$m_1 m_3 \qquad m_1/m_3 \qquad m_3/m_1 \qquad 1/m_1 m_3$$

Now if the field ratios are designated $1, r_1, r_2$

$$\text{then } (m_1 m_3)^2 = r_2$$

$$m_1^2 = r_1$$

$$m_3^2 = \frac{r_2}{r_1}$$

For preliminary specified fields 2.5, 20, 60 arc mins the field ratios become 24 : 3 : 1 and the magnifications tabulate as in Table 7.1.

Table 7.1 Theoretical magnifications for specified field ratios

$m_1 = 1.73, \quad m_3 = 2.83$	r	Field
$m_1 m_3 = 4.90$	24	3'.0
$m_3/m_1 = 1.634$	8	9'
$m_1/m_3 = 0.612$	3	24'
$1/m_1 m_3 = 0.204$	1	72'

Four criticisms may be made each of which disallows the choice of the above configuration.

- (a) $m_1 = 1.73$ does not at all use the resolution capability of the objective for any field.
For this to occur $m_1 \geq 4$.
- (b) $m_3 = 2.83$ images up the limited resolution of the intensifier.
- (c) $m_3 = 2.83$ increases the stellar disc area 8 x on TV target with corresponding loss in sensitivity.
- (d) The m_3/m_1 situation represents the classis sin of demagnifying and then magnifying.

Two further combinations of field ratios are tabulated in Tables 7.2 and 7.3.

Table 7.2

	$m_1 = 2.24$	$m_3 = 2.24$	
r_2	25	$m_1 m_3 = 5.0$	3.0'
r_1	5	$m_1/m_3 = 1.0$	15'
1	1	$1/m_1 m_3 = 0.20$	74'

Table 7.3

	$m_1 = 3.46$	$m_3 = 1.414$	
	24	$m_1 m_3 = 4.90$	3.0'
	12	$m_1/m_3 = 2.45$	6.0'
	2	$m_3/m_1 = 0.41$	36'
	1	$1/m_1 m_3 = 0.20$	72'

It is clear that the values in Table 7.2 show only a marginal improvement while in Table 7.3 $m_3 = 1.414$ may be almost acceptable. However in the latter the useful fields of view 3, 6, 72 arc min. are not regarded as an acceptable distribution of fields.

The conclusion that must be drawn is that acceptable values for m_1 and m_3 do not give fields (3 at once) similar to those specified and another selector lens must be added.

(ii) TWO LENS FIELD SELECTOR/ONE LENS TRANSFER

The individual magnifications possible are -

$$m_{11}, \frac{1}{m_{11}}, m_{12}, \frac{1}{m_{12}}, m_3, \frac{1}{m_3}$$

where subscripts 11 and 12 refer to the each of the two lenses before the intensifier.

Potentially useful combination are then,

$$\begin{array}{lll} m_{11} m_3 & m_{11}/m_3 & 1/m_{11} m_3 \\ m_{12} m_3 & m_{12}/m_3 & 1/m_{12} m_3 \end{array}$$

with the exclusions being m_3/m_{11} and m_3/m_{12} for reasons previously given.

For consumer convenience m_{11} , m_{12} , m_{13} , need to be chosen so that field of view ratios form a geometric progression.

$$\text{Therefore } \frac{m_{11}}{m_{12}} = r$$

$$\text{and } \frac{m_{12}m_3}{m_{11}m_3} = r$$

$$\text{giving } m_3 = r$$

$$\begin{aligned} \text{and } (m_{11}m_3)^2 &= r^5 \\ &= 24 \end{aligned}$$

$$\begin{aligned} \text{Hence } m_{11} &= r^{\frac{5}{2}} = 2.59 \\ m_{12} &= r^{\frac{1}{2}} = 1.374 \\ m_3 &= r = 1.89 \end{aligned}$$

The fields and the relative brightness of 2 arc sec. seeing stars are tabulated in Table 7.4.

Table 7.4

		Ratio	Field	Relative Brightness
$m_{11}m_3$	= 4.90	24.0	3.0	0.073
$m_{12}m_3$	= 2.59	12.7	5.7	0.26
m_{11}/m_3	= 1.37	6.7	10.8	0.92
m_{12}/m_3	= 0.73	3.6	20.3	1
$1/m_{11}m_3$	= 0.39	1.9	38.3	1
$1/m_{12}m_3$	= 0.20	1.0	72.4	1

Nowhere above is information that was finer than intensifier resolution magnified up by m_3 . If seeing is worse than 1.3 arc sec. as is often the case then m_{12} and m_{11} exceed the smallest element resolvable on the photocathode.

Stellar image brightness will remain constant for wider fields but tapers down for narrow fields as light spreads over neighbouring pixels, the amount depending on seeing conditions.

Suddenly the range of fields appears almost cinematographic as the interchange button is pressed repeatedly. However this design allows for $m_3 = 1.89$ which by the discussion in the previous chapter is larger than desirable. Coupling this with earlier statements on tolerances on depth of fields for a F1.4 lens, the question is asked, can some fields of view be traded off for a fixed but lower magnification of image transfer system and preferably at $m_3 = 1$.

(iii) TWO LENS FIELD SELECTOR. $m_3 = 1$

The only magnification possibilities are:

$$m_{11}, \frac{1}{m_{11}}, m_{12}, \frac{1}{m_{12}}$$

therefore $\frac{m_{11}}{m_{12}} = r$

and $\frac{m_{12}}{1/m_{12}} = r$

$$\begin{aligned}
 \text{therefore } m_{12} &= r^{\frac{1}{2}} \\
 m_{11} &= r^{\frac{3}{2}} \\
 \text{now } r^3 &= 24 \\
 \text{therefore } r &= 2.28 \\
 m_{11} &= 4.90 \\
 m_{12} &= 1.70
 \end{aligned}$$

The fields are as tabulated in Table 7.5.

Table 7.5

$m_3 = 1$	Ratio	Field	Relative Brightness	Δm_v
$m_{11} = 4.90$	24.0	2.7	0.059	- 3.07
$m_{12} = 1.70$	8.3	7.8	0.49	- 0.77
$1/m_{12} = 0.589$	2.9	22.4	1	0
$1/m_{11} = 0.204$	1.0	64.8	1	0

The table demonstrates the sought after result:

- (a) Four very appropriately scaled fields employing only two sets of optics in the field selector system.
- (b) An optimum magnification for the transfer system of high efficiency that also leaves it mechanically fixed.

OPTICAL CONFIGURATION POSSIBILITIES OF FIELD SELECTOR

Having determined the optimum magnifications for each of four fields it remains to establish the exact form of optical system what will best satisfy the two criteria of passing all light and maintaining resolution. In principle the efficient transmission of light can be effected by large apertures coated with multilayer thin films but this mitigates against low aberration of components. Space considerations also require the system to be physically compact.

The foremost possibilities to be investigated are:

- (a) Single lens.
- (b) Single lens plus field lens.
- (c) Twin lens fixed focus imaging at focal points.
- (d) Twin lens system including a zoom.
- (e) Catadioptric folded system.

(a) Single lens

Extreme rays from F15 objective and passing through the edge of the prime field stop must be collected by the selector lens for imaging on the intensifier faceplate. It is immediately evident from Fig. (7.1) that for smaller values of m_1 , i.e. wide fields the apertures need to be very large indeed, and the F numbers exceedingly low.

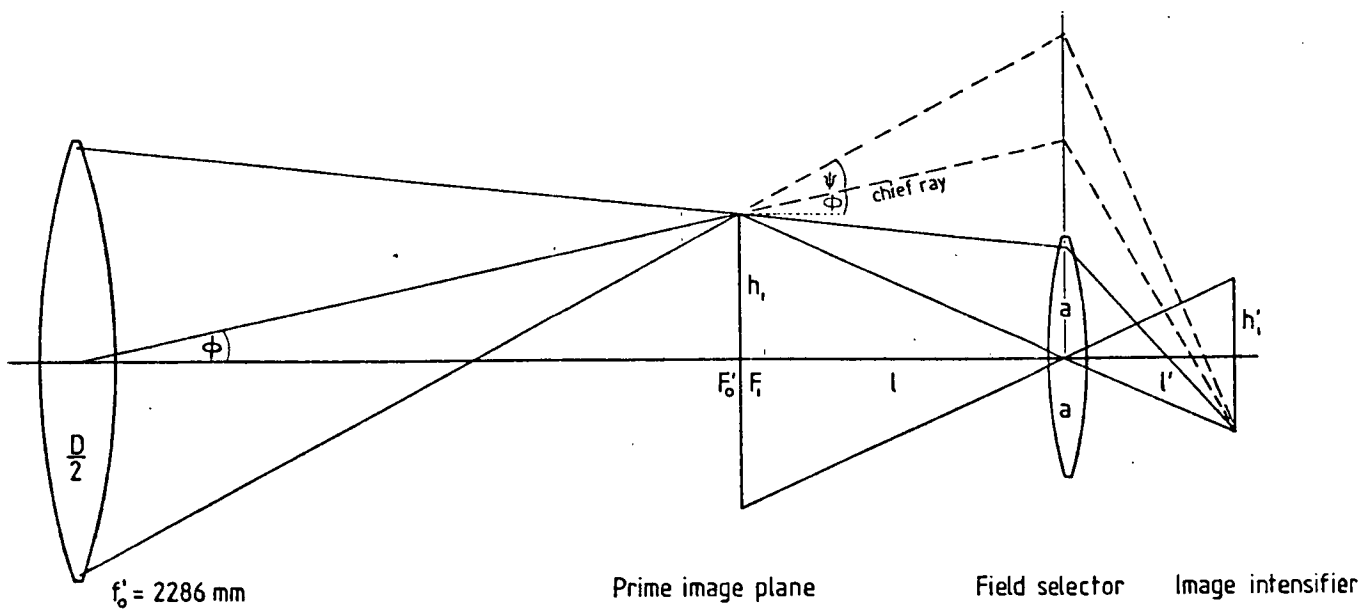


Fig. (7.1) A single lens field selector. Rays are not transmitted unless the selector lens has very large aperture.

Using the notation in the figure, for no light loss, the selector aperture must be -

$$2a = 2h_1 + 2l \tan(\phi + \psi)$$

Now
$$\phi_{\max} \approx \arctan \frac{h_{1\max}}{f'_0} = 0.54^\circ$$

and
$$\psi \approx \frac{D}{2f'_0} = 1.9^\circ$$

therefore
$$2a = 2h_1 + 2l \left(\frac{h_1}{f'_0} + \frac{D}{2f'_0} \right)$$

$$= \frac{Q(f'_0 + l)}{m_1 m_2 m_3 f'_0} + \frac{lD}{f'_0}$$

Further, to a good approximation,

$$\begin{aligned} \ell' &= (1 + m_1) f_1' \\ \ell &= \left(\frac{1 + m_1}{m_1} \right) f_1' \end{aligned}$$

so that the optical length is

$$\ell + \ell' = \frac{(m_1 + 1)}{m_1} f_1'$$

Putting in values $Q = 8.8 \text{ mm}$, $f' = 2286 \text{ mm}$

$$m_2 = m_3 = 1, \quad \ell + \ell' = 300 \text{ mm}$$

yields the tabulated results of Table 7.6.

Table 7.6 Simple single lens selector parameters.

Field	m	f_1'	ℓ	2a	FN
2.7'	4.90	42.2	50.9	5.2	8.07
7.8'	1.70	70.0	111.2	12.9	5.45
22'	0.589	70.0	189	28.9	2.43
65'	0.204	42.2	249	64.4	0.66

Considering the 65' field parameters the aperture is very large and the F number absurdly low. A simple single lens selector is therefore ruled out.

(b) Single Lens Selector Plus Field Lens

The function of a field lens is to image the illumination from the preceding component into the one following without affecting the position or scale of image points. Fig. (7.2) shows how the extreme rays are deviated into the selector lens.

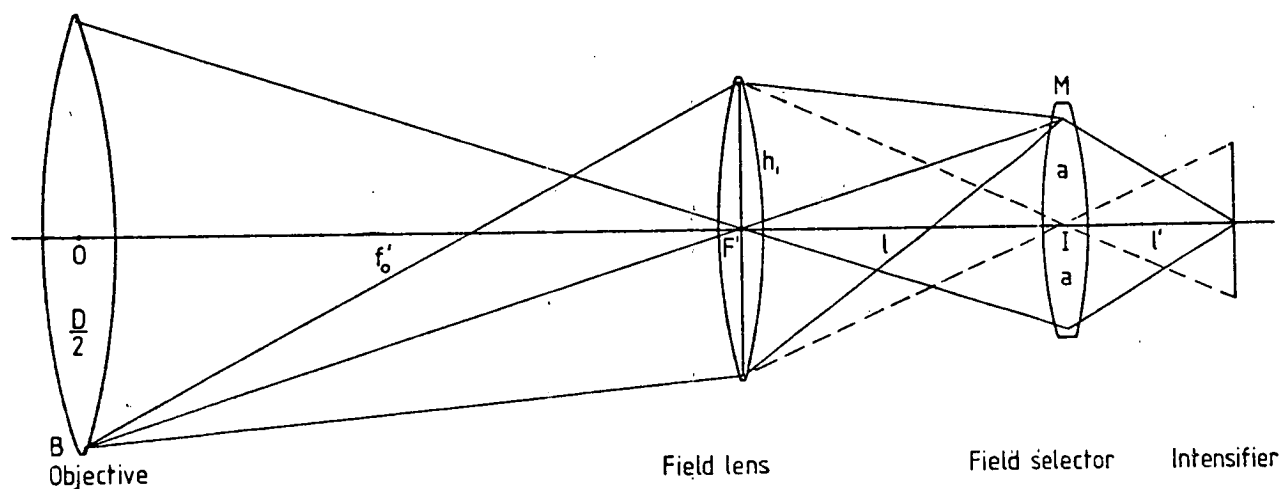


Fig. (7.2) Effect of field lens insertion. Small aperture selector lens still passes all light.

Considering the most critical field situation, the widest, for the objective to image into the selector, $2a = \frac{Dl}{f'_0}$ using values calculated in Table 7.6 for l gives the new selector aperture as $2a = 16.6\text{mm}$ with $\text{FN} = 2.54$.

This has been reduced from $2a = 64\text{mm}$ at $F0.66$, a rather dramatic improvement and immediately acceptable.

With regard to the field lens specifications the gaussian lens equation gives $f'_{FL} = 224\text{mm}$. At 65' field the aperture is 43mm and the $FN_{FL} = 5.2$. Since the image quality restrictions on a field lens need only be slight a simple doublet was purchased from an optical clearing house. The match was $f'_{FL} = 220\text{mm}$ and aperture 48mm!

It must be clarified whether the field lens needs to be changed with the selector, or if the field lens for the 65' field be used for the other fields without a change in its position. For the 22' field the selector lens with a field lens especially chosen for it would have had a new aperture $2a = 12.6\text{mm}$ and $FN = 5.6$. As it is the 65' field lens will also deviate considerable energy into the 22' selector. In fact a diameter of 16mm is sufficient to collect all the light energy. Fig. (7.3) illustrates this in a reduced scale diagram.

Thus the insertion of the field lens only has the effect of increasing the F number of the selector lenses to more desirable values. The two selector lenses must therefore have the following specifications:

- (i) 65' and 2.7 fields : $f'_1 = 42\text{mm}$
 $FN = 2.5$
 Aperture 17mm

To operate at conjugate ratio 4.9 : 1.

- (ii) 22' and 7.8 fields : $f' = 70\text{mm}$
 $F = 4.4$
 Aperture 16mm

To operate at conjugate ratio 1.7 : 1

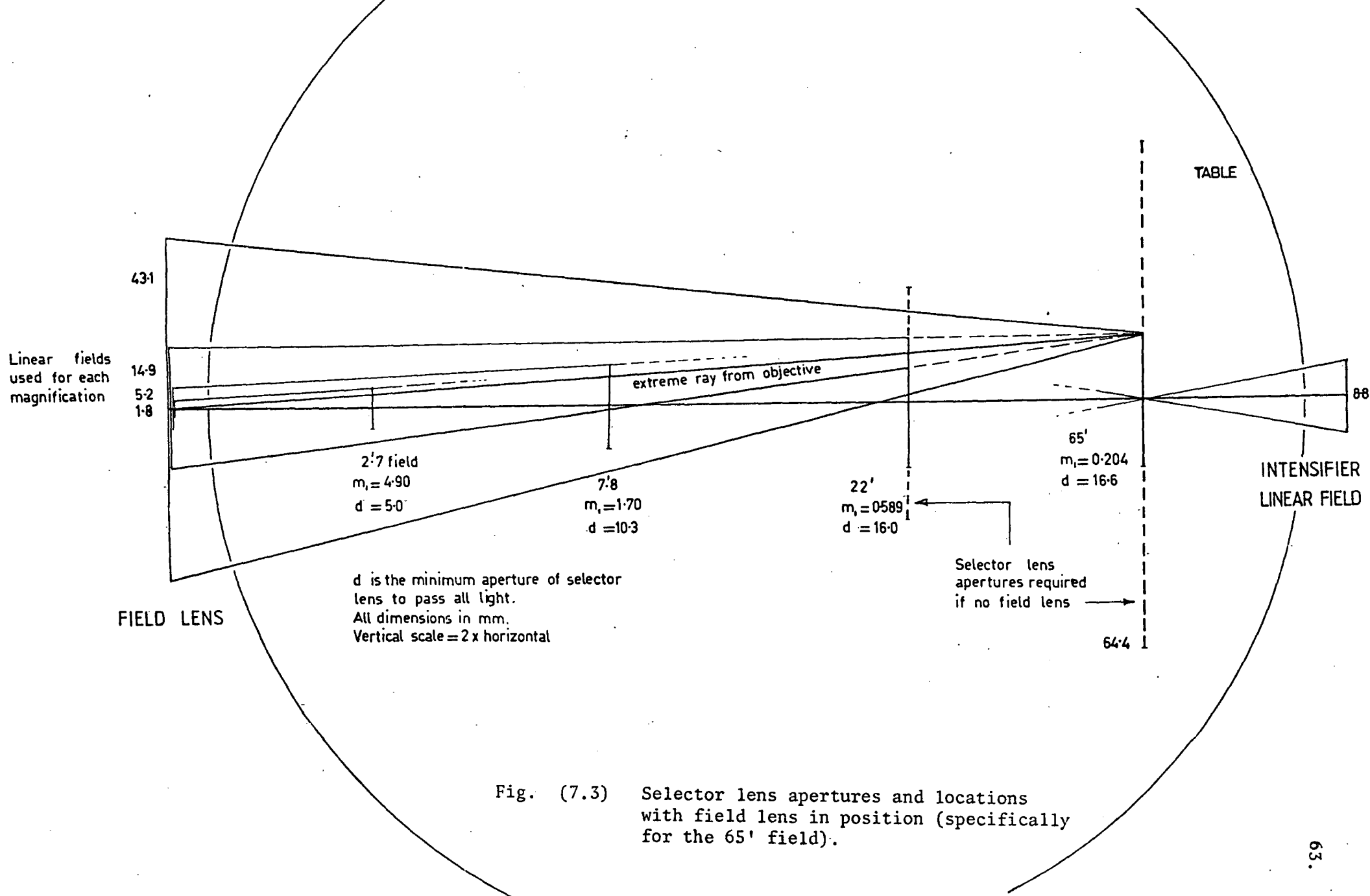


Fig. (7.3) Selector lens apertures and locations with field lens in position (specifically for the 65' field).

Exhaustive efforts failed to find any lenses that exactly matched those desired, firstly, since quality off-the-shelf lenses seem to have standardised on 50 and 75mm focal lengths (as nearest approximations), and secondly, because the conjugate ration $1.7 : 1$ is very abnormal. There being little choice, photographic lenses designed for best quality at infinite conjugates and at focal lengths 50 and 75mm were accepted although of course the fields of view now changed slightly. As will be pointed out later the 75mm F2.8 Switar lens had its normal resolvability compromised by being forced to operate at short conjugates. The 50mm F1.2 Canon lens at $4.9 : 1$ conjugates performed splendidly.

(c) Twin Lens (Fixed focus)

A lens pair is mounted front to front at infinite conjugates so that object and image are at focal points and collimated beams exist between the pair. For the four fields of view two such pairs are required and would be positioned orthogonally on the rotating table with suitable interlens spacing so as not to obstruct the beams.

The advantages would be:

- (i) Total physical length is short.
- (ii) The optical length can easily be adjusted to match the other pair or any particular length.
- (iii) Focussing is simplified.
- (iv) Lenses are used at their designed optimum performance conjugates.
- (v) Aperture of the leading lens is not as large as in case (a).

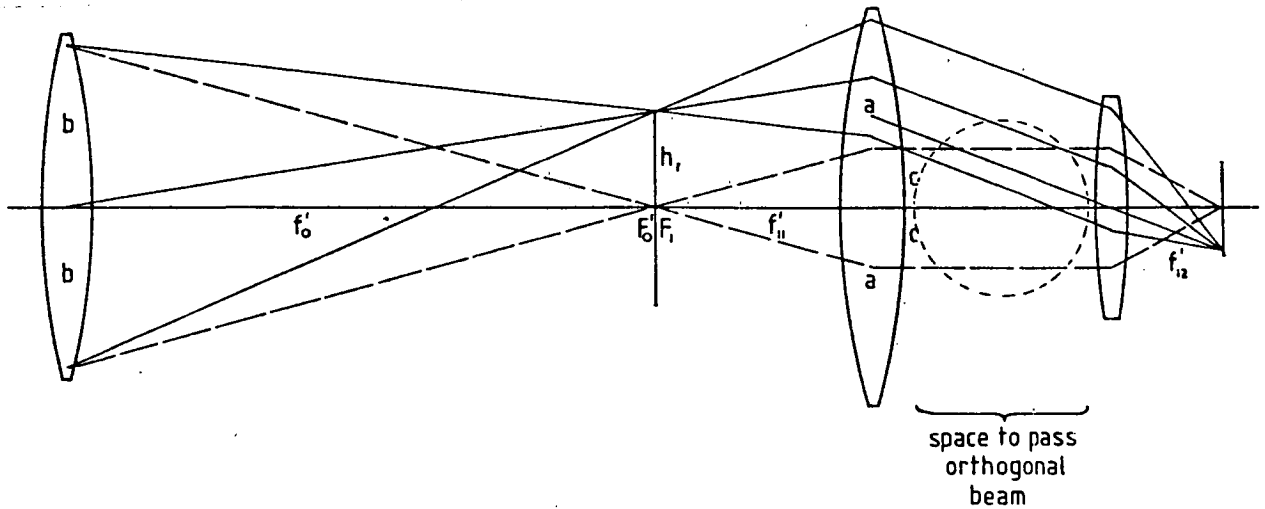


Fig. (7.4) Twin lens field selector imaging at focal points.

The magnification is determined by -

$$m_1 = \frac{f'_{12}}{f'_{11}}$$

which can create the practical problem in that it is not possible to arbitrarily select any focal length. The aperture of leading lens is -

$$\begin{aligned} 2a &= 2h \left(1 + \frac{f'_{11}}{f'_0}\right) + \frac{2bf'_{11}}{f'_0} \\ &= \frac{Q(f'_0 + f'_{11})}{m_1 m_2 m_3 f'_0} + \frac{2bf'_{11}}{f'_0} \end{aligned}$$

For wide field configuration, the leading lens must have greater aperture while the second can be akin to a 16mm cine lens.

$$\text{Now} \quad \frac{2c}{f_{11}} = \frac{2b}{f_0} = \frac{1}{FN_0}$$

$$\text{and} \quad \frac{F_{12}}{2c} = FN_{12}$$

$$\text{Therefore } FN_{12} = m_1 FN_0$$

The F number of the beam from any star image received by the leading lens is FN_0 whereas the beam emerging is $m_1 FN_0$.

Hence for widest field ($m_1 = 0.204$)

$$\begin{aligned} FN_{12} &= 0.204 \times 15 \\ &= 3.06 \end{aligned}$$

Actual exit lenses may be 25mm F1.4 or 15mm F1.3 cine. This would still leave considerable flexibility with respect to aperture and hence physical location. However for each of the above the leading lens requires $f_{11} = 122$ or 74 mm respectively, and with necessary apertures of 54 and 49 mm respectively, the corresponding F numbers are F2.3 and F1.5. Each of the leading lenses therefore seem somewhat formidable. It should be noted that the bundle of rays from a single star is incident on only a small area of the aperture thus reducing the aberrations, notably spherical.

While a field lens may reduce aperture four quality lenses are still necessary.

(d) Twin Lens Selector Including a Zoom

Of all field selectors possible a zoom system would be the ideal. Not only would a continuously variable magnification be the epitome of convenience but would be mechanically the most robust and precise of systems since no rotations and relocations are necessary. However for the desired field range the necessary focal length zoom ratio of 24 : 1 is impracticable to say the least. A more feasible system employs the zoom and fixed focus lenses as a pair reversibly as discussed earlier in this chapter so that the zoom range requirement is only $\sqrt{24} = 4.9$. Such are procurable but costly.

It is the steep rays that are difficult to accommodate and these are associated with the wide fields.

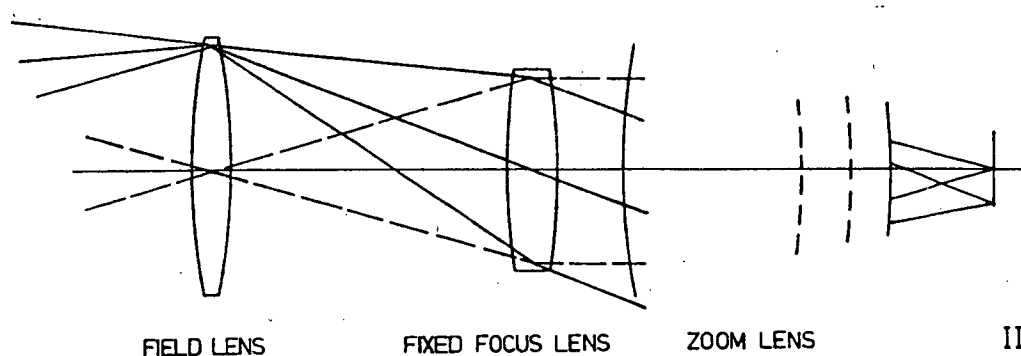


Fig. (7.5) Fixed Focus + Zoom configuration.

For no vignetting the exit pupil of the fixed focus lens must be coincident with the entrance pupil of the zoom lens, but it is characteristic of many zooms to be of great length as well as soft in focus. The interpupil distance is therefore large and vignetting very considerable.

Because of the very high desirability of such a system a prototype was built and field tested using a 75mm F1.9 Macro Switar fixed focus with 17-75mm F2 PanCinor zoom. Each lens intended for normal 16mm use is regarded as excellent quality. The results of tests at magnifications 4.2x, 2.7, 1.8, 1x on open star cluster NGC 3293 are shown in Fig. (7.6) and should be compared with Fig. (7.7a) and (7.7b). The latter photographs were taken with a single fixed focus 50mm lens as selector, at magnifications $m_1 = 4.2$ and 1 respectively while transfer system at 135/50 was the same throughout.

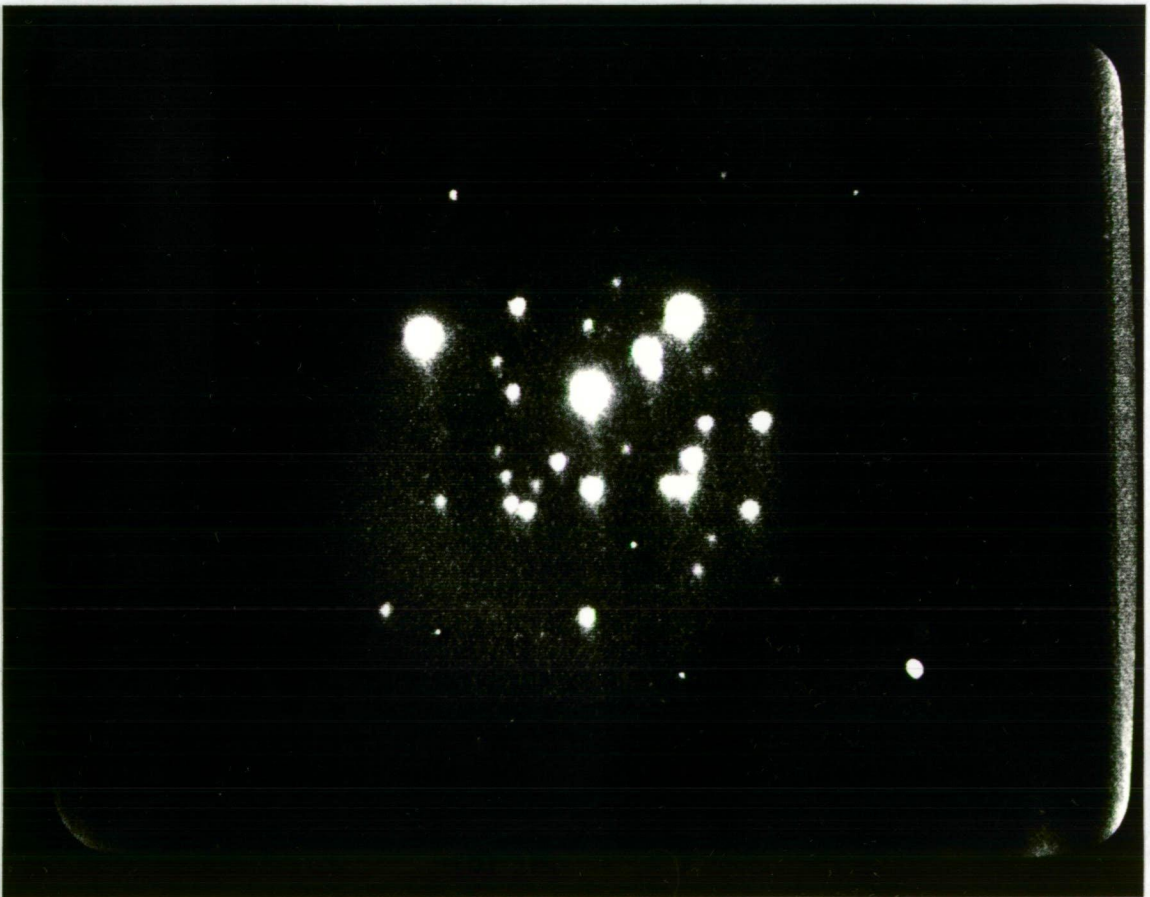
The evaluation and conclusions are regrettably clear and simple : the system is expensive to purchase, resolution poor, light loss large, and vignetting colossal.

(a) $m_1 = 1$ (b) $m_1 = 1.8$ (c) $m_1 = 2.7$ (d) $m_1 = 4.2$

Fig. (7.6) Open Cluster NGC 3293. $\frac{1}{2}$ sec. exposure.
Field test using a zoom selector system.
Compare with Fig. (7.7) using fixed focus
lenses.



(a) $m_1 = 1$



(b) $m_1 = 4.2$

Fig. (7.7) Open cluster NGC 3293. $\frac{1}{2}$ sec. exposure. Fixed field selector. Compare zoom system of Fig. (7.6) with respect to resolution and limiting sensitivity. Note the full TV monitor screen.

(e) Catadioptric Folded System

For compactness this folded system shown in Fig. (7.8) may have much to commend it. Three fields only are available using two lenses and four plane mirrors mounted on two sliding tables. The rectilinear motion ensures accurate location by firm end stops. A field at magnification $m_1 = 1$ is obtained by sliding in a pair of mirrors and fields for $m_1 \lesssim 1$ by positioning the positive or negative barlow ends.

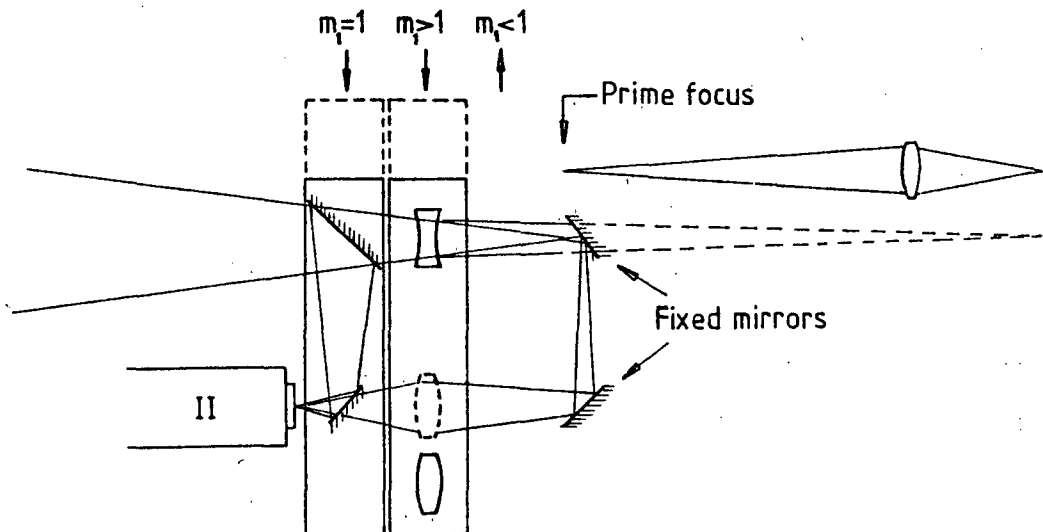


Fig. (7.8) Folded Field Selector.

When it is said that the range of focal lengths of commercially available positive lenses is limited then the range for negative lenses is even more limited. Only 2x and 3x lens multipliers seem to be readily accessible and these generally yield poor quality images on axis and worse off axis. A second limitation of this system is one of gross inconvenience in that the insertion of the positive lens inverts the image relative to the other two fields.

Conclusion:

It is clear that the system offering greatest promise and simplicity is the single lens plus field lens with a possible hesitation over the performance of the short conjugate use of one lens.

PROJECTED SENSITIVITY PERFORMANCE

To estimate the limiting stellar magnitude detectable with an intensifier television system it is necessary to establish a relationship incorporating the light flux collected and imaged and the gains and losses throughout the optoelectronic chain.

Combining Pogson's equation with the fact that a zeroth magnitude star provides a light flux of $L_0 = 2.54 \times 10^{-6}$ lux outside the atmosphere (Allen 18) gives a value for the illumination L produced by a star of magnitude m_v :

$$\log L - \log (2.54 \times 10^{-6}) = 0.4(0 - m_v)$$

$$\text{i.e.} \quad 0.4 m_v = -\log L - 5.595$$

If the collecting area of the telescope is A and the transmission coefficient of the atmosphere is T_a , then the total flux received is,

$$F = T_a LA \text{ lumens}$$

$$= T_a L \pi D^2 / 4$$

When the flux is passed through the system and concentrated on the picture elemental area dA of photocathode the target illumination is F/dA lux where $S = F/dA$ is the limiting sensitivity of the TV target, m_v becomes the limiting magnitude detectable.

Hence substitution yields

$m_v = 5 \log D - 2.5 \log S - 2.5 \log dA + 2.5 \log T - 14.34$ (8.1)
--	-------------

where dA is the star image spread on the target and T is the resultant transmission all factors such as atmosphere, lens components, intensifier gain, etc.

If the variables were controllable one would of course select very low light camera sensitivity, S , imaged into minute area of dA provided that the target resolution matched, good transmission, and high gain. It is suggested that this to a large degree has been achieved.

Very many experimental tests were performed using a range of objective apertures, different TV cameras, with and without intensification, and field selector lenses of varying complexity.

The figures for the final acquisition system will be of first interest. Analysis of 9', 25' and 60' photographs show a 2 TV line pair stellar

diameter = 0.0518 mm on TV target so that $dA = 2.104 \times 10^{-9} \text{ m}^2$.



National Newvicon camera WV 1350 has sensitivity, $S = 0.3 \text{ lux}$

Objective diameter, $D = 150 \text{ mm}$.

The loss factors for each lens component are difficult to determine but reasonable estimates are tabulated below.

	T	Δm_v
Atmosphere transmittance	$T_a = 0.80$	-0.242
Objective losses (4 surfaces + absorption)	$T_{obj} = 0.84$	-0.189
Field lens transmittance	$T_{fl} = 0.95$	-0.056
Selector lenses transmittance (multiple element)	$T_{sl} = 0.75$	-0.312
Transfer lens pair		
- transmittance	$T_{tl} = 0.64$	-0.485
- collection efficiency	$T_{col} = 0.113$	-2.367
	0.035	-3.65
Image Intensifier gain	145 000	+12.90
Net gain	5 020	$9^{m.25}$

Insertion of these values into equation (8.1) then gives an anticipated limiting magnitude sensitivity for the complete intensified television system as faint as $m_V = 13^m.9$ which is quite impressive for this small aperture system.

It is quite possible that transmittance estimates are slightly optimistic. Worst reasonable case figures could make transmission losses:

$$0.75 \times 0.80 \times 0.88 \times 0.65 \times 0.60 \times 0.10 = 0.021 \equiv -4^m.2,$$

a marginal lowering of expected limiting magnitude of

$$0.6 \text{ to } m_V = 13^m.3.$$

In the situation where the star image disc is enlarged 50% either by magnification in the narrowest field or by bad seeing conditions, a corresponding fall in sensitivity occurs of $\Delta m_V = -0.88$

BACKGROUND AND NOISE

SKY BACKGROUND MEASUREMENTS

Estimates of sky background intensity were necessary for two reasons:

- (a) In the design of the image transfer system from intensifier to TV target only information carrying photons need to be allowed for. No useful purpose is served in collecting and transferring low level II screen noise. It will be understood of course that such noise is a function of direction of pointing, presence of moon light, and magnification before the intensifier.
- (b) Comparisons need to be made between the equivalent background input (E.B.I.) of the intensifier photocathode and sky noise to establish which will be dominant as a function of both gain and field of view. The possibility of adding a fourth stage of gain is discussed in Chapter 12. and noise characteristics are investigated in the next section.

Tests were made with a small area (6mm dia.) photo-conductive cell pressed in close contact with the output screen of the intensifier whichⁱⁿ turn was in train with the prototype system shown in Fig. 9.1. Readings were made using a good quality electronic microammeter and were corrected for non linearity of the cell.

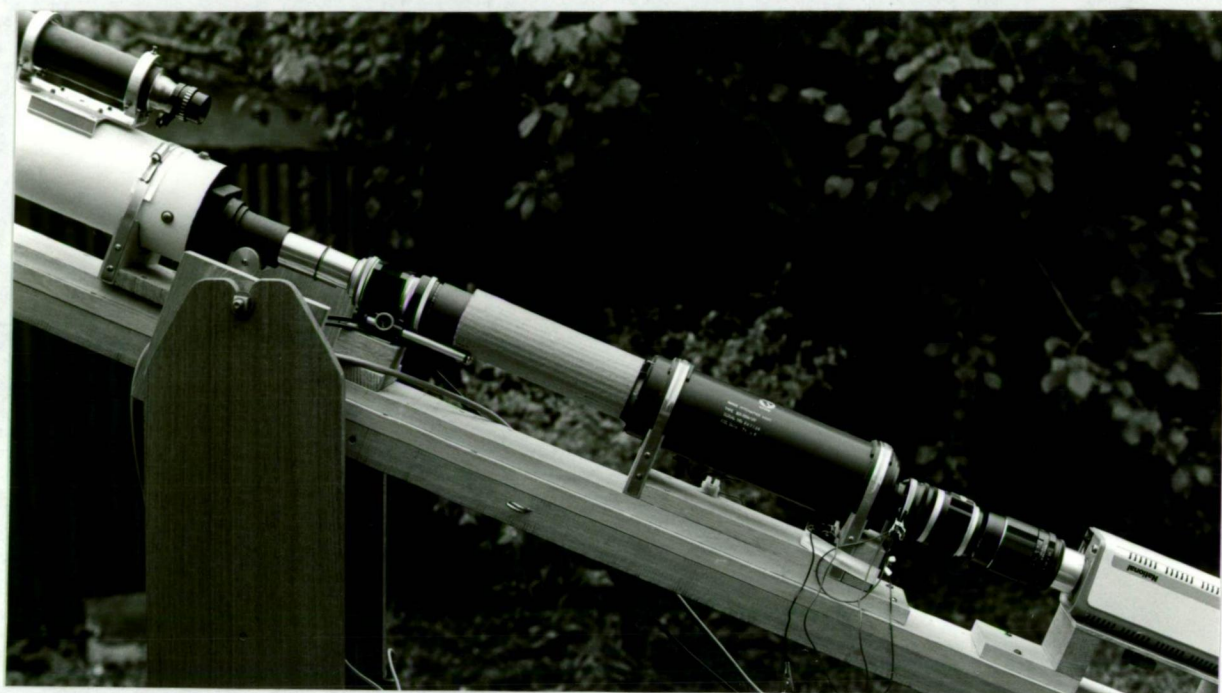


Fig. (9.1) Prototype arrangement for various tests including sky background. The objective is 100mm F15. A 50mm Tessar lens on the bellowscope provides $m_1 = 4$ while the transfer system is a pair of 135mm telephoto lenses front to front.

The proximity of Hobart city centre being only 2km away on the one hand was a problem but on the other allowed a diverse range of sky light conditions. Sky profiles through the zenith were therefore taken in situations of clear and moonlight sky and also with field selector magnifications $m_1 = 1$ and 4.

In Fig.(9.2) graphs are shown for clear moonless nights with the above two magnifications. A neighbouring dark roof edge provided a convenient zero setting. The dramatic contrast of city sky light is demonstrated in Fig. (9.3) for interest.

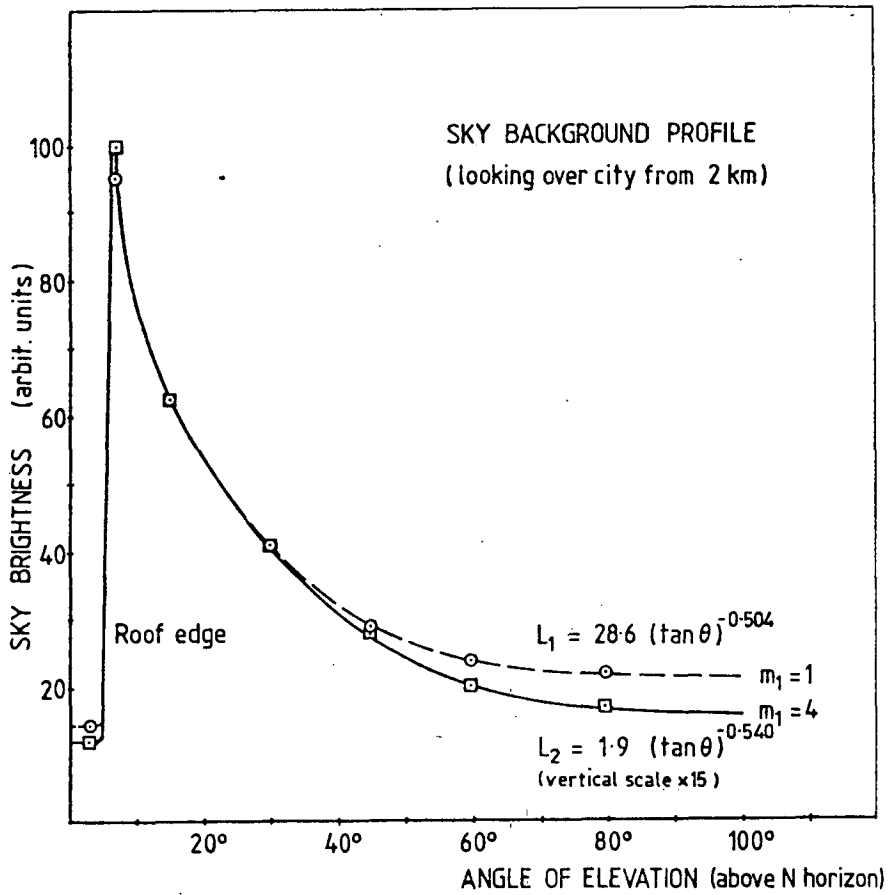


Fig. (9.2) Sky background profile through zenith from location 2km south of Hobart centre. Vertical scale is arbitrary.

The two curves of best fit have equations $L_1 = 28.6 (\tan \theta)^{-0.504}$ and $L_2 = 1.9 (\tan \theta)^{-0.540}$ respectively where θ is the elevation above north horizon so that $L_1/L_2 = 15.1$. Inspection shows that three important features stand out:-

- (a) That sky noise becomes constant past the zenith.
- (b) That the ratio of this asymptotic sky noise to equivalent background input equals 1.5.

- (c) That the $m_1 = 4$ curve multiplied by 15.1 closely fits the $m_1 = 1$, confirming experimentally that background is inversely proportional to the square of the focal length ($\sqrt{15.1} = 3.9$).

It was mostly for general interest that sky light was also measured with a near full moon (7/8) in the sky. Between $30^\circ - 90^\circ$ from the moon sky readings were 10 - 20 times higher than on moonless nights and even the darkest section of sky was four times brighter than under moonless conditions.

For the particular image tube used in this project the EBI is known to be 1.85×10^{-7} lux so that sky noise has a value 2.78×10^{-7} lux. There will of course be some variations to this as atmospheric constituents change and also due to the more distant location of Mt. Canopus observatory.

An example of the contrast between high and low backgrounds possible is shown in the photograph Fig. (9.3). It is somewhat exaggerated in that the viewing direction was low over the city and $m_1 = 1$, $m_3 = 0.37$ which concentrates flux in a small film area.



Fig. (9.3) Sky brightness looking north low over Hobart city 1.7 km. away. An out of focus roof line at 6° altitude illustrates a dramatic change. The 1 sec exposure on HP5 is typical of those taken for most star fields.

Stellar magnitude equivalent of background.

On a similar basis to the derivation of the equation (8.1) for limiting magnitude sensitivity one can straightforwardly find expression for the luminous intensity S inside an image disk of star of magnitude m_v on the faceplate of the intensifier. T' is now the transmission coefficient of all components and atmosphere before the faceplate.

$$m_V = 5 \log D - 2.5 \log S - 2.5 \log dA + 2.5 T' - 14.242 \quad \dots\dots (9.1)$$

$$\text{Taking } T' = 0.80 \times 0.84 \times 0.95 \times 0.75 = 0.479$$

$$S = \text{EBI} = 1.85 \times 10^{-7} \text{ lux}$$

$$D = 0.15 \text{ m}$$

$$dA = 2.104 \times 10^{-9} \text{ m}^2$$

$$\text{gives an EBI star, } m_V = 19^{\text{m}.4}$$

Hence star equivalent of sky background

$$\begin{aligned} \text{is } m_V &= 19.36 - 0.44 \\ &= 18^{\text{m}.9} \end{aligned}$$

Sky Background as a Function of Magnification

It will be most useful in considering further possible gains to ascertain what are the present sky background values for each of the fields of view. Already at widest field a faint background glow can be visually detected on the TV monitor that is not present with other fields and for photographs taken of the monitor the brightness had to be reduced.

Now it is clear that sky noise imaged on the focal plane (in lumens/metre²) is inversely proportional to the square of the F number, or for fixed aperture, inversely proportional to the focal length squared.

Therefore if dA subtends one arc sec at an objective the focal length must be $f_B' = d/\tan \Delta\theta$
 $= 10677\text{mm}$

and, if the field selector magnification m_1 operates on f_0' to give an effective focal length $m_1 f_0'$, the background intensity will vary

as
$$\left(\frac{m_1 f_0'}{f_B'} \right)^{-2}$$

Thus the sky magnitude is given by

$$m_V(\text{sky}) = 19.4 - 2.5 \log k + 2.5 \log \left(\frac{m_1 f_0'}{f_B'} \right)^{-2}$$

where k is the relative brightness of sky to EBI measured at $m_1 = 4$.

$\therefore m_V(\text{sky}) = 16.0 - 2.5 \log k + 5 \log m_1$

..... (9.2)

These are tabulated below in Table 9.1.

Table 9.1 Limiting sky brightness as function of field of view.

2θ	m_1	$m_V(\text{sky})$
$3\frac{1}{2}$ arc min	4.070	19.0
9	1.670	17.1
25	0.596	14.9
60	0.247	12.6

Note that the value $k = 1.5$ was used as measured at the test location nearer the city. Over the observatory k may be less than one (yet to be determined).

Thus it is concluded that:-

- (a) background should just be visible in the 60' field.
If not background limited stars of $13^m.4$ would have been just discernable as for the 25' field;
- (b) the choice of F1.4 lenses in the transfer system is justified as appropriate to the 3-stage intensifier;
- (c) since background levels for the $3\frac{1}{2}'$ and 9' fields are very low the practical possibility of the addition of a further gain element exists. This is proposed and explored in Chapter 12.

INTENSIFIER NOISE

Thermal Emission

The dark emission from photo detectors is very important in setting the lower limit to the flux levels that may be detected. For intensifiers the principle cause of dark emission is thermal emission of electrons from the photocathode. Since noise characteristics tend to be rather rapidly varying functions if the intention is to increase the applied voltage these characteristics must be determined. This investigation also serves as a check on the manufacturer's claims about EBI.

As for measurements of sky noise the photoconductive cell was placed flush with the phosphor screen while the faceplate was in total darkness. The night ambient temperature in the laboratory was 23°C (February) so that for field use significant reduction in noise effects can be expected. An empirically deduced formula was used to correct for the non linear response of the cell and to convert microamps readings to lux incident on the surface:

$$\text{viz.} \quad L = \left(\frac{b}{c - \log I} \right)^{\frac{1}{a}} \quad \text{where} \quad \begin{array}{l} a = 0.0348 \\ b = 12.53 \\ c = 7.98 \end{array}$$

The results are plotted in Figure (9.4) and indicate a linear log curve in the neighbourhood of the upper voltage range of interest. The slope of the graph is a rather steep 4.9 compared to a power law of 3.04 for the signal gain.

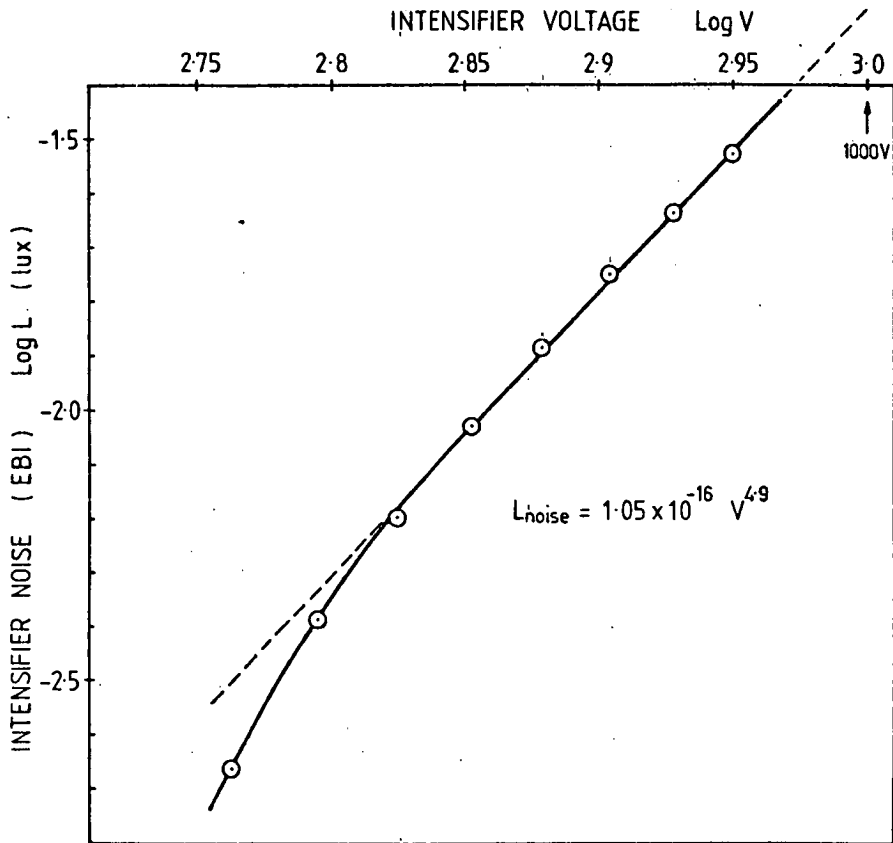


Fig. (9.4) Intensifier noise as a function of applied voltage.

$$\text{Log } L_{\text{noise}} = -15.98 + 4.9 V_{II}$$

$$\text{or } L_{\text{noise}} = 1.05 \times 10^{-16} V^{4.9}$$

Substitution of normal operating voltage gives a screen output noise of 29.6 millilux which with a gain of 145000 makes the EBI 2.04×10^{-7} lux compared to Varo's rating of 1.85×10^{-7} lux. Such confirmation is gratifying.

Fractional changes in anticipated noise can now be extrapolated for higher voltages as tabulated in Table 9.2.

Table 9.2 Noise increments as function of voltage.

V	Fractional voltage increase	Fractional noise increase
890	1.00	1.00
1000	1.12	1.77
1100	1.24	2.82

Considering the fact that it has been shown that sky background dominates over noise and that the characteristics was determined under warmer than intended field situations it can safely be stated that thermal noise will not be a problem.

Two other albeit minor effects are visible on the intensifier screen: ion shot noise and phosphor boil.

Ion Shot Noise

Ion emissions occur as a result of electron bombardment of heavy atoms in the leading assembly. These appear as pulses of light whose duration are determined by the persistence of the phosphors and whose distribution is random. For direct monitor viewing there is no ambiguity or inconvenience but during time exposures of the screen a number may be collected and become confused as stars. Figure (9.5)

shows the effect by deliberately exaggerating the normal exposure from 1/15 sec. to 8 sec. The count rate is approximately 5-10/sec.



Fig. (9.5) Ion shot noise count in 8 sec.
Direct photograph of the intensifier screen.
Grain is that of the film.

Phosphor Boil

When bright extended objects such as a few nebulae and planetary discs are viewed the screen demonstrates a time varying mottled appearance. It could be said that resolution would be lost in any case due to the abundance of light. The problem is not very significant as by changing down to narrow fields extended objects quickly reduce their

flux density. An example of phosphor boil frozen at $\frac{1}{5}$ sec. is shown in Fig. (9.6), while in Fig.(6.1b) the $1\frac{1}{2}$ sec. time exposure has had boil removed by averaging.

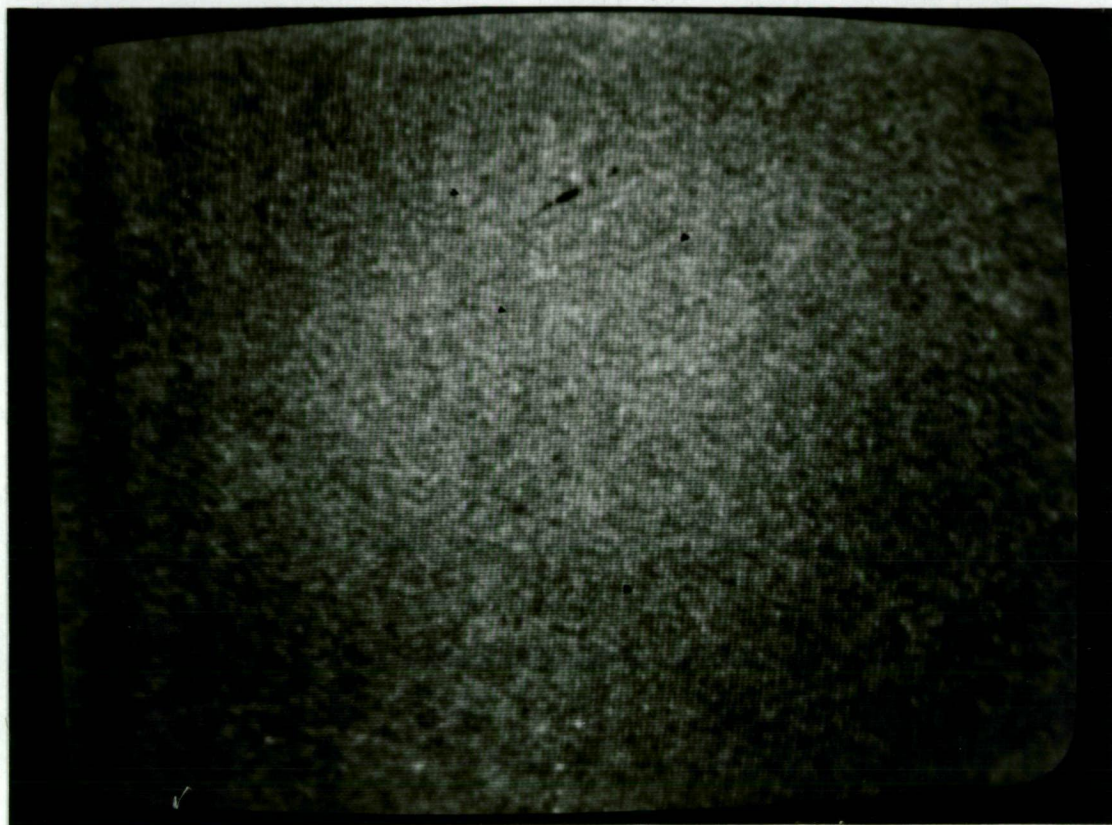


Fig. (9.6)

Intensifier screen phosphor boil evident at $\frac{1}{5}$ sec. The vertical striations are a temporary resolution grating on the faceplate.

Chapter 10.

TECHNICAL ASPECTS OF CONSTRUCTION

FIELD SELECTOR TABLE ROTATION

When the astronomer calls for a particular field angle, the appropriate table mounted lens must rotate rapidly into position and locate with a precision of at most one star diameter, preferably less. For design purposes such star diameter is taken as one arc second, and this must be transformed into a tolerance on table axis seating, motor rotation and gear ratio.

It will be evident that a most suitable transport mechanism will be a geared stepping motor. The basic increments of the Sigma motor used are $1.8^\circ/\text{step}$ (200 steps per rev) with a non cumulative error of $\pm 3\%$ of one step.

In the first instance a relationship is sought between table rotation $\Delta\phi$, the linear movement of the star image on the faceplate Δx , the field selector magnification m_f and the optical length $(a + b)$ of the field selector system. Other symbols are as denoted in Fig. (10.1).

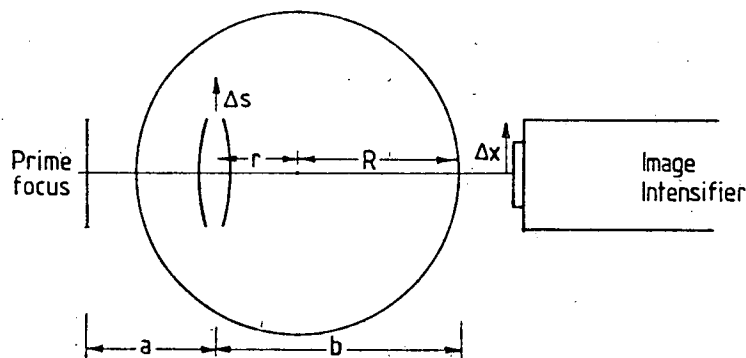


Fig. (10.1) Selector table rotations.

Since Δx is the permissible variation in reproducible settings caused by a translation Δs in the lens,

$$\frac{\Delta s}{a} = \frac{x}{a+b}$$

$$\begin{aligned} \text{and } \Delta\phi &= \frac{\Delta s}{r} \\ &= \frac{a}{a+b} \frac{\Delta x}{r} \end{aligned}$$

$$\text{Now } m = \frac{b}{a}$$

$$\text{so that } r = \left(\frac{m+1}{m} \right) \frac{a+b}{2}$$

Substitution yields

$$\Delta\phi = \frac{2 \Delta x}{(a+b)(m-1)}$$

If the narrowest field ($3\frac{1}{2}'$) is taken as the most critical,

$$\Delta x = \frac{1 \times 8.8}{3.5 \times 60} = 0.419 \text{ mm}$$

$$\begin{aligned} \text{and } m &\doteq 4.07 \\ a+b &\doteq 315 \text{ mm} \end{aligned}$$

$$\begin{aligned} \text{so that } \Delta\phi &= 8.67 \times 10^{-5} \text{ rad.} \\ &= 1.38 \times 10^{-5} \text{ rev.} \\ &= 2.76 \times 10^{-3} \text{ step} \end{aligned}$$

If the stepping error is $\pm 3\%$ the gearing required is,

$$\begin{aligned} \text{Gear ratio} &= \frac{2.76 \times 10^{-3}}{0.03} \\ &= 0.0920 \end{aligned}$$

Hence to keep star displacements to within one arc sec. it is necessary to gear down by at least 10.9 : 1.

To satisfy the patience of the astronomer the motor must operate at the highest speed reasonable commensurate with the power of the motor to drive the table and the maximum stepping speed. For no ramping to be required the maximum rate is 500/steps sec so that if 1 revolution in 16 sec. is satisfactory then the gear ratio becomes 40 : 1.

The ramifications are firstly that the reproducible star setting accuracy reduces to $\frac{1}{4}$ arc sec. (from the above), and secondly, the waiting time to position a new field, since there are four stations, requires at best 4 sec and at worst 12 sec. There are therefore 2000 steps between stations.

The single step parameters are tabulated in Table 10.1.

Table 10.1

Field	$3\frac{1}{2}$ arc min	9'	25'	60'
m_1	4.07	1.66	0.578	0.241
ΔX	0.380 mm	0.082	-0.052	-0.094
Field movement per motor step	9.5 arc sec	5".0	-9".3	-39".8
Tolerance (3%) by stepping motor	0.28 arc sec	0".15	0".28	1".2
Fractional field per step	4.3%	0.9%	0.6%	1.1%

INCREASING EFFECTIVE FIELD BY LATERAL DISPLACEMENT

A secondary question that arises is whether or not lateral image displacements can be used to increase the effective field. This would have particular merit if there happened to be no sufficiently bright star for guiding in the immediate neighbourhood of the faint object of interest.

Shifting the lens laterally has the same effect as moving the object point off axis. It must be determined how far can this be done without affecting image quality. Fig. (10.2) defines the angular relationships.

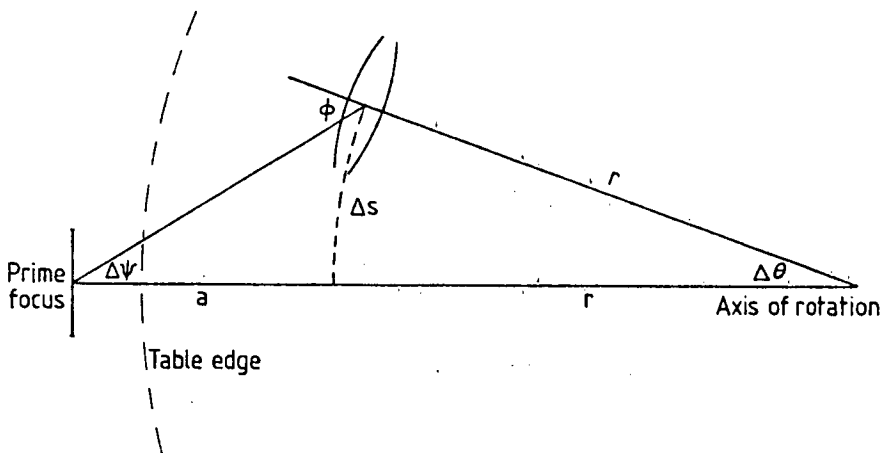


Fig. 10.2

The off axis angle,

$$\begin{aligned}\theta &= \Delta\phi + \Delta\psi \\ &= \Delta\phi + \frac{r\Delta\phi}{a} \\ &= \Delta\phi \frac{(m+1)}{2}\end{aligned}$$

As it is greatest for the narrow field the inclination corresponding to a linear displacement of one field width is calculated.

$$\begin{aligned}\text{For 25 steps } \Delta\phi &= \frac{25 \times 2\pi}{8000} \\ &= 0.0196 \text{ rad} \\ &= 1.12^\circ\end{aligned}$$

$$\text{so that for } m_1 = 4.07, \theta = 2.85^\circ$$

Since the lenses used are designed to perform at much greater angles ($\approx 20^\circ$) it is evident that lateral displacement of several field widths can be easily and usefully accommodated. Actual tests performed indicate no significant deterioration in image quality although some vignetting does occur at the edge of the 60' field.

TABLE MECHANICS

The table was a cast aluminium plate ribbed at the underside to prevent distortion and lens movement at a later stage. Angular contact bearings in the housing shown in Fig. (10.3) produced a fit such that no play could be detected.

FIELD SELECTOR TABLE

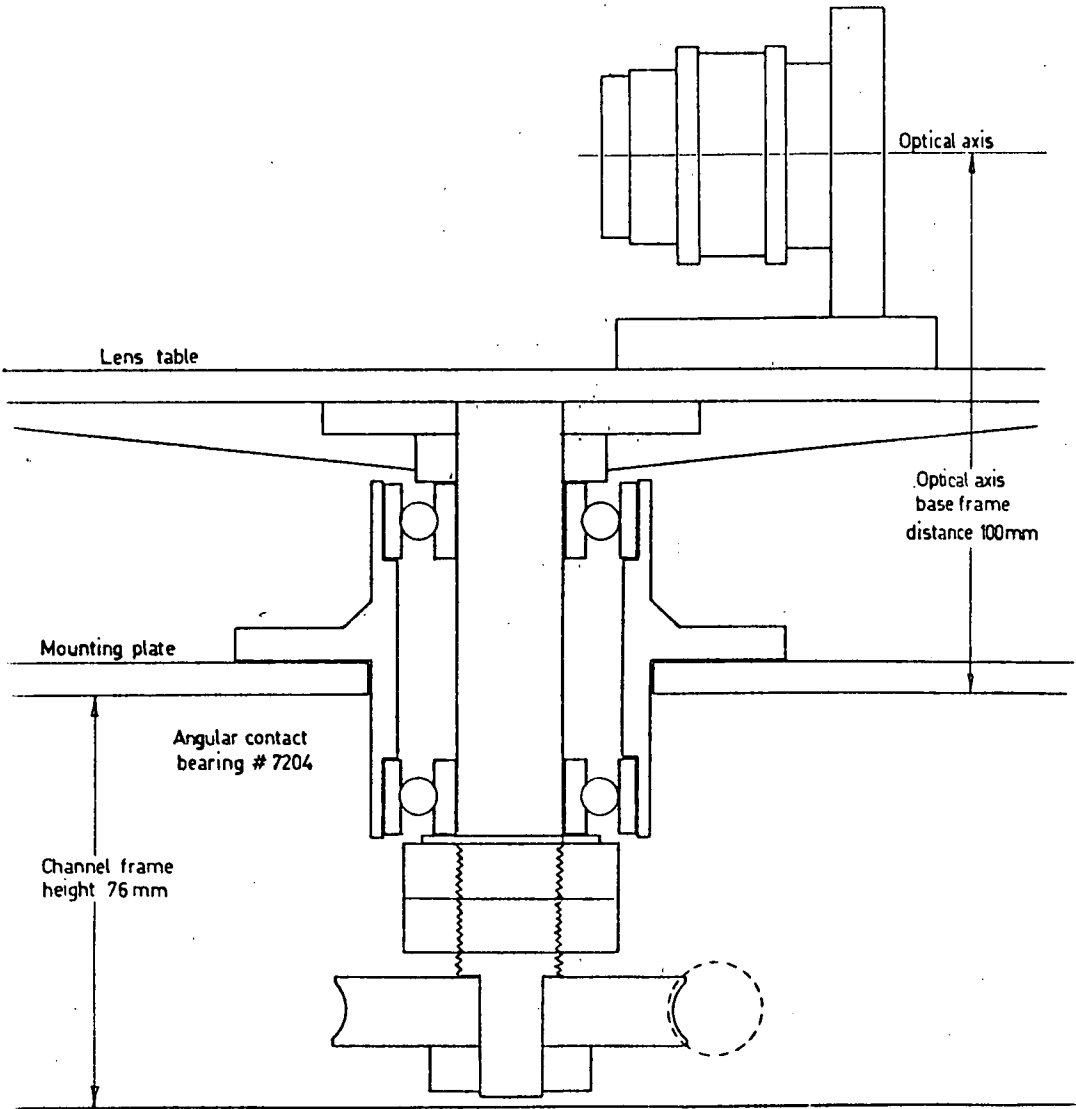


Fig. (10.3) Selector table bearing housing.

The 40 : 1 worm shaft also in its own bearing housing was driven by the motor via an oldham coupling. Any backlash was small compared to the 3% motor stepping tolerance. The photograph of Fig. (10.4) shows the worm and gear and motor on the underside of the mounting plate with slotted holes. After precise mounting of the optics at 90° positions the table was very carefully balanced about the axis by lead weight at the opposite periphery so that it was in neutral equilibrium at any angle.

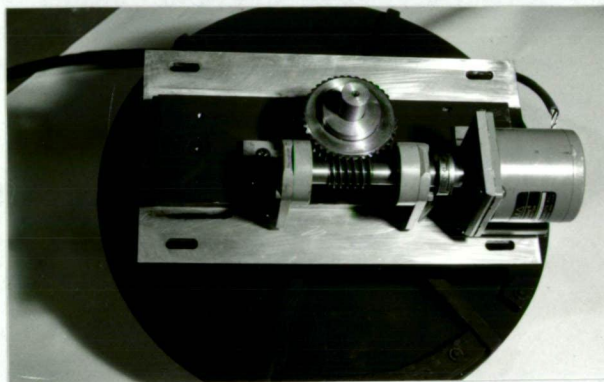


Fig. (10.4) Underside of the field sector assembly.

Experimental evidence was sought for the accuracy and repeatability of table rotations with respect to the design values. Displacements in a 0.01 x 100 mm objective micrometer situated on the edge of the 300 mm table were observed with a microscope as motor steps were incrementally advanced. Over 20 steps the average shift was 0.118mm with standard deviation of 0.003mm. This corresponds to a mean accuracy of 0.24 arc sec. in the $3\frac{1}{2}$ arc min. field of view and is marginally less than $0''.28$ calculated in table (10.1). For 360° rotations the repeatability had a similar standard deviation of 0.0035mm or precisely $0''.28$!

Attention is drawn to the fact that the above measurements were taken with motor motion in one direction only. The pulse power supply was capable of motor operation in either direction. In switching from forward to reverse the anomolous effect was produced of the addition or subtraction of a motor stop, depending upon the actual armature position. It appears likely that this is a function of magnetic polarity. However, since the astronomer is not normally cognizant of the motor polarities use of the reversing switch therefore adds an uncertainty in setting of two steps. The selector table should thus always be operated unidirectionally thereby reducing the possible error from $9\frac{1}{2}$ arc sec. to ± 0.25 arc sec.

As each selector lens is used for two fields the sequence of the field angles cannot be arbitrarily predetermined, in fact they cannot be monatonic. The cycle order can only be in the form : $3\frac{1}{2}'$, $9'$, $60'$, $25'$ as is illustrated in Fig. (10.5).

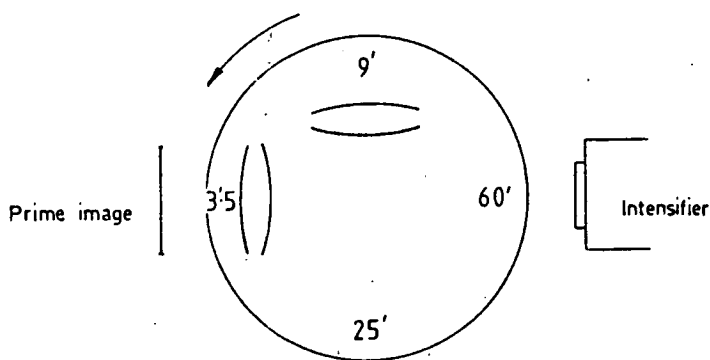


Fig. (10.5) The cyclic order of fields.

The selector table is seen in situ in Fig. (9.6)

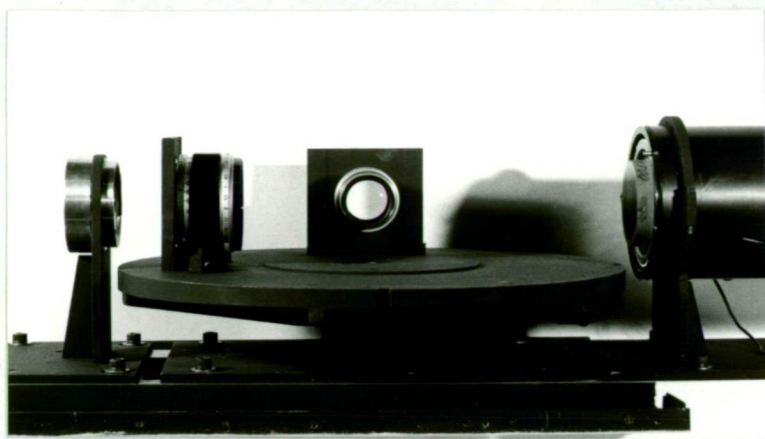


Fig. (10.6a) Selector imaging $3\frac{1}{2}'$ field (Canon lens)



Fig. (10.6b) Selector imaging $60'$ field.

ACQUISITION SYSTEM SUPPORT FRAME

Attachment to the side of the main telescope demands a stable support for each segment of the acquisition and guide system that is independent of the skew pointing angles. Neither flexure nor warp can be tolerated. The one metre telescope provides three rigid support points : at the Cassegrain ring, the centre ring and the mirror support, so that it is convenient for the 2.3 m focal length of the 150 mm objective to straddle the upper section while smaller components are arrayed over 1.2 m to span the lower section. The frontispiece shows the arrangement.

ACQUISITION SYSTEM SUPPORT FRAME

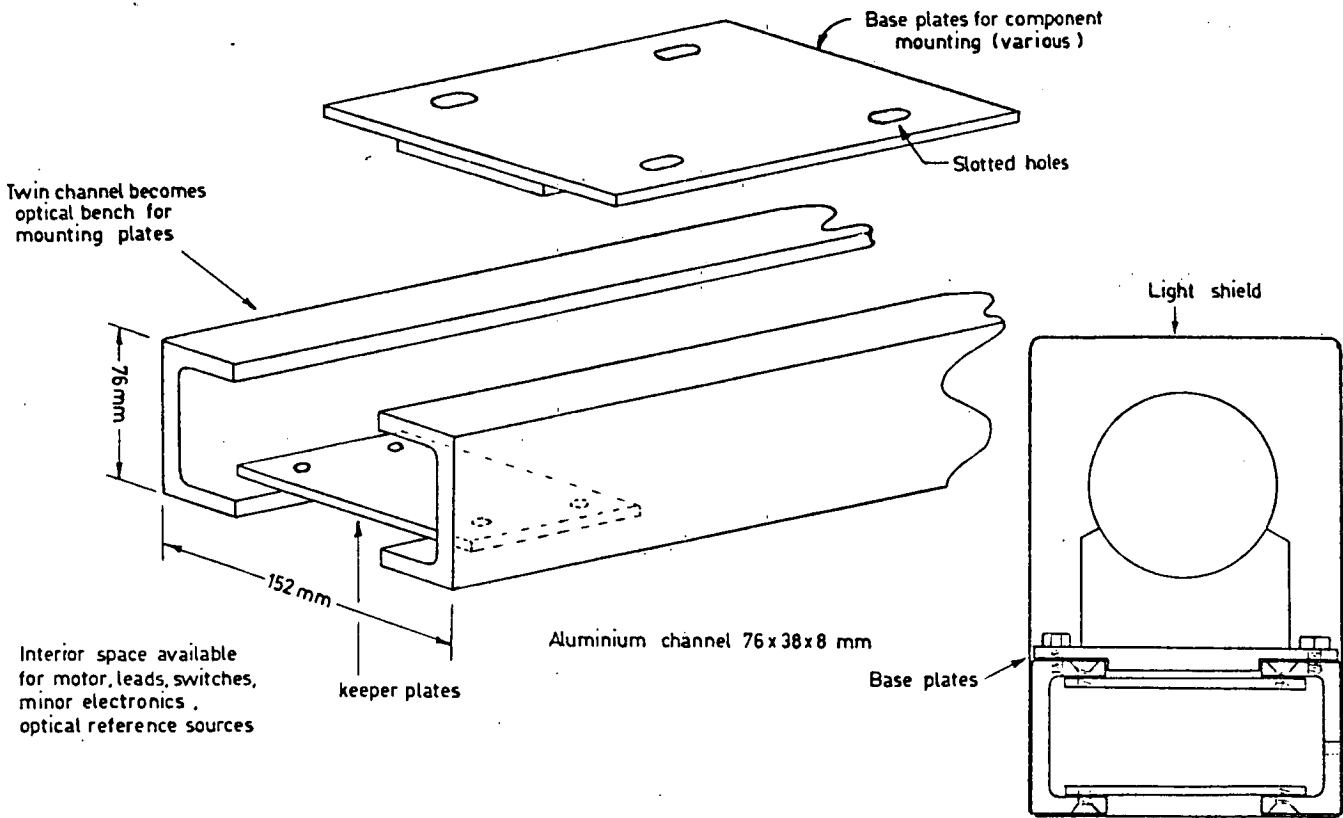


Fig. (10.7)

Other than the objective all components are mounted on a specially constructed light weight optical bench comprising two duralumin channels and a number of separation plates. The 76 x 150 x 1500mm rigid box beam so produced was milled on inside edges and top faces to provide a true edge for the component mounting plates. Figs. (10.7) and (10.8) illustrate the assembly.

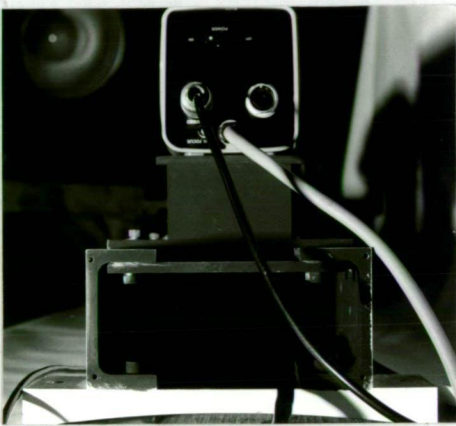


Fig. (10.8a)

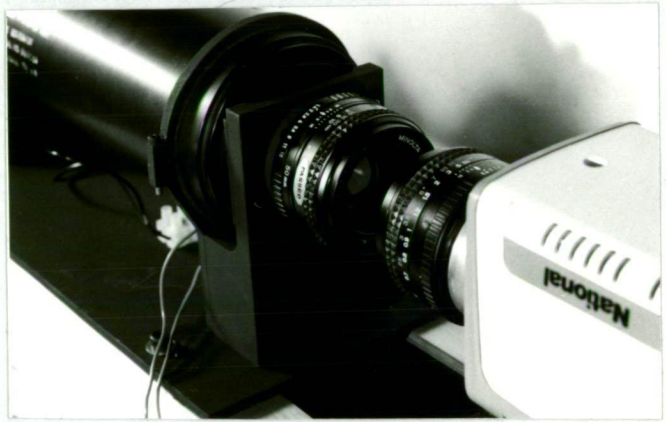


Fig. (10.8b)

Each component is mounted on its own plate for individual adjustment although each of the image transfer lenses was fixed to the intensifier and TV camera respectively. The collimated beam between the two lenses made relative spacing of the two components somewhat flexible and therefore desirable. For fine focussing a suitable object was simply the phosphor boil on the intensifier screen which could be viewed on the TV monitor. Off-the-shelf lenses also have the added convenience of inbuilt fine focussing rings.

The field lens also is on its separate stand and has a plane glass graticule at its rear side on which an angular scale is marked to indicate field of view. It is this graticule that coincides with the prime focus.

Of any adjustments the field selector system is by far the most difficult. Not only must the lens focus the graticule on the faceplate but a table rotation to the conjugate position must leave these planes unchanged. The same applies for the second lens. In the first instance it is critical that the table axis be central between graticule and faceplate. Some use can be made of the fact that for $m_1 = 4.07/0.241$ the beams emerging from the Canon lens are F 61 and F 3.6 so that a slight image plane shift may be accommodated by the depth of the field of the former. However, even with use of iterative procedures the practical problem is laborious.

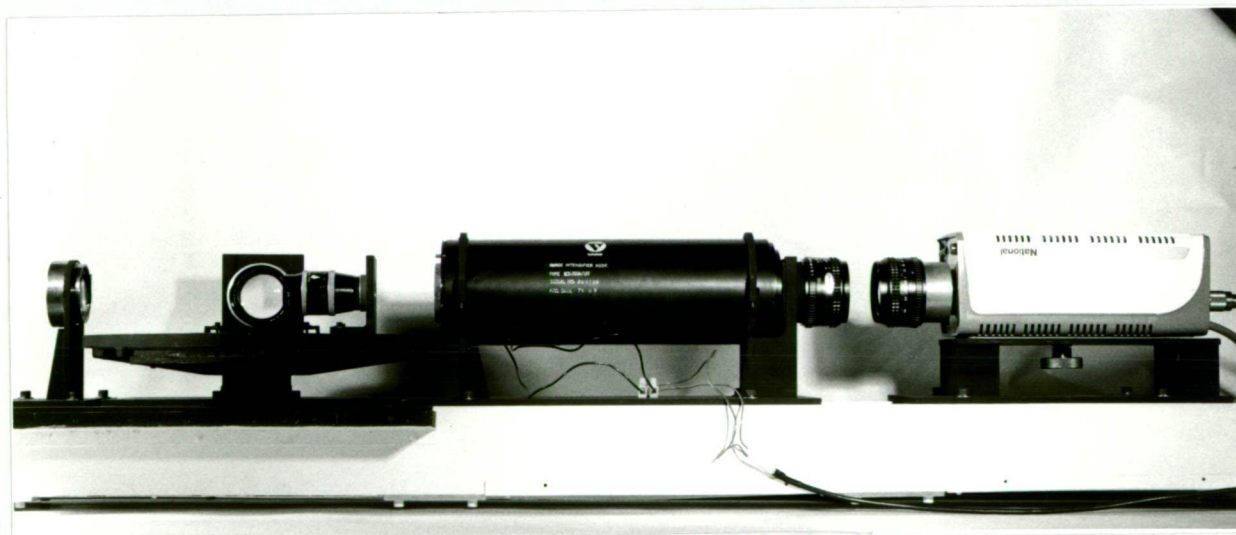


Fig. (10.9) The acquisition and guide system.

The fully assembled and adjusted guiding system on its optical bench is shown in Fig. (10.9) ready for mounting. Only tight fitting light covers with black foam edgings remain to be screwed into place.

System Mounting

The system of course must be positioned somewhere around the periphery of the one metre telescope tube. From the viewpoint of convenient tracking of stars on the monitor screen with the hand paddle it is very preferable that the two directions of motion be horizontal and vertical. The only locations of the system on the telescope which permit this are at 90° , 180° , 270° around the tube from the declination axis. Since the Nasmyth focus is at 180° one of the two other stations was chosen. This is clear from the frontispiece.

2

LOCATION OF SYSTEM OPTICAL CENTRE

Only one point common to all four fields will remain stationary on the TV monitor as the magnification is changed. It is the point away from which all stars appear to "zoom" as m_1 increases. It is therefore also the point at which a star must be placed if guiding is to be performed interchangably in more than one field of view.

Furthermore this optical centre of field must needs be reliably coincident with the axial point of the various foci of the one metre telescope such as the photometer aperture (even the smallest at 7 arc sec) at Cassegrain and the spectrograph slit at Coude. Of course if the star to be observed is very faint or even invisible off-set guiding on a brighter star on the monitor is necessary. If no sufficiently bright star is available in the $3\frac{1}{2}$ min. field guiding would have to be performed on the wider 9 min. field with it attendant slightly higher guiding errors (3 arc sec/mm of TV scale as opposed to $1\frac{1}{2}$ "/mm).

A practical problem is the location of the optical centre and how stable it is whilst the table cycles through its four stations. If the two optical axes are not quite orthogonal a shift of a star on the centre will be detectable.

On the TV monitor two distinct scales are visible. One is simply the pair of perpendicular transparent mm cursors that slide smoothly over the screen. The other is the TV image of a scale secured in the prime focus of the 150mm guidescope objective having undergone magnification

$m_1 m_2 m_3 m_4$ of the field selector, intensifier, transfer system TV system and where $m_3 = 1$ and $m_2 = 0.82$ (depends on distortion). If an arbitrary reference mark is taken on the prime image x axis indicated by cursor reading a , the actual difference between this and the optical centre in the prime image plane will be b and will scale on the TV cursor as $m_1 m_2 m_3 m_4 b$, so that the centre as read on the cursor will be

$$x_0 = 1 + m_1 m_2 m_3 m_4 b$$

By rotation between conjugate positions m_{11} and $\frac{1}{m_{11}}$ two values each for a and b are obtained and the consequent pair of simultaneous equations may be solved for x_0 . Similarly for the y ordinate,

$$y_0 = a' + m_1 m_2 m_3 m_4 b'$$

Hence the coordinates of the optical centre are (x_0, y_0) and are permanently marked on the TV monitor cursors.

To discover a variation, if any, with the second pair of conjugate positions $(m_{11}, \frac{1}{m_{12}})$ the procedure is repeated, the coordinates averaged and the half differences recorded as errors. The mean position of the optical centre for all fields is therefore,

$$x_0 = 160.4 \pm 0.9\text{mm}$$

$$y_0 = 88.1 \pm 0.4\text{mm}$$

In the $3\frac{1}{2}$ arc min field the small shift amounts to $\Delta x_0 = 1.1''$ and $\Delta y_0 = 0.5''$. However if the observer takes cognizance of which field he is using the setting accuracy reverts to that 0.25 arc sec limited by motor stepping as discussed earlier.

Chapter 11.

SYSTEM EVALUATION

Prototype Tests (100mm objective)

A number of variants of a prototype system were assembled principally with the object of assessing sensitivity and resolution as a function of real optical configurations before and after the image intensifier. The design aspects and some observations have already been treated.

In every case the objective was a 100mm F15 doublet anchored to a timber box beam supported on a yoke mounting as shown in Fig. (11.1). Mechanical instabilities (torsional), wind, and the non-tracking ability of the lengthy structure restricted photographic exposure times generally to a maximum of 1 sec, while the system damping constant of about 10 sec. was often sufficient for the object of interest to drift right out of the field, especially narrow ones. Needless to say not all the 1000 negatives taken over many months recorded useful information. The 35mm camera was focussed on the TV monitor screen with exposure time to allow at least two TV frame scans but limited so as not to be fogged by CRT fluorescence. The latter effect occurs rapidly with the Ilford HP5 film used. Typical exposures range over 1/15 to 1 sec.



Fig. (11.1) Final variant of prototype.
Note camera in position to photograph
monitor screen.

For ease of recognition and the securing of a number of standard brightness stars in the same field the test objects were always chosen as southern star clusters on which detailed photometric analyses had been published in the literature. Although 15 such clusters were photographed regularly with different optical configurations it was not always possible to find stars of appropriate magnitudes. Only the observations on three clusters are presented here.

One of the leading questions raised earlier was whether or not the transfer system would be efficient enough to image noise onto the TV target. This is analogous to asking, will the limiting magnitude of stars on the TV screen be the same as that on the intensifier screen? Direct photography of the intensifier is possible simply by removal of the TV camera and rear transfer lens and replacing this by a 35mm camera.

For the cluster 47 Tucanae the photographs of figs. (11.2a) and (11.2b) are comparable since both used the same 135mm F2.8 transfer pair.

E



N

W

Fig. (11.2a) Globular cluster 47 Tuc. Flags on the direct photograph of the intensifier screen show stars as faint as 14^m .



Fig. (11.2c) 47 Tuc. in a 50' field with higher F number transfer system shows same resolution and sensitivity as Fig.(11.2b).

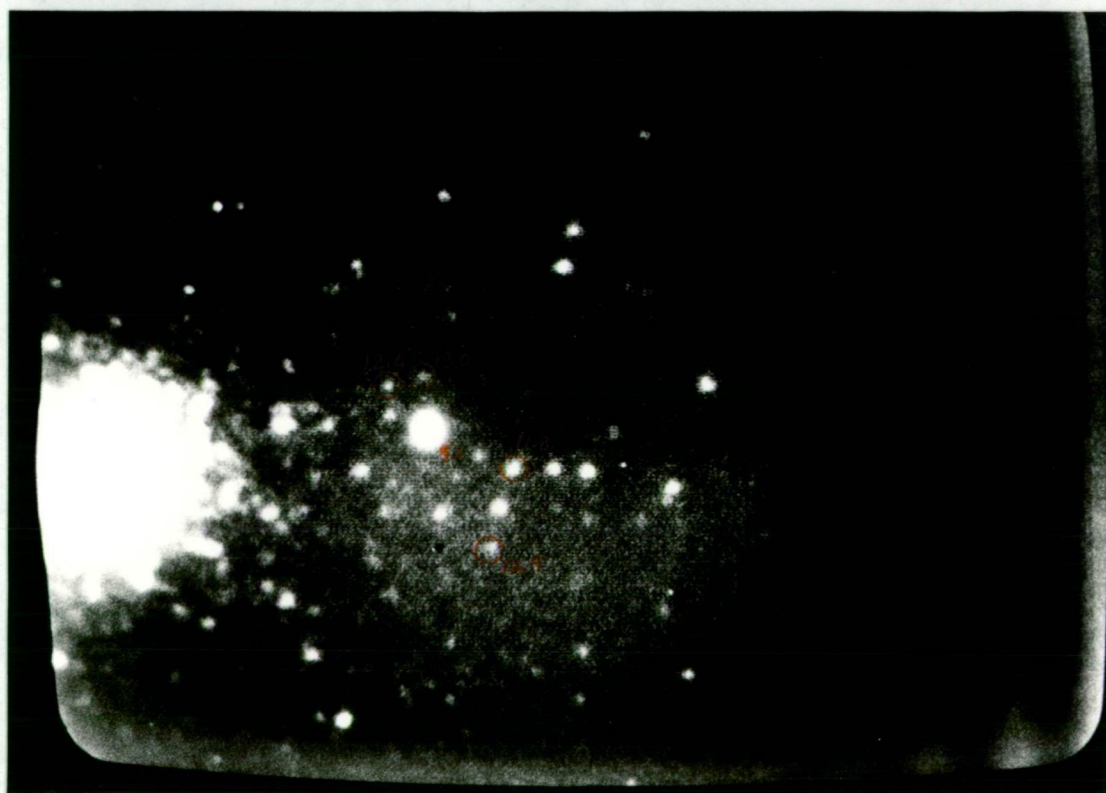


Fig. (11.2d) 47 Tuc. in 20' field with F1.4 transfer system shows marked improvement in sensitivity over Figs. (11.2b and c). Magnitude data for all stars in this figure was not available.

The globular cluster NGC 6752 has a more suitable distribution of stellar brightness for estimating quantitatively the limiting magnitude. A direct screen photograph Fig. (11.3a) shows a sample of five stars of known brightness (Cannon and Stobie 22) yielding an average of $m_{v\ell} = 14^m.3$. The comparable TV screen photo Fig. (11.3b) which is the key test gives a desirable $m_{v\ell} = 13^m.5$. It should be noted that results from a number of other clusters, e.g. NGC 4103, 4755, 3766 give a similar value.

E



W

Fig. (11.3a)

Globular cluster NGC 6752. A direct photograph of the intensifier screen revealing a number of stars fainter than 14th magnitude.



Fig. (11.3b) Cluster NGC 6752 as viewed on the TV Monitor
with a 20 arc min. field.

Permanent System (150mm objective)

Despite the many intermediate tests carried out under all extremes of weather conditions over various seasons time allowed only two nights of final system appraisal, one under poor seeing conditions and one acceptable.

The selector system with 50mm Canon and 75mm Switar lenses are in position with some attendant aberration evident in the latter probably due to close conjugate use. A sequence of four photographs of the κ Crucis cluster is shown at the designated fields - $60'$, $25'$, $9'$, $3\frac{1}{2}'$. Fig. (11.4a, b, c, d). Assessment of several clusters NGC 4755, 4103, 3292, for magnitudes and resolution give the results in Table 11.1.

Columns of expected limiting magnitudes at voltage 1000 and 1100 volts are also included. For comparison with Fig. (11.4d), Fig. (11.4e) illustrates the anticipated effect discussed much earlier than when the seeing deteriorates sensitivity will also drop off dramatically due to flux spread over target pixels.

Table 11.1 Final system, resolution and limiting magnitude

Field	Star diameter (half height gaussian width)	m_{VL}		
		890V	1000V	1100V
$3\frac{1}{2}'$	$1.4''$	11.3	11.7	12.0
$9'$	$3.5''$	12.3	12.7	13.0
$25'$	$7.5''$	13.0	13.4	13.7
$60'$	$24''$	12.6		

Comparative results with the projected values for m_{VL} therefore show a very close correlation.



Fig. (11.4a) Open Cluster NGC 4755 (K Cru) at 60 arc min
viewed on TV monitor.

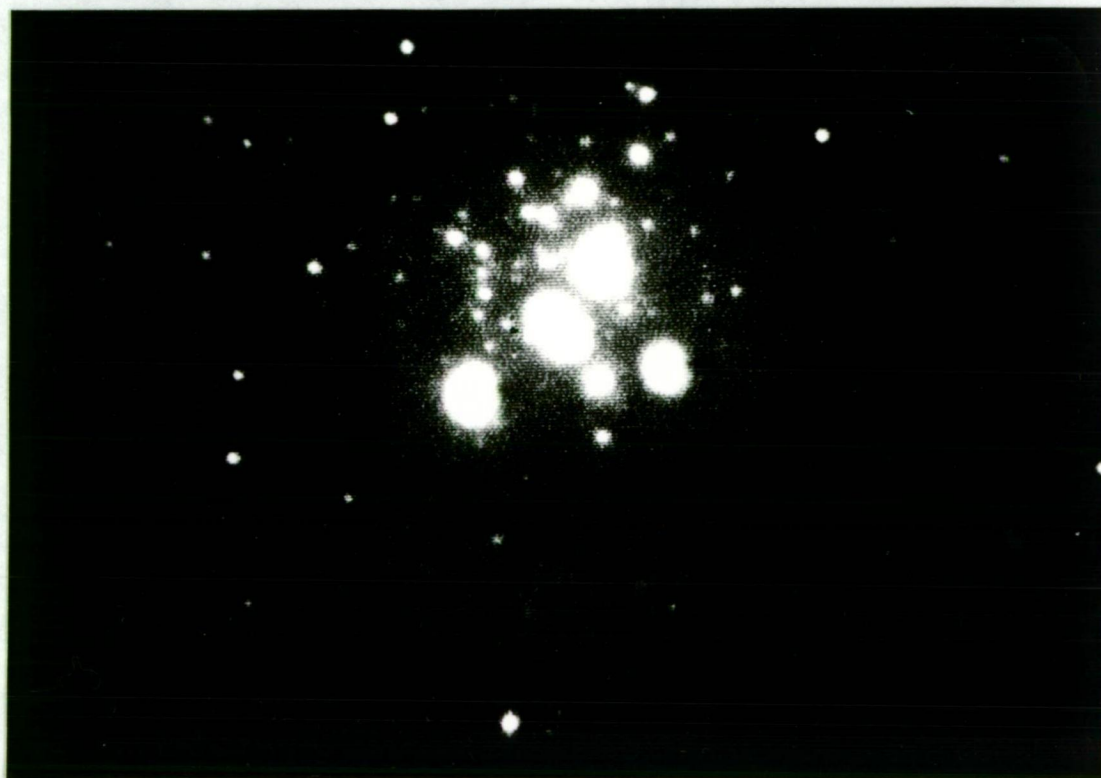


Fig. (11.4b) Cluster NGC 4755, 25 arc min field.

S

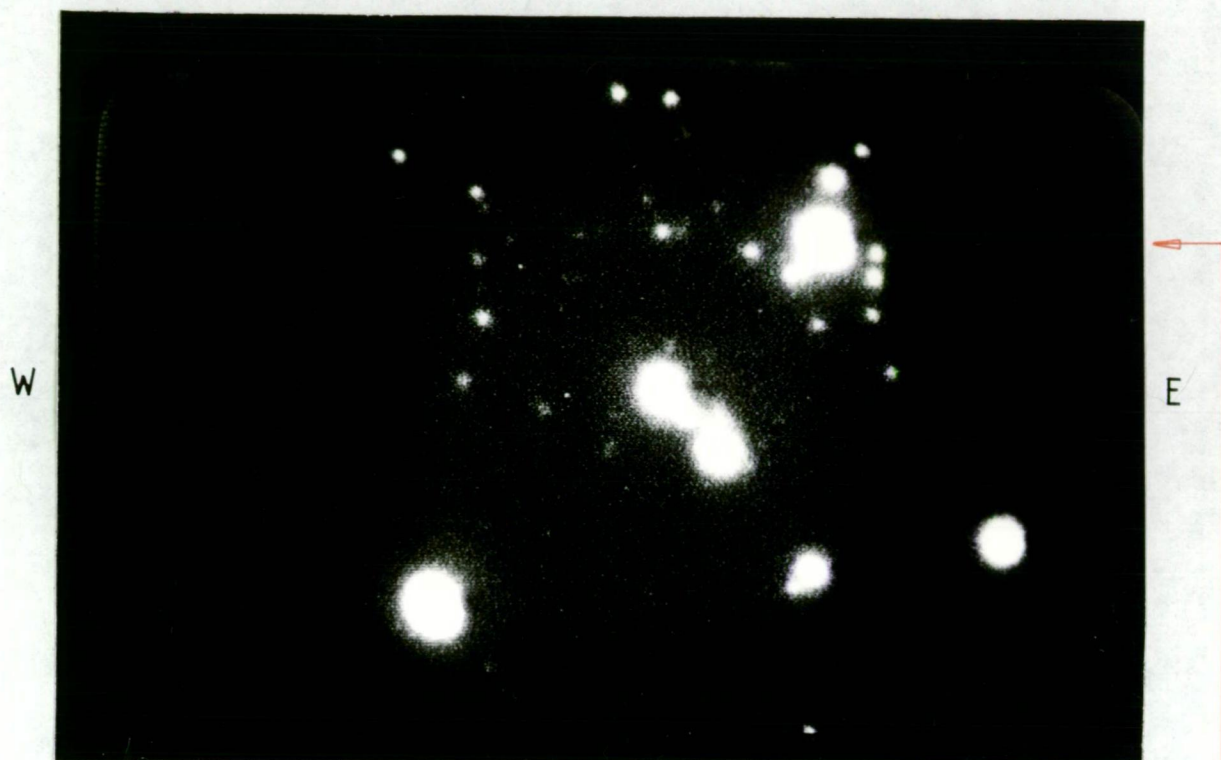


Fig. (11.4c) NGC 4755, 9 arc min. field. The improvement in angular resolution with narrowing field should be observed. Note the area around the southernmost star (top) in the triangle.

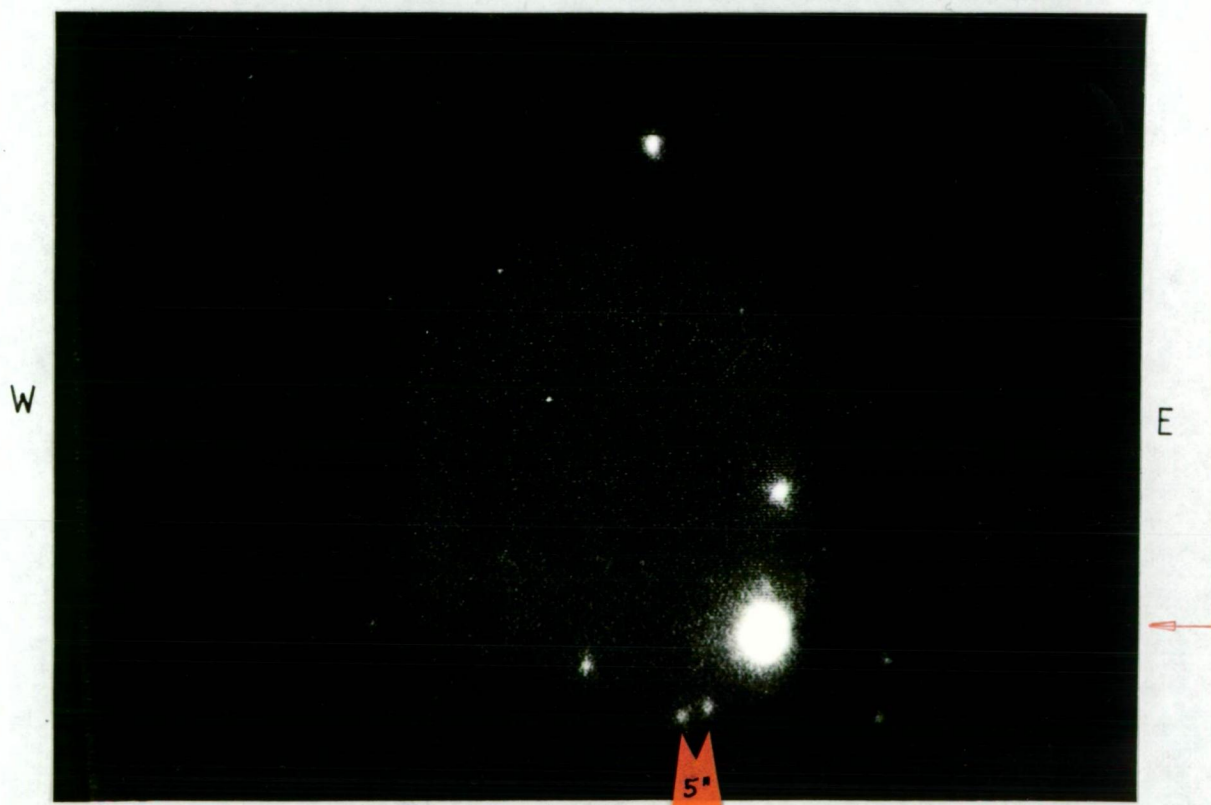


Fig. (11.4d) NGC 4755, Southernmost star in $3\frac{1}{2}$ arc min. field. The excellent resolution obtainable with the completed system is indicated by the double star near the lower edge. The pair separation is 5 arc sec and the stellar disc diameter is 1.4 arc sec.



Fig. (11.4e) Effect of deteriorating seeing.
Compare Fig. (11.4d).

Conclusion

An intensifier television acquisition and guide system has thus been developed step by step and demonstrated to have limiting magnitudes of $13^m.4$, and resolution of $1.4''$ and setting accuracy of $0.28''$, all with rather limited resources.

Chapter 12.

FUTURE DEVELOPMENTS

It seems to be almost a universal reaction that having completed an instrument, and sometimes even before completion, one considers how one would build Mark II version or else what additions or frills could be constructed for increased versatility. Such facilities may further information gathering capabilities, or be protective in nature, or merely increase convenience in use. Various possibilities are briefly considered.

A Fourth Stage of Intensification

Adding a further stage of intensification will certainly increase sensitivity and usefully so, particularly in the narrow field. The detrimental effects in the first case will be some reduction in resolution but even more obviously the sky background will appear very much brighter.

The present intensifier has a gain of 52.5 per stage ($= 4^m.3$) and a single stage resolution of 60 $\ell p/mm$. Use of the cascade formula

$\frac{1}{R_T^2} = \frac{1}{R_1^2} + \frac{1}{R_2^2}$ gives an approximate value of 24 $\ell p/mm$ for a for a four stage system with a consequent slight increase in point spread function on ^{the} TV target and loss of about 0.^m3. The net gain in sensitivity is therefore 4.^m0 and is shown in Table 12.1. Sky noise dominates by far for two fields. The left hand column gives the empirical stellar magnitude limits measured from photographs.

Table 12.1 Useful gains anticipated with fourth stage of intensification.

20	m_v	m_v	m_v sky
	3 stage	4 stage	background
$3\frac{1}{2}$ arc min.	11.7	15.7	19.0
9	12.7	16.7	17.1
25	13.4	14.9	14.9
60	12.6	12.6	12.6

Internal noise will no doubt also become significant and some form of cooling may need to be employed at the front end. The full 4^m gain may need to be slightly restricted. To prevent the output phosphor flooding with light and possible burn in a gain limiter by way of input voltage control on the 25' and 60' fields is necessary and can be automatically indexed from the field selector table. Clearly the gain may be substantially increased for the two fields that are most pertinent to guiding.

The following have been considered:

- A. 4th stage of intensification
- B. Integration facility in TV camera (vary framing but not sweep)
- C. Use of channel plate intensifier
- D. Fibre Optic transfer
- E. Access port for direct photography of intensifier screen
- F. Electronic fiducial markers on TV monitor
- G. Standard stellar comparison magnitudes
- H. Illuminated angular scale
- I. Protective shutter
- J. Photochromic window over intensifier faceplate
- K. Objective grating or prism
- L. Reflective optics of larger aperture

Each of the above have been investigated in some detail to demonstrate feasibility. Experimental progress has already been achieved on some items such as the protective overload shutter, illuminated angular scale, objective grating, and provision for direct photography of the intensifier screen. The time for submission of this thesis has precluded detailed discussion here but this can be appended later if requested.

APPENDIX I

VIGNETTING IN ROKKOR TRANSFER LENS PAIR

Since the focal length of each lens is of the order of the thickness it can hardly be assumed that the pair separation is negligible. This would be the case if the rear principle point of the first lens were in fact coincident with the front principle point of the second. That this is not so means some vignetting must occur for off axis object points. Whether this is significant depends not only on the fraction but also on the flux concentration near the lens centre due to the point source on the phosphor having a Lambertian excitance.

For each of three 50mm F1.4 MD Rokkor lenses tested by autocollimation methods the following values were determined:-

Front focal distance	11.2 mm
Axial thickness	43.8 mm
Back focal distance	37.5 mm

The necessary front to front orientation of the lenses and an eight mm gap of convenience thus yields an interprinciple point distance

$$\begin{aligned}
 P_1' P_2 &= 83.2 + 8 \\
 &= 91.2 \text{ mm}
 \end{aligned}$$

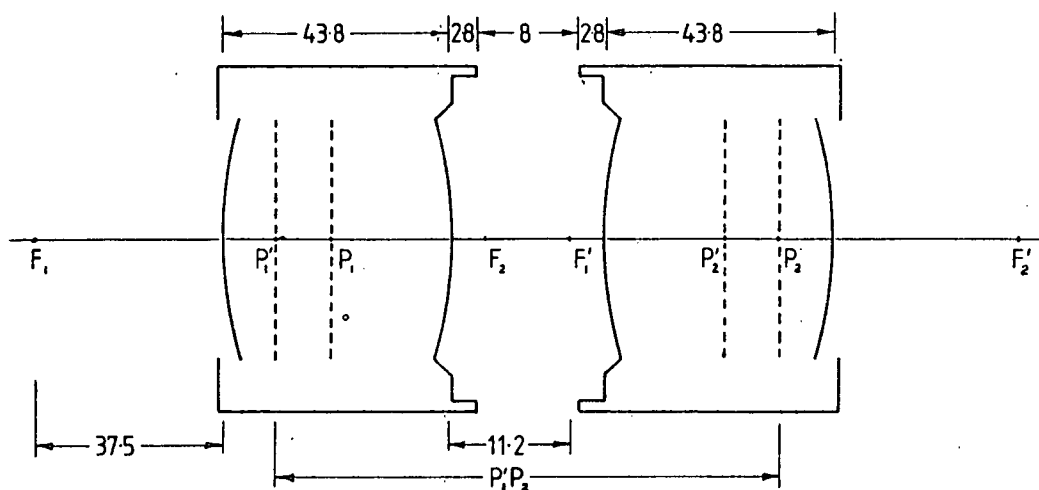


Fig. (A1) Location of Cardinal points of lens pair.

The 1 : 1 transfer lens configuration with an 8.8mm quality rectangle TV target places the extreme object point 4.4mm off axis, i.e. the inclination of the chief ray is a $\theta = \arctan \frac{4.4}{50} = 5.03^\circ$.

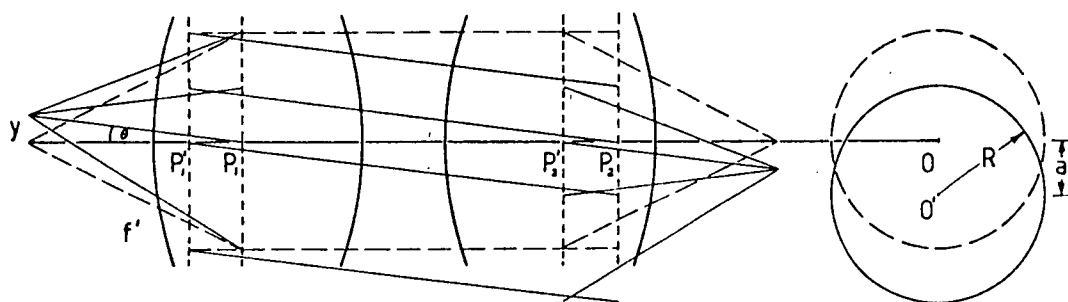


Fig. (A2) Vignetting as a result of interlens spacing.

The area of the beam transmitted to the TV target, being the intersection of the circles shown in Fig. (A2), by straight-forward geometry can be shown to be $A = 2(R^2 \arctan \frac{1}{a} \sqrt{R^2 - a^2} - a \sqrt{R^2 - a^2})$ where R is the radius

of the maximum lens aperture and $a = P_1' P_2 \tan \theta = P_1' P_2 y / f'$ is the lateral displacement of the incident beam on plane P_2 . Substituting the values above puts $R = 17.9$ and $a = 8.0\text{mm}$ so that fractional area transmitted is 0.449 and vignetting is 55.1% for an extreme off-axis object point.

However, the $\sin^2 \theta$ weighting of the Lambertian distribution for a phosphor point reduces the light flux in the crescent above by about 13% thus diminishing the vignetting to approximately 42% at edge of field.

APPENDIX II

SCENE ILLUMINATION V TARGET ILLUMINATION

When marketing low light level television cameras manufacturers in eagerness to impress that their product is sensitive to lower light levels will sometimes resort to non-uniform descriptions. Two systems are generally used each specifying the sensitivity in lux. One refers to the actual TV tube faceplate illumination while the other gives the illumination on the scene to be imaged.

The question is: how are these figures compatible? Obviously lens parameters^{and} scene reflectance will be relevant.

Suppose an object of area dA and reflectance R is illuminated by L lux, dA is imaged by the lens into dA' with magnification m .

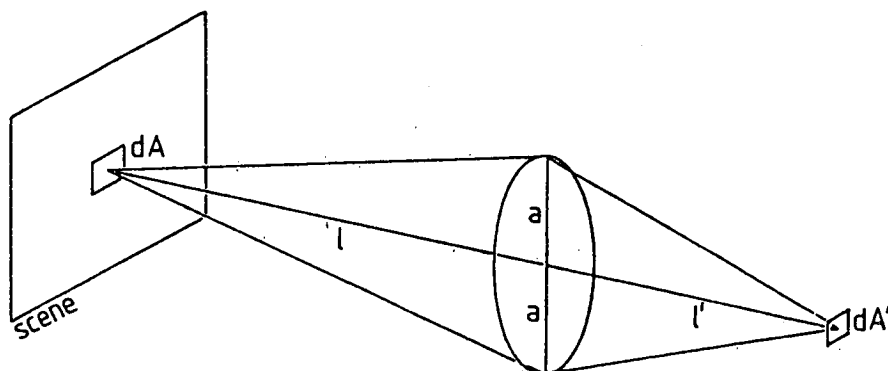


Fig. (A3) Imaging of conjugate elemental areas.

Using the elementary formula $m = \ell'/\ell$ and $FN = f'/2a \approx \frac{\ell}{2a}$ it has been shown in the discussion on transfer lens systems that the fraction of photons reflected by the object and collected by the lens aperture is $\sin^2(\arctan \frac{m}{2(1+m)FN})$. Since the image is magnified (less than unity) the intensity change due to this alone is $\frac{dA'}{dA} = m^2$.

The illumination on the TV faceplate is thus

$$L' = \frac{RL}{m} \sin^2(\arctan \frac{m}{2(1+m)FN})$$

If the conjugates are long as is normally the case this may be approximated to

$$\begin{aligned} L' &= \frac{RL}{4(1+m)^2 FN^2} \\ &\approx \frac{RL}{4FN^2} \end{aligned}$$

$$\text{or} \quad \frac{L'}{L} = \frac{R}{4FN^2}$$

A typical example may be taken with scene reflection of 40% and an F1.4 lens, so that $L'/L = 0.050$.

Hence if the lens F number is given a conversion factor is obtained.

APPENDIX III

RESOLUTION TESTS ON MD ROKKOR LENSES

The combined resolution of the transfer lens pair must not degrade the image significantly. If the resolution of each lens can be measured then by using the cascade formula $\frac{1}{R_T^2} = \frac{1}{R_1^2} + \frac{1}{R_2^2}$ (Kapany 23) an approximate value for total resolution is found.

While MTF methods are no doubt very desirable the photographing of a test chart can give meaningful results. Recordak microfilm was used to photograph a Paterson test target and was analysed with a travelling microscope.

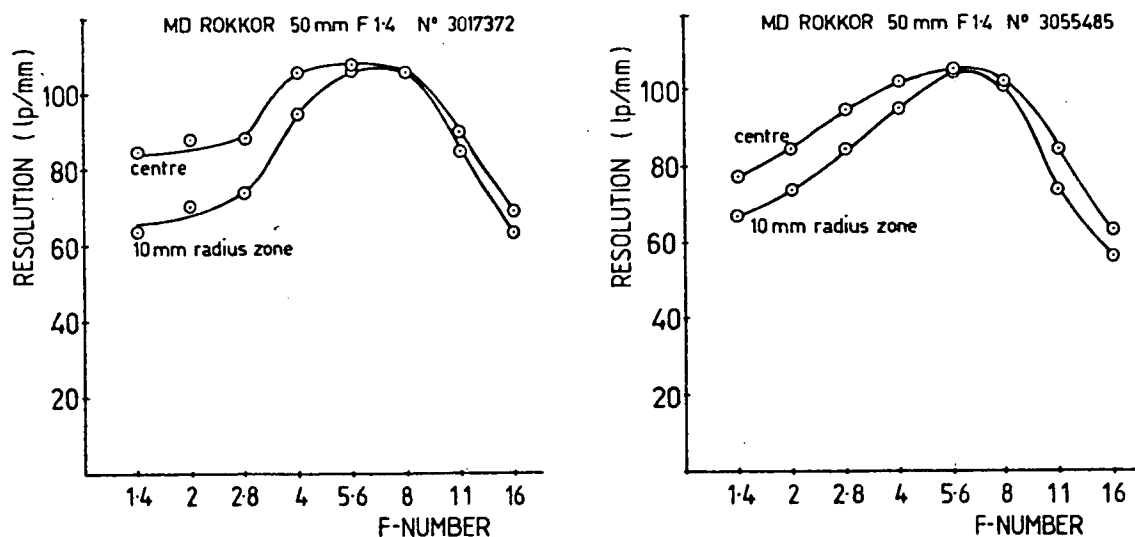


Fig. (A4) Resolution as function of F number.

Of the rather excellent results only the resolution at F1.4 is pertinent to this project yielding a total axial resolution for the pair of $R = 56 \text{ lp/mm}$. Note that since the linear field is only 8.8mm diameter the extreme off axis rays are at 5.0° to the axis and the resolution only degrades to 53 lp/mm .

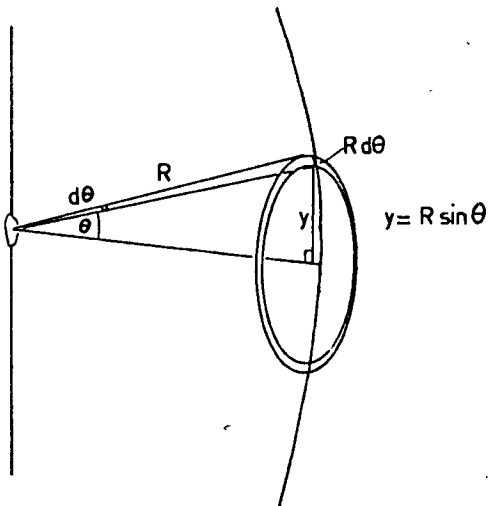
APPENDIX IV

PHOTON FLUX COLLECTED FROM STAR IMAGE ON PHOSPHOR

A transparent phosphor as on the output screen of an image intensifier behaves as a uniform diffuser so that the radiation pattern is

Lambertian, i.e. $I = I_0 \cos \theta$

The flux emitted by a star image into an annular cone is $dF = I d\omega$



$$\text{Solid angle } d\omega = \frac{dA}{R^2}$$

Now area of annular ring is

$$\begin{aligned} da &= 2\pi y \cdot R d\theta \\ &= 2\pi R \sin \theta \cdot R d\theta \end{aligned}$$

$$\text{Therefore } d\omega = 2\pi \sin \theta d\theta$$

Fig. (A5)

Therefore the flux into cone of half angle θ is,

$$\begin{aligned} F &= \int_0^\theta I \cos \theta d\omega \\ &= 2\pi I_0 \int \sin \theta \cos \theta d\theta \\ &= \pi I_0 \int \sin 2\theta d\theta \\ &= \pi/2 I_0 (1 - \cos 2\theta) \\ &= \pi I_0 \sin^2 \theta \end{aligned}$$

Thus, if the cone is subtended by a collecting lens, the fraction of light collected from an axial point is

$$\begin{aligned} E &= \frac{F_{\theta}}{F_{\text{total}}} \\ &= \frac{\pi I_0 \sin^2 \theta}{I_0} \\ &= \sin^2 \theta \end{aligned}$$

APPENDIX V

SOME OBSERVATIONS

As an indication of the possible functions other than acquisition and guiding that can be served by the completed system some examples of observations of rapid time varying events are described. Occultations or near occultations of three stars by minor planets and the moon were observed. The stage of development of the instrument at that time did not permit rapid change to narrow fields so that fine angular resolution was precluded. However event timing is still possible and is limited chiefly by the response times of the phosphors. For the intensifier the decay time is 5 millisecc while for the TV monitor it is approximately 20m sec. If electronic image processing were employed after the TV camera then only the intensifier decay time is relevant and significant accuracies can be expected. In this instance only visual measurements could be made.

Minor Planet 532 Herculina $9^m.3$

This body was predicted to occult the bright star SAO 120774 of $6^m.4$ on 7 June 1978. An intensity drop of $3^m.2$ should very readily be seen. The exact area of visibility on the earth's surface is small and difficult to predict as the precise location of the occulted stars may not be known to an accuracy better than several arc seconds which can shift the occultation path by a thousand kilometers. In this case the anticipated 23 sec. cut out was not observed from Tasmania.

A continuous sequence of photographs was taken to cover the event and two are shown in Fig. (A6a) and (A6b)



Fig. (A6a) The brightest star, SAO 120774 of $6^m.2$ is shown in a 50 arc min field at the scheduled time for the occultation by Herculina. The system was not tracking.

This was the same event for which a secondary occultation was observed at Lowell Observatory that sparked the present profuse debate over whether a minor planet can sustain its own satellite. A momentary dip in brightness of $3/4$ sec. duration was in fact observed by the writer. However several other explanations could also satisfy this observed time interval.



Fig. (A6b) Photograph taken 82 min after the expected occultation time clearly shows the asteroid separation from the star. The field of view is 20 arc min.

Minor Planet 52 Europa $10^m.4$

This expected occultation of 16 February 1978 would have displayed only a $0^m.7$ change in intensity if the path had passed across Hobart.

Three of a sequence of photographs shown in Figs. (A7a), (A7b), (A7c) follow the asteroid's progress 25 hours (11 arc mins) before the event to 46 min after.

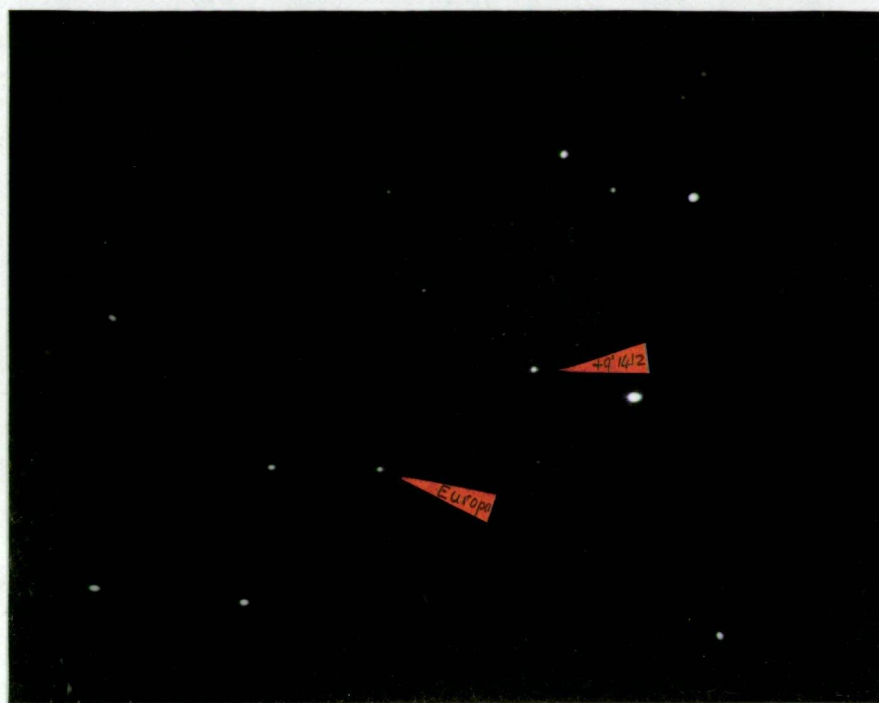


Fig. (A7a) Asteroid 52 Europa proceeding towards the star AGK3 + 9° 1412 indicated 25 hours before the expected occultation.



Fig. (A7b) Star and Europa are not resolved in the 50 arc min. field at the predicted time of occultation.



Fig. (A7c) Europa has passed the star and is very easily resolved 46 min. later.

Lunar Occultation

On March 24 1978 a total lunar eclipse occurred permitting occultation observations at the "bright" limb of the Moon. Neutral density filters were inserted before the intensifier faceplate to obtain the photographs of Fig. (A8a), (A8b), (A8c).

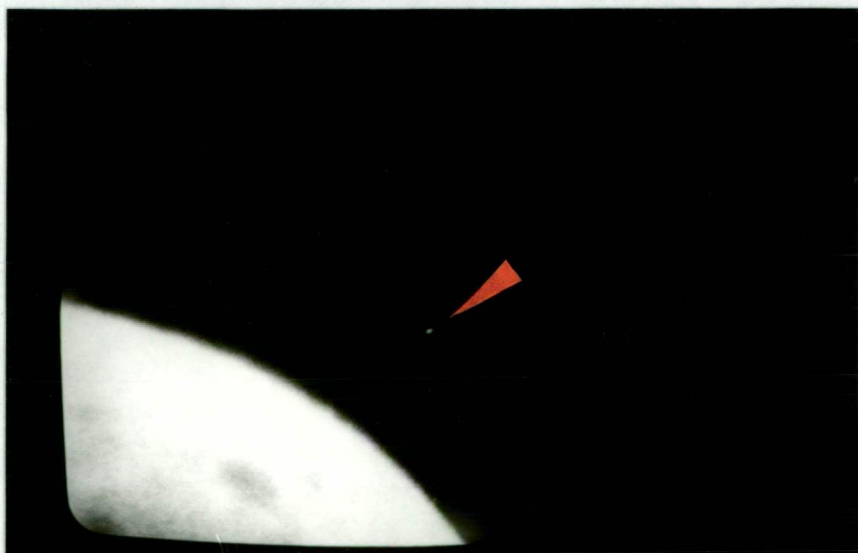


Fig. (A8a) Star is 6 min from lunar occultation.

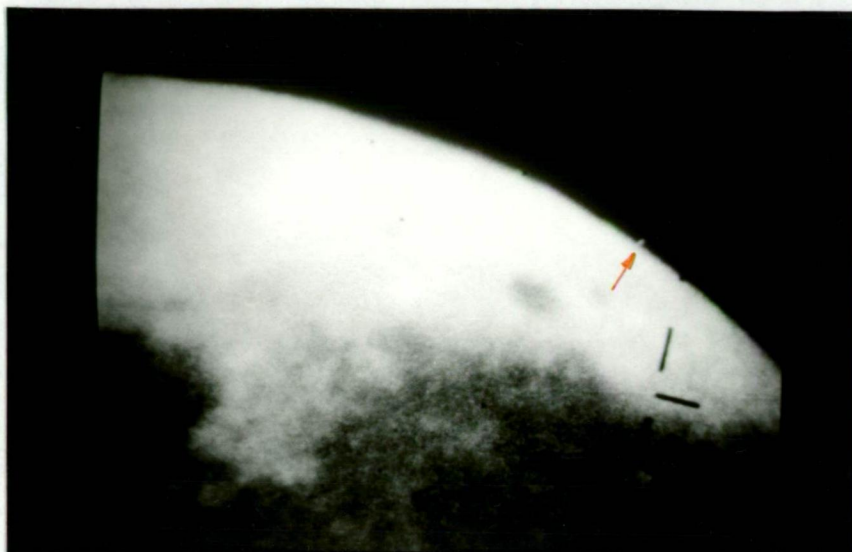


Fig. (A8b) Star is 10 sec. from occultation.

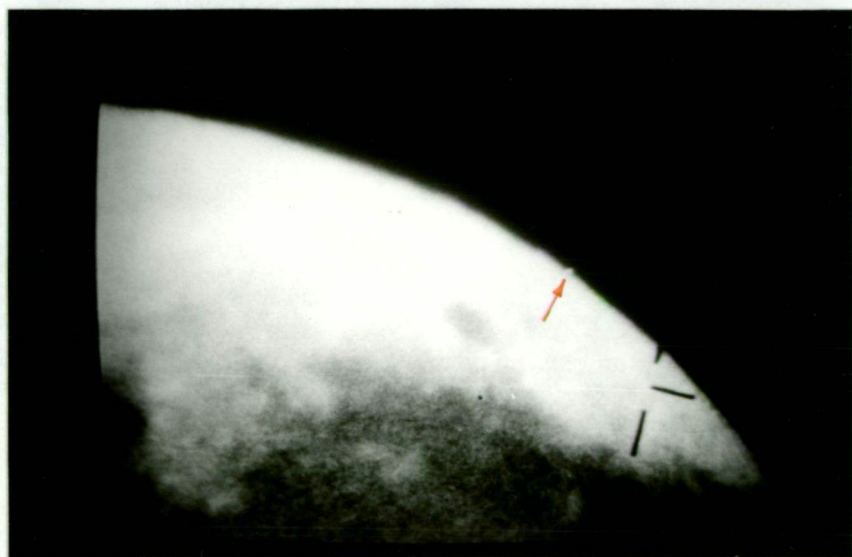


Fig. (A8c) Star is 1.5 sec. from occultation.

REFERENCES

1. YOUNG, A.T., Applied Optics 8, 869, (1969).
2. McGEE, J.D., Vistas in Astronomy Vol.15, Beer (ed), 1973.
3. WAMPLER, E.J., Methods in Experimental Physics, Vol.12A,
Ch. 6.1, 1974
4. LOWRANCE, J.L. and ZUCCHINO P.Op.cit. Ch. 6.3
5. SAUERMANN, G.O., Optical Engineering, Vol.14, No.3., S91,
1975.
6. BIBERMAN, L.M., and NUDELMAN, S. (eds.) Photoelectronic Imaging
Devices, Plenum Press, 1971.
7. FLYNT, W.E., Varo Tube Development Dept., private communication.
8. EBERHARDT and HERTEL, Applied Optics 10, 1972, (1971).
9. WEYLAND, W.P., Electronics Engineering, p.31., Aug. 1975
10. BAILEY P.C. Electronics, p.8., July, 1976.
11. DAWE, A., Video Review, p.22. Feb. 1977.
12. COPE, GRAY, HUTTER, Photoelectronic Imaging Devices, Vol. 2., p.15,
Bibermann and Nudelman (eds.)
13. LEVI, L., Applied Optics, Wiley, p.260, 1971.
14. CARNT, P.S. and TOWNSEND, G.B., Colour Television, p.85, Iliffe
15. GROB, B., Television, p.81, McGraw Hill.
16. DAWE, A., Video Review, p.22., Feb., 1977.
17. PHILIPS, Internal data sheets, 8P:3802 (1976).
18. ALLEN, C.W., Astrophysical Quantities, p.197, Athlone Press (1973).
19. WILDEY, R.L., Astrophysical Journal 133, p.430 (1961)
20. MENZIES, J., Mon. Not. Roy. Astr. Soc. 163, p.323, (1973)
21. TIFT, W.G., Mon. Not. Roy. Astr. Soc. 126, p.16, (1962)
22. CANNON, R.D. and STOBIE, R.S., Mon. Not. Roy. Astr. Soc., 162
p.227, (1973)
23. KAPANY, N.S., Fibre Optics - Principles and Applications, Acad.
Press (1967)